# THE EFFECTS OF ANTI-CD20 THERAPY ON SUSCEPTIBILITY TO *PNEUMOCYSTIS* INFECTION AND THE CD4+ T-CELL SIGNALS THAT MEDIATE CLEARANCE

by

**Waleed A Elsegeiny**

Bachelor of Science, Louisiana State University, 2008

Submitted to the Graduate Faculty of

School of Medicine in partial fulfillment

of the requirements for the degree of

Doctor of Philosophy

University of Pittsburgh

2015

UNIVERSITY OF PITTSBURGH

SCHOOL OF MEDICINE

This dissertation was presented

by

Waleed A Elsegeiny

It was defended on

July 8, 2015

and approved by

Jennifer Bomberger, Ph.D. Assistant Professor, Microbiology and Molecular Genetics

Geetha Chalasani, M.D. Assistant Professor, Medicine

Shabaana Khader, Ph.D. Associate professor, Molecular Microbiology

Penelope Morel, M.D. Professor, Immunology

Dissertation Advisor: Jay K. Kolls M.D. Professor, Pediatrics and Immunology

**The Effects of Anti-CD20 Therapy on Susceptibility to *Pneumocystis* Infection and the CD4 Signals that Mediate Clearance**

Waleed A Elsegeiny, PhD

University of Pittsburgh, 2015

*Pneumocystis* is an opportunistic fungal pathogen that presents as a pulmonary pneumonia. Originally characterized as an AIDs-defining illness, *Pneumocystis* has now reemerged in non-HIV immunocompromised patients. It has been shown that *Pneumocystis* prophylaxis of can reduce the incidence of infection, severity of disease, and mortality rate in immunocompromised patients. However, prophylaxis is relatively toxic, and only prescribed to defined at risk populations. Anti-CD20 was originally a therapy for B-cell non-Hodgkin lymphomas, but now it's also used to treat hematological malignancies, autoimmune diseases, and post-transplant lymphoproliferative disease. Studies have shown that up to 30% of patients receiving anti-CD20 antibodies developed *Pneumocystis* pneumonia, however, many of these patients were also on concomitant immunosuppressive drugs which complicates any analyses of clinical studies. Thus, we generated a murine model of anti-CD20 therapy, and demonstrated treatment does induce susceptibility to *Pneumocystis* infection. This correlated to an overall decrease in immune response, but more specifically a loss in CD4+ T-cell mediated protection.

The predominant factor required for immunity against *Pneumocystis* infection is the presence of CD4+ T-cells. This has been validated several times over by clinical data and experimental animal models. Early on, studies have examined the role of T helper 1 (Th1), T helper 2 (Th2), and T helper 17 (Th17) cells. To briefly summarize these studies, Th1, Th2, and Th17 cells can all be detected in the lung during infection, however, removal of their classically

defined effector molecules only delayed clearance or had no effect. We examined the importance of each subset of T helper cells by deleting the Stat transcription factors that mediated differentiation. We found that specifically Stat3 was required, however, it was independent of IL-17 and IL-23 signals. We also identified IL-21 as a key cytokine required to mediate clearance. Using a variety of approaches, we determined that GM-CSF and IL-22 play important roles during *Pneumocystis* infection. GM-CSF+ CD4+ T-cells are critical for T-cell mediated clearance, however, it alone is not sufficient. While IL-22, although not required, was sufficient to reduce burden in IL-21 receptor knockout mice. These data suggest a model of clearance, requiring non-classical T helper cell function.

## TABLE OF CONTENTS

**PREFACE** ..... **XIII**

**1.0 CHAPTER ONE: INTRODUCTION** ..... **1**

**1.1 THE PATHOGEN** ..... **1**

**1.1.1 History and Taxonomy of *Pneumocystis*** ..... **1**

**1.1.2 *Pneumocystis* Host Specificity and Nomenclature** ..... **2**

**1.1.3 *Pneumocystis* Morphology and Life-Cycle** ..... **4**

**1.2 THE HOST** ..... **7**

**1.2.1 *Pneumocystis* Epidemiology** ..... **7**

**1.2.1.1 HIV associated *Pneumocystis* pneumonia** ..... **8**

**1.2.1.2 Non-HIV associated *Pneumocystis* pneumonia** ..... **9**

**1.2.2 Clinical Features and Diagnosis** ..... **11**

**1.2.3 Treatment and Prophylaxis** ..... **14**

**1.2.4 Immune Reconstitution Inflammatory Syndrome** ..... **15**

**1.3 THE IMMUNE RESPONSE** ..... **17**

**1.3.1 Pulmonary immunity and disease** ..... **17**

**1.3.2 Lung-resident dendritic cells and macrophages** ..... **18**

**1.3.3 T-cell mediated immunity in the lung** ..... **23**

**STATEMENT OF PURPOSE** ..... **28**

**2.0 CHAPTER TWO: ANTI-CD20 THERAPY AND SUSCEPTIBILITY TO *PNEUMOCYSTIS* PNEUMONIA..... 30**

**2.1 INTRODUCTION ..... 31**

**2.1.1 Anti-CD20 Therapy ..... 31**

**2.1.2 B-cells and *Pneumocystis* infection ..... 32**

**2.1.3 Anti-CD20 Therapy and immune reconstitution inflammatory syndrome 32**

**2.2 MATERIALS AND METHODS ..... 33**

**2.2.1 Mice. ..... 33**

**2.2.2 *Pneumocystis* Isolation, Inoculum and Antigen Preparation..... 34**

**2.2.3 Whole Lung Cell Preparation and Antigen Stimulation. ..... 34**

**2.2.4 Flow Cytometric Analysis. ..... 35**

**2.2.5 RNA Isolation and *Pneumocystis* Quantification by RT-PCR. ..... 35**

**2.2.6 Serum Collection and *Pneumocystis murina* Antigen ELISA..... 36**

**2.2.7 Antibody Mediated Cell Depletion. ..... 36**

**2.2.8 Preparation of Splenocyte, Purified-CD4, and Purified-B220 Cells for Adoptive Transfer. ..... 37**

**2.2.9 Pulse Oximetry and Lung Injury Qualification from BALF. ..... 37**

**2.2.10 Statistical Analysis. ..... 38**

**2.3 RESULTS ..... 38**

**2.3.1 Anti-CD20 treatment induces susceptibility to *Pneumocystis*. ..... 38**

**2.3.2 CD20 depletion blocks type 2 immune responses in the lung. ..... 40**

**2.3.3 Anti-CD20 treatment eliminates CD4+ T-cell protective responses. ..... 44**

**2.3.4 Mice with convalescent immunity are resistant to anti-CD20 mediated susceptibility. ..... 47**

**2.3.5 B-cells are dispensable during T-cell immune reconstitution inflammatory syndrome (IRIS). ..... 49**

**2.4 DISCUSSION ..... 53**

**3.0 CHAPTER 3: CD4+ T-CELL INTRINSIC IL-21R SIGNALING AND THE FACTORS THAT MEDIATE *PNEUMOCYSTIS* CLEARANCE ..... 57**

**3.1 INTRODUCTION ..... 58**

**3.2 MATERIALS AND METHODS ..... 59**

**3.2.1 Mice. ..... 59**

**3.2.2 *Pneumocystis* Isolation, Inoculum and Antigen Preparation. ..... 60**

**3.2.3 Whole Lung Cell Preparation and Antigen Stimulation. ..... 60**

**3.2.4 RNA sequencing ..... 61**

**3.2.5 Flow Cytometric Analysis. ..... 62**

**3.2.6 RNA Isolation and *Pneumocystis* Quantification by RT-PCR. ..... 62**

**3.2.7 Serum Collection and Direct ELISA. ..... 63**

**3.2.8 Antibody Mediated Cell Depletion. ..... 63**

**3.2.9 Preparation of Purified-CD4+ T-cells for Adoptive Transfer. ..... 64**

**3.2.10 Histology ..... 64**

**3.2.11 Statistical Analysis. ..... 64**

**3.3 RESULTS ..... 65**

**3.3.1 Classical Th1, Th2, and Th17 effector cytokine signals are not required for *Pneumocystis* clearance. ..... 65**

**3.3.2 IL-21R signaling is necessary for control of *Pneumocystis* infection. ..... 69**

**3.3.3 IL-21 signaling is required for protective B- and T-cell responses. ..... 71**

**3.3.4 Defining a role for IL-22 during *Pneumocystis* infection. ..... 74**

**3.3.5 IL-22 supports the clearance of *Pneumocystis* ..... 78**

**3.3.6 GM-CSF-producing CD4+ T-cells are required for clearance of *P. murina* infection. ..... 82**

**3.4 DISCUSSION ..... 86**

**4.0 CHAPTER 4: CONCLUSIONS AND FUTURE PERSPECTIVES ..... 90**

**APPENDIX A ..... 99**

**BIBLIOGRAPHY ..... 127**

## LIST OF TABLES

Table 1. Genes Associated with *Pneumocystis* Susceptibility ..... 10

Table 2. Dendritic cell and macrophage surface marker expression ..... 21

Table 3. CD4+ T-cell Subtypes ..... 25

## LIST OF FIGURES

Figure 1. *Pneumocystis* morphology ..... 4

Figure 2. *Pneumocystis* reproduction ..... 6

Figure 3. *P. murina* quantification mitochondrial LSU vs SSU rRNA ..... 13

Figure 4. Macrophage phagocytosis of *Pneumocystis* ..... 23

Figure 5. Anti-CD20 treatment during *Pneumocystis* infection ..... 39

Figure 6. CD4 and B220 cell assessment post anti-CD20 treatment ..... 41

Figure 7. Cytokine analysis of supernatants from *Pneumocystis* antigen stimulated WLCs ..... 43

Figure 8. Adoptive transfer of naïve CD4+ cells protects Rag1-/- from *P. murina* infection ..... 44

Figure 9. Loss of CD4+ cell specific protection after anti-CD20 treatment ..... 46

Figure 10. Humoral immunity is sufficient for protection against *Pneumocystis* ..... 48

Figure 11. Influence of CD20 depletion on Immune Reconstitution Inflammatory Syndrome ... 50

Figure 12. Influence of naïve and antigen-experienced B220 cells on IRIS ..... 52

Figure 13. Classical Th1, Th2, and Th17 factors are dispensable during *P. murina* infection .... 66

Figure 14. CD4 intrinsic Stat3 required for clearance ..... 68

Figure 15. IL-21 signaling required for *P. murina* clearance ..... 70

Figure 16. IL-21 signaling required for B-cell mediated clearance against *P. murina* infection . 73

Figure 17. CD4 intrinsic IL21r signaling is required for protection ..... 75

Figure 18. IL-22 signaling is increased during *Pneumocystis* infection ..... 77

Figure 19. IL-22 supports clearance of *P. murina* infection ..... 79

Figure 20. CD4+ T-cells produce GM-CSF during infection ..... 81

Figure 21. GM-CSF is required for *P. murina* clearance ..... 84

Figure 22. GM-CSF and IL-22 work cooperatively to clear *Pneumocystis* infection ..... 85

Summary Figure. Immune Response to Pneumocystis Infection ..... 97

Figure 23. RNA sequencing of whole lung shows a prominent CD4-dependent eosinophil signature at day 14 of *Pneumocystis* infection..... 112

Figure 24. CD4-dependent recruitment of eosinophils to the lung at day 14 of *Pneumocystis* infection ..... 114

Figure 25. Eosinophils contribute to control of *Pneumocystis* infection both *in vitro* and *in vivo* ..... 115

Figure 26. Treatment of CD4-depleted C57Bl/6 and Rag1-/- mice with pIL5 results in eosinophilia in whole lung and decreased *Pneumocystis* burden ..... 118

Figure 27. Eosinophil numbers correlates with *Pneumocystis* killing in vivo..... 119

Figure 28. pIL5 treatment can reduce *Pneumocystis* burden in CD4-depleted BALB/c mice ... 121

Figure 29. pIL5 treatment cannot rescue eosinophil-deficient Gata1tm6Sho/J knockout mice . 123

# PREFACE

These past four years at the University of Pittsburgh have been a difficult and rewarding journey. I was fortunate to have the support and encouragement from numerous individuals, without whom the completion of this study would not have been possible. I would first like to thank my mentor, Dr. Jay Kolls, for his guidance and patience through my training and development as an independent scientist. I would also like to thank all the past and present member of the Kolls lab, especially Taylor Eddens, Kong Chen, David Ricks and Leticia Monin for their continuous assistance with my research in theory and in practice. I am also grateful to my committee and the members of the Alcorn, Khader, Sanders, and Maricich labs for providing a sense of community through their technical assistance and intellectual discussions. A special thanks to Ryan Moeslein and Dr. Larry Kane for their motivational encouragement and making sure that I was always moving forward during my doctoral studies. I would also like to thank all the collaborators that have provided samples and/or reagents during the course of this study.

I would like to acknowledge my parents, Siham Yassin and Abdel-Wahab Elsegeiny, who have always been supportive of my ambitions and goals. Much gratitude must go to my friends for keeping my life balanced and full of wonderful/necessary distractions. Finally, I would like to thank my undergraduate mentor, Dr. Tin-wien Yu, for building a strong foundation in molecular biology and research practices which have supported the development of my career.

# 1.0 CHAPTER ONE: INTRODUCTION

## 1.1 THE PATHOGEN

### 1.1.1 History and Taxonomy of *Pneumocystis*

*Pneumocystis* is a fungal genus that was first discovered in 1909 by Carlos Chagas (1979-1934). Chagas was investigating trypanosomiasis in the Minas Gerais state of Brazil, and observed the cyst form of *Pneumocystis* in *Cavia porcellus* (guinea pigs) inoculated with blood from two children infected with Trypanosoma [1, 2]. He misidentified the cysts as a new genus of trypanosomes, calling them *Schizotrypanum*. In 1910, Antonio Carini (1872-1950), at Instituto Pasteur de São Paulo, also identified the same cystic organisms in the lungs of *Rattus norvegicus* (rats) during an experimental model of Trypanosoma lewisi infection, but also mischaracterized these cysts as a new genus of trypanosome [3]. Shortly after, Delanoë and Delanoë, fellows under Alphonse Laveran at Instituto Pasteur de São Paulo, received samples from Chagas and compared them to similar organisms they found in rats that were negative for *Trypanosoma*. These organisms did not acquire dissemination to the blood, and displayed a strict tropism to the lung, very uncharacteristic of trypanosomes. Thus, Delanoë and Delanoë reported that the organisms identified by both Chagas and Carini are unique from trypanosomes, and named the

genus *Pneumocystis carinii*, Pneumo- for the lung, -cytis for its circular morphology, and carinii after Antonio Carini [4, 5].

The taxonomy of *Pneumocystis* had been under debate for many years due to its morphological features and life cycle. Its small cyst and large trophozoite lifeforms initially lead many scientists to conclude that *Pneumocystis* is a coccidian Protozoa [6, 7], however, there were still those who suggested that the organism more accurately resembled Fungi [8, 9]. In 1988, Jeffrey Edman, with the use of small subunit ribosomal RNA analysis, was able to settle this debate by comparing the structural distances (average number of base changes per position) of the rRNA among several fungal, protozoan, and mammalian organisms. He concluded that *Pneumocystis* has strong structural similarity with Fungi, especially *Sacchromyces cerevisiae*, and a large structural distance from Protozoa [10]. Other studies have also shown that the thymidylate synthase and dihydrofolate reductase, beta tubulin, and mitochondrial DNA sequences of *Pneumocystis* have greater homology with Fungi than Protozoa. More recently, the sequencing of the *Pneumocystis* genome has validated it's strong homology with other Fungi [11]. Thus, *Pneumocystis* has been listed under the Ascomycota phylum (subphylum Taphrinomycotina), closest known relative being *Schizosacchromyces pombe*, and given a unique class, order, and family [12]. Eukaryote Fungi Ascomycota Pneumocystidomycetes Pneumocystidales Pneumocystidaceae *Pneumocystis carinii* [13].

### 1.1.2 *Pneumocystis* Host Specificity and Nomenclature

Since its initial discovery in rats and guinea pigs, *Pneumocystis* has been identified in nearly all mammalian species. The earliest known documentation of pneumocystosis was during World War II at an orphanage in Poland, where two malnourished infants presented with a diffuse

interstitial pneumonia. The investigation was led by two Dutch physicians, van der Meer and Brug who identified *Pneumocystis* as the causative agent of the infection in the infants [5]. However, it wasn't until 1952 that a Czech pathologist by the name, Otto Jirovec received credit for describing the first human case of *Pneumocystis* pneumonia. Initially, it was believed that humans infected with *Pneumocystis* acquired a zoonotic infection [14]. Experimentally however, although it was shown that *Pneumocystis* could be transmitted via an airborne route between animals of the same species, there were no successful attempts of interspecies infection. It was an unprecedented discovery, within the kingdom Fungi, for *Pneumocystis* to have such stringent host specificity. For example, *Pneumocystis* from an infected rat cannot successfully infect a mouse, and vice versa [15]. Historically, this required *Pneumocystis* to be labeled as distinct forms i.e. forma specialis (f.sp.). For example, the form of *Pneumocystis* that infects mice was referred to as *Pneumocystis carinii* f.s*p. murina*, while *Pneumocystis carinii* f.sp. *hominis* was reference to the form that infected humans [16].

The exact reason for this host and tissue tropism is still not known, however, *Pneumocystis* spp. have genetic and antigenic variations between the different forms. This discovery triggered a nomenclature change in the research community [17], so each form of *Pneumocystis* is now referred to as a distinct species. For example, *Pneumocystis carinii* f.s*p. murina* is now simply *Pneumocystis murina*. Since Antonio Carini discovered the organism in rats; now only the rat form is named *Pneumocystis carinii*, and the human form is named after the pathologist Jirovec, *Pneumocystis jirovecii* [16, 18].

### 1.1.3 *Pneumocystis* Morphology and Life-Cycle

*Pneumocystis* is a dimorphic organism with cystic and trophic lifeforms **(Figure 1)**. The life-cycle and basic biology of *Pneumocystis* is unique but very much understudied. The biggest limitation of *Pneumocystis* research is the inability for the organism to grow *in vitro*, so most studies of *Pneumocystis* morphology and life-cycle were done in a rabbit model of infection with *Pneumocystis oryctolagi* [19]. The majority of data generated on the specific structural features of *Pneumocystis* was generated in the 90's by transmission electron microscopy, ultrastructural cytochemistry, and computational 3D reconstructions [20-22].

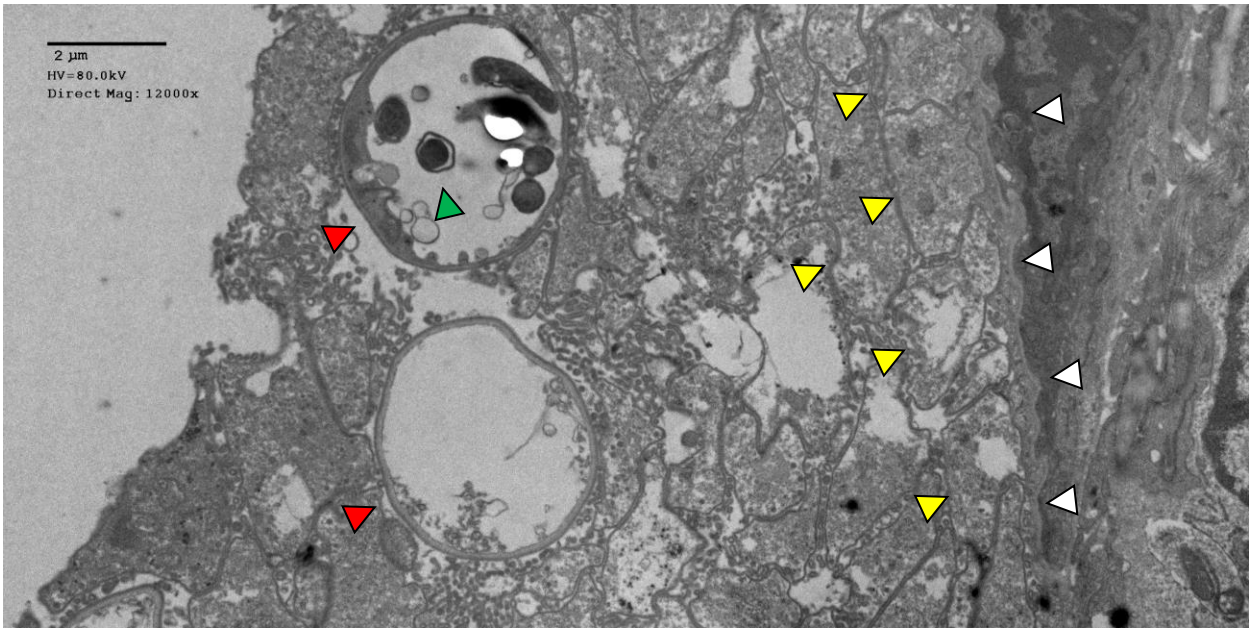


**Figure 1. *Pneumocystis* morphology**

Transmission electron microscopy of murine alveolar epithelial cells during *Pneumocystis* infection. The trophic form of *Pneumocystis* (yellow arrow) is amoeboid and binds directly to the surface of alveolar epithelial cells (white arrows) and each other. The cystic form of *Pneumocystis* (red arrows) is round, with a thick, β-1,3-glucan rich cell wall, and up to 8 ascospores per cyst (green arrows).

The accepted life-cycle of *Pneumocystis* begins with the transmissible and infectious form of the pathogen, the ascospore filled cyst. The ascospore has a visible outer membrane with a single layered electron-dense cell wall [23]. These grow/differentiate into trophozoites (trophs) that start off small (1-2 μm) and ellipsoid, but become larger (4-8 μm) and have irregular shapes (amoeboid). This irregularity is due to the numerous filopodia that sometimes are described as tree-like. The trophic forms attach specifically to alveolar type-I (AT1) epithelial cells and begin their transition through three sporocytic stages (early, intermediate, and late) finally forming a mature cyst or ascus **(Figure 2A)**. Early sporocytes are very similar to the trophic form (mononuclear, single-layered cell wall), except they have a rounded morphology. The intermediate sporocyte have an increase in cell wall thickness, primarily from β-1,3-glucan synthesis of the middle layer of the cell wall, and undergo multiple nuclear replications. The late sporocyte is denoted by the visual appearance of up to 8 nuclei; the invagination of the cyst membrane establishes the ascospores and completes the cystic stages [23, 24]. The surfaces of mature cysts have highly polymorphic mannose-rich antigens, known as major surface glycoproteins (MSG) [5, 25]. The MSGs are heterogeneous among the different species of *Pneumocystis*, however, intracellular proteins, such as kinases, are more closely conserved. It is speculated that the heterogeneity of the MSGs of *Pneumocystis* may play a role in their strict host specificity (Eddens et al. unpublished). Finally, the mature cysts release the ascospores through a small pore.

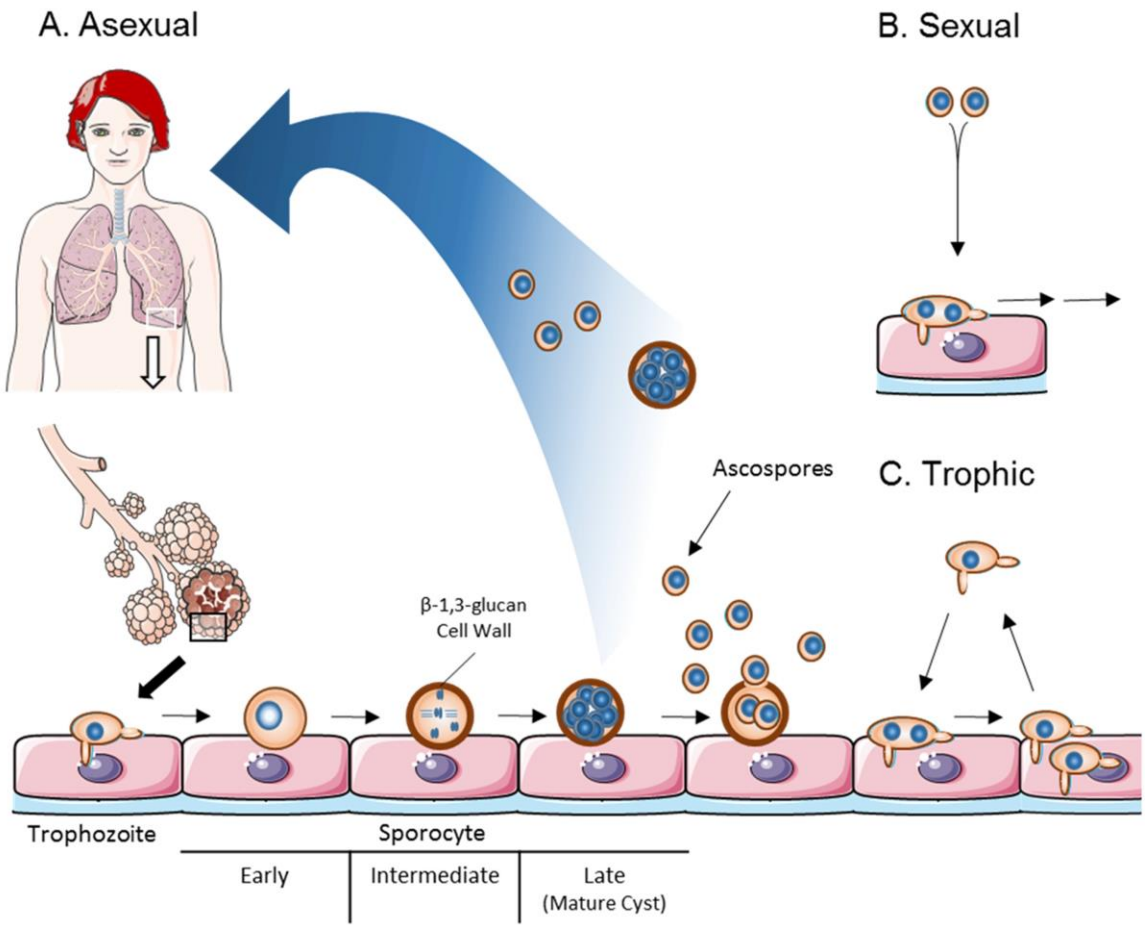


**Figure 2. *Pneumocystis* reproduction**

A. The asexual method of *Pneumocystis* reproduction begins with the ascospore attaching to the alveolar epithelium and growing into a trophozoite. The trophozoite then matures into a mature cyst through 3 sporocytic stages (early, intermediate, and late). The mature cyst releases up to 8 ascospores through a tiny pore in its membrane. B. Two ascospores or trophs are suspected to be able to fuse with each other to initiate a sexual method of reproduction. C. Trophs are also suspected to be able to replicate without progression through sporocytic stages. Servier Medical Art was used to generate this figure.

It is believed that *Pneumocystis* is also capable of sexual reproduction **(Figure 2B)**, a trait more commonly found in plant-pathogenic fungi [26]. The *Pneumocystis* genome project revealed many genes homologous to other Ascomycota that are involved in mating, meiosis, and

mitosis regulation, such as α-mating factor pheromone receptors and mitogen-activated protein kinases [11, 27, 28]. Although the *in vitro* limitations have made it difficult to confirm this hypothesis, modern tools including library screening, yeast complementation, and computer modeling have provided strong supporting evidence. Presence of diploid trophozoites is considered strong supporting evidence for this hypothesis, however, it is also believed that the trophozoite may also be able to replicate by an asexual binary fission **(Figure 2C)**. Furthermore, rodents treated with β-1,3-glucan synthase inhibitors (caspofungin) are effectively depleted of the cyst form, but are still burdened by the trophic form. This suggests that the trophozoite can replicate without transitioning through sporocytic stages. Interestingly, these animals also lose their capacity to transmit infection, further confirming that the ascus is the transmissible form [29]. There is still much to be learned about the *Pneumocystis* life-cycle, however, discovering a means to culture the organism will be crucial.

## 1.2 THE HOST

### 1.2.1 *Pneumocystis* Epidemiology

Populations with the highest risk for *Pneumocystis* pneumonia can be divided into two categories: Human Immunodeficiency Virus (HIV) positive, and HIV negative populations. The following section discusses the significance of each.

#### 1.2.1.1 HIV Associated *Pneumocystis* Pneumonia

*Pneumocystis* was originally considered a rare infection found in only malnourished and congenitally immunocompromised patients. There was a small increase in incidence with the start of solid organ transplantations, with 5-25% of transplant patients developing *Pneumocystis* pneumonia. However, rates nearly diminished after the introduction of chemoprophylaxis. It wasn't until 1981, when the Center for Disease Control revealed its first report of *Pneumocystis* pneumonia, among homosexual men and intravenous drug users in Los Angeles, that pneumocystosis shifted from a rare disease to a common pneumonia [30]. This marked the beginning of the HIV-AIDS epidemic, with *Pneumocystis jirovecii* pneumonia (PJP) becoming the AIDS-defining diagnosis in HIV infected patients. Patients with CD4+ cell counts less than 200 cells per microliter had an incidence rate as high as 20% per year, with a 75% risk of all HIV positive patients to develop PJP in their lifetime [31, 32].

In the developed world, PJP accounted for two thirds of AIDS-defining illnesses, thus in 1989 began the implementation of anti-*Pneumocystis* prophylaxis to all patients with CD4+ cell counts less 200 cells per microliter. The frequency PJP in AIDS patients reduced from 53% to 42% over the next three years, however, the total number of *Pneumocystis* cases remained unaffected due to the spread of HIV [30, 33]. Another major decrease occurred in late 1995 with start of combined Anti-Retroviral Therapy (cART), in which the yearly *Pneumocystis* infection rate had decrease by half. Unfortunately, this has had little to no effect on the mortality rate, which only shifter from 10.1% to 9.7% [34].

Even with the advent of anti-*Pneumocystis* prophylaxis and cART, *Pneumocystis jirovecii* still remains the most diagnosed AIDS-defining opportunistic infection in the United States [35]. In the past, studies have shown that most cases were of patients unaware of their

HIV status and/or were not receiving treatment, however, up to 40% of HIV positive patients diagnosed with PJP were in fact receiving prophylaxis. These patients may have acquired a drug resistant strain of *Pneumocystis* or were too immunocompromised for the prophylaxis to be efficacious [36].

In developing countries, where anti-*Pneumocystis* prophylaxis and cART availability are limited, HIV associated *Pneumocystis* pneumonia is still a major clinical complication. Studies have shown that over 30% of southern Africans presenting with diffuse pneumonia have tested positive for the presence of *Pneumocystis* in bronchoalveolar lavage fluid (BALF) [37, 38]. Many Southeast Asian countries have up to a 25% incidence of *Pneumocystis* infection in HIV-positive populations, while South American countries, such as Chile and Venezuela, report incidences as high as 37%.

#### 1.2.1.2 Non-HIV Associated *Pneumocystis* Pneumonia

At the turn of the century, *Pneumocystis* infection has reemerged in developed countries, primarily in HIV-negative populations. In Sweden, a 10-year study at Sahlgrenska University Hospital revealed that the numbers of *Pneumocystis* cases over the course of the study had not changed, and more surprisingly, 75% of the patients were HIV negative. Less than 20% of patients received prophylaxis prior to developing *Pneumocystis* suggesting that many at risk populations have not been identified [39]. Another study reported that, although the incidence of HIV-positive PJP had decreased, the total number of confirmed *Pneumocystis* cases had increased an average of 7% per year. The primary at risk populations were patients that had received a transplant, or had a hematologic malignancy [40]. A large number of conditions (and therapeutic agents) can be statistically correlated with *Pneumocystis* infection, briefly these include: hematological malignancies and solid tumors (alkylating agents), transplantation

**Table 1. Genes Associated with *Pneumocystis* Susceptibility**

| Loss-of-function Gene Mutation | Susceptibility to *Pneumocystis* | |
|---|---|---|
| | **Human** | **Murine** |
| **RAG1** | + | + |
| **RAG2** | + | + |
| **CD40-CD40L** | + | + |
| **PRKDC** | + | + |
| **IL-2Rγ** | + | + |
| **CD4** | + | + |
| **HLA/MHC class II** | + | + |
| **IKBKΓ** | + | N/I |
| **ICOS** | + | N/I |
| **BTK** | + | N/I |
| **STAT3 (polymorphism)*** | + | + |
| **IL-21R*** | + | + |

Human (+): Clinical diagnosis in patients with mutation.
Murine (+): Validated using experimental models.
N/I: Not yet investigated. *: To be described in Chapter 3.

(antimetabolite chemotherapeutics and azathioprine), autoimmune disorders (corticosteroids and TNF inhibitors), hyper-IgM syndrome, B-cell lymphomas and leukemia's (Rituximab and Alemtuzumab), and congenital immunodeficiency [41]. Some of these conditions and/or associated treatments affect non-CD4+ T-cell compartments, but these patients are remarkably susceptible to *Pneumocystis* infection. In addition, these cases typically have increased morbidity

and higher mortality rates than HIV-positive associated PJP cases [42, 43]. Many genetic mutations have been associated with *Pneumocystis* susceptibility, and interestingly, most of these targets have also been replicated experimentally using murine studies **(Table 1)**.

### 1.2.2 Clinical Features and Diagnosis

HIV positive and non-HIV associated *Pneumocystis* pneumonia have very different clinical presentations. HIV positive patients' symptoms typically present with a low-grade fever, progressive dyspnea (shortness of breath), and an unproductive cough. Immunocompromised HIV negative patients have substantially more acute symptoms such as severe dyspnea and high fevers. Urgent need for mechanical ventilation is not uncommon, and respiratory failure accounts for 40% of the mortality rate. Although the non-HIV populations typically have greater disease severity, the HIV-positive populations usually have higher fungal burden, as measured in BAL [44]. Disease severity closely correlates with neutrophil and inflammatory cell numbers [45].

These symptoms, especially in immunocompromised patients, should be the primary indicator for physicians to request further evaluation for *Pneumocystis* infection. In many cases, radiological findings such as bilateral pulmonary infiltrates may be seen on chest X-ray (CXR). However, *Pneumocystis* infection may present less common patterns such as lobar infiltrates, pneumothorax, pneumatoceles, or pulmonary nodules, or may even present with normal radiographs. These cases are typically followed up by high-resolution chest CT, which generally reveal bilateral ground-glass opacities [44]. Although symptomology and radiographic evidence may strongly suggest an underlying *Pneumocystis* infection, microscopic visualization is still the gold standard for diagnosis. Typically, organisms from bronchoalveolar lavage or induced sputum samples are stained with Gomori-methenamine silver (GMS) stain, however, other stains

such as Wright-Giemsa, Calcofluor white, and toluidine blue O can also be used to detect *Pneumocystis* organisms. Currently, fluorescently-labelled monoclonal antibodies appear to have the greatest sensitivity and specificity [46].

Unfortunately, visual examination may generate false-negative results, primarily in non-HIV patients who tend to have a lower infectious burden [47]. A few molecular methods have been adopted to help with the diagnosis of these patient populations. One of these was single round Polymerase Chain Reaction (PCR), which amplified the mitochondrial ribosomal RNA of *Pneumocystis*. To increase the sensitivity, nested-PCR (two round of PCR amplification) was incorporated on a variety of target genes, including rRNAs, major surface glycoproteins (MSG), dihydrofolate reductase (DHFR), and dihydropteroate synthase [48, 49]. However, these could not distinguish patients colonized with *Pneumocystis* versus patients with active *Pneumocystis* pneumonia [50].

To help distinguish colonization from active infection, techniques such as quantitative real-time PCR (RT-PCR) have been incorporated. This assay provides expedient, specific, highly sensitive, and most importantly quantifiable results that can be used to estimate fungal burden in patients. This has been demonstrated in several studies using a variety of genes including MSG, which has been shown to have a 100% specificity and 98.6% sensitivity in both HIV-positive and HIV-negative patients [51]. However, before RT-PCR can be fully implemented as a primary tool for diagnosing *Pneumocystis*, standardization of the assay to distinguish colonization and active human infection is still required. In the research community, using RT-PCR to quantify burden in infected animals has become common practice. The mitochondrial Large Subunit (LSU) ribosomal RNA is more broadly used to assess *Pneumocystis* burden. However, our lab had determined that primers and probes against the

mitochondrial Small Subunit (SSU) ribosomal RNA had less background genomic amplification **(Figure 3)**. In addition, RNA sequencing of trophozoite enriched organism has allowed us to identify troph and cyst specific genes, arp1 and sp, respectively (unpublished).

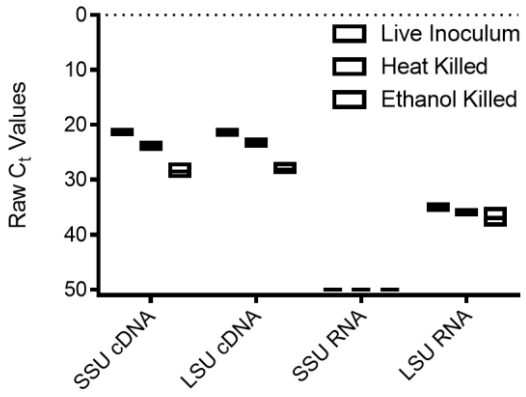


**Figure 3. *P. murina* quantification mitochondrial LSU vs SSU rRNA**

Live *Pneumocystis* inoculum was either washed with 70% ethanol (right boxplot), heat killed at 95ºC for 15 minutes (center boxplot), or left untreated (left boxplot). Samples were reverse transcribed (labeled cDNA) or underwent no RT reactions (labeled RNA). Then amplified by Large Subunit (LSU) or Small Subunit (SSU) primer/probe combinations. The SSU primer/probe set had the least background in the no RT control samples.

As described in 1.1.3, the *Pneumocystis* ascus cell wall is composed of β-1,3-glucans, and can be detected in serum during active infection. Diagnosing *Pneumocystis* infection with serum β-1,3-glucans levels above 100pg/mL had a sensitivity and specificity of 100% and 96.4%, respectively [52]. However, β-1,3-glucans are also present on other fungal species, thus as a marker, it is unable to discriminate *Pneumocystis* from other fungal pathogens. Another serum marker *Pneumocystis* pneumonia is KL-6, a surface glycoprotein. Although KL-6 is a more specific marker, studies have only confirmed elevated serum KL-6 levels in HIV-positive cases.

### 1.2.3 Treatment and Prophylaxis

The recommended first-line therapy for mild to severe *Pneumocystis* pneumonia is trimethoprim-sulfamethoxazole (TMP-SMX). The standard dose is given by separate administrations of 15-20 mg/kg/day of TMP and 75-100mg/kg/day SMX orally, however, intravenous (IV) administration may be used for severe cases. SMX requires extensive hepatic metabolism followed by renal excretion, thus doses are typically adjusted for patients with liver and kidney failure. It is standard to measure drug levels at least once after administration to insure adequate dosing and to avoid toxicities. TMP-SMX have adverse side-effects such as rash, vomiting, diarrhea, and cytopenia, and is not recommended for patients with sulfa allergies [53-55]. Aerosolized pentamidine was an alternative option for treatment, however, it was associated with disease dissemination, and is currently a last resort medication. Intravenous pentamidine has better success at controlling infection, however it also has more severe side effects such as hypotension and pancreatitis. More recently, combination drugs (e.g. primaquine and clindamycin) have been effective treatments, with higher tolerance than IV pentamidine [44]. Echinocandins inhibit β-1,3-glucan synthesis, which affect the development of the ascus cell wall. Rodents treated with echinocandins have reduced asci, but are still burdened by the trophic form. Caspofungin, an echinocandin, has been shown to have a therapeutic effect when administered with a low-dose of TMP-SMX. This was particularly effective with renal transplant patients that cannot handle the typical dose of TMP-SMX [56]. Patients treated with echinocandins should be monitored for *Pneumocystis* burden by quantitative PCR, because the disruption of the cell wall may render false-negatives by visual GMS staining [29].

A typical regimen for treating *Pneumocystis* pneumonia lasts for approximately 3 weeks, however, if disease is still progressing past the first week of treatment, then drug-resistance

should be suspected. Drug resistance is associated with *Pneumocystis* gene mutations, such as dihydropteroate synthase gene (DPHS) [57, 58]. Prophylaxis administration depends on the particular condition inducing immunosuppression, thus should be individualized. HIV-positive patients maintain treatment for as long as their CD4 counts are below 200 cell per microliter. Similarly, HIV-negative patients categorized for at risk of *Pneumocystis* infection are treated for as long as the immunosuppressive agents are in effect. This becomes complicated for HIV-negative patients who may remain immunosuppressed months after completion of a cytotoxic regimen such as cyclophosphamide. Thus patients should be monitored for at least 6 months post immunosuppression.

### 1.2.4 Immune Reconstitution Inflammatory Syndrome

Immune reconstitution inflammatory syndrome (IRIS) is a pathological immune response to an opportunistic infection that occurs during the recovery from an immunosuppressive condition or agent. This syndrome was originally characterized in HIV/AIDS patients that have a positive response to cART, followed by an inflammatory condition. Approximately 16% of HIV-positive patients on cART develop IRIS, and typically present with fever, dyspnea, and may develop respiratory failure. Combination antiretroviral therapy would deplete HIV, repopulate CD4+ T-cells, and restore the host's adaptive immunity. Infections developed during immunosuppression become unmasked, and the immune system initiates an exaggerated immune response that can cause serious damage to the host. There is a second form of IRIS, referred to as paradoxical IRIS, which occurs despite the absence of a serious infection. In cases where patients may have had treatment for an acquired infection, however, residual antigens from the infection linger and trigger the exaggerated response [59-61].

*Mycobacterium* and *Cryptococcus* are the infections most commonly associated with IRIS, however, *Pneumocystis* accounts for up to 4% of cases. It is important to note that an accurate measure of IRIS incidence is difficult due to the lack of a consensus of diagnostic criteria, and variability in the time of onset post cART, spanning from 2 months up to a year [59, 62, 63]. The direct relationship between severity of immunosuppression (i.e. low CD4 counts, high viral load) and the risk for development of *Pneumocystis*-associated IRIS can be concluded. Interestingly, studies have also suggested that early treatment with cART also increases risk of IRIS, in contrast, delayed treatment with cART increases *Pneumocystis* related mortality [64, 65].

Treating the underlying infection with TMP-SMX is the primary approach to help manage the severity of IRIS. If possible, recognizing the immunosuppressive cause of infection and complementing the immune system is considered most efficient in treating IRIS. In HIV-positive cases that may develop life-threatening IRIS due to large *Pneumocystis* burden, treatment of the inflammatory environment with glucocorticoids may become necessary [66-68]. Treatment with glucocorticoids reduced risk of respiratory failure and death in a controlled trial of 327 HIV patients [69]. Other anti-inflammatory medications are also being investigated to help control the rapid progression of respiratory failure, such as PDMP, a glycosphingolipid synthesis inhibitor, and Muromonab, an anti-CD3 T-cell depleting antibody [70, 71].

## 1.3 THE IMMUNE RESPONSE

### 1.3.1 Pulmonary Immunity and Disease

The respiratory system is responsible driving oxidative metabolism through the exchange of carbon dioxide for oxygen. To efficiently do so, the trachea, bronchi, bronchioles, and alveoli form a tree-like organization in the lungs which provides a very large surface area (approx. 10 $m^2$ in healthy human adults) that can filter around 9,000 liters of air, daily [72]. This process is coupled by continuous bombardment with particulates, allergens, and microbes, which represents one of the largest immunological challenges for the host. The front line of defense is the epithelial barrier of the alveolar spaces which is lined by type-I and type-II epithelial cells. This innate host defense is managed by production of a mucus barrier, tight-junctions between cells, and anti-microbial peptides which all aid in ciliary clearance [73, 74]. Secretory cells such as goblet cells have relatively low numbers and minimal activity in normal airways but will increase during injury and infection.

Mucins, large glycoproteins complexed with abundant O-linked polysaccharides, help create the mucus barrier which acts as a mucociliary escalator for the transport of pathogens out from the conducting airways. Mucins that are secreted, such as Muc5AC and Muc5B, can bind pathogens directly to prevent aggregation and binding to the epithelial surface. However, hyper production of mucus is characteristic of airway diseases, such as cystic fibrosis (CF), chronic obstructive pulmonary disease (COPD), and asthma. Mucus production is directly linked to Toll-like receptor (TLR) signaling through IRF and NF-κB families and cytokine signaling via the Jak-Stat pathway [75, 76]. These TLR signals also lead to the successive production of anti-microbial peptides, such as defensins, cathelicidin, surfactant proteins, and lysozyme, in addition

to chemokines and cytokines which recruit and activate innate and adaptive immune cells. The role epithelial cell-mediated immunity in the context of *Pneumocystis* infection has been largely understudied.

### 1.3.2 Lung-Resident Dendritic Cells and Macrophages

In order to form the appropriate and effective response to an infection, the lungs are monitored by an intricate network of sentinels known as dendritic cells (DCs). DCs can fall under a number of categories based on their origin and function, these include conventional (cDC), plasmacytoid (pDC), and monocyte-derived (moDC). In the lung, cDCs and moDCs can be identified by having high CD11c and MHC class II. cDCs can be further be distinguished by expression of CD103 or CD11b, in absence of the Fc receptor CD64. pDCs have intermediate CD11c and uniquely express high levels PDCA-1 and B-cell associated marker, B220. These subsets have their own distinct and overlapping functions, and are generally crucial for initiating immunity in response to a pathogen. DCs are typically located on the basolateral side of the alveolar epithelium, and project across the epithelial layer to sample antigens in the lumen [77-79].

Upon acquiring an immunogenic antigen, DCs migrate to the draining lymph nodes to induce T-cell and B-cell responses. This is performed through antigen presentation and costimulation through major histocompatibility complexes (MHCs). The two MHCs, MHC class I and MHC class II, function similarly in presenting peptides on the surface of the DCs, but present specifically to either CD8+ or CD4+ T-cells, respectively. Typically, MHC class I molecules acquire their processed antigen from intracellular sources, thus they are the primary mechanism to mount immune responses against viruses, intracellular bacteria, and abnormal/mutant cellular proteins. Alternatively, MHC class II acquires antigens exogenously

thus mounting responses against extracellular pathogens and allergens. However, MHC class I can sometimes acquire exogenous antigens through a process termed cross-presentation, while MHC class II molecules can present cytosolic proteins degraded through autophagy [80]. For both MHC classes, antigen to peptide-bound MHCs can be broken down into six general steps: 1) acquisition of antigenic protein or peptides, 2) ubiquitination of the antigen which directs them to 3) a degradation process into smaller peptides by proteasomes, 4) transport of peptides into the endoplasmic reticulum or endolysosomal compartments where they 5) bind MHC class I or MHC class II molecules, respectively, and 6) are finally transported to the cell surface to interact with T-cells.

MHC class I molecules are ubiquitously expressed on all nucleated cells, unlike MHC class II molecules which are only expressed on "professional" antigen present cells (APCs) i.e. macrophages, B-cells, and DCs [81]. In addition to antigen presentation, professional APCs also provide costimulation to T-cells by engaging two classes of molecules on T-cells. The first class of costimulatory molecules includes CD28 and inducible T-cell costimulatory (Icos), which reduces the threshold for quantity and duration of MHC contact with T-cells required for activation. The second class which includes TNF receptor family member: CD40, OX-40, and CD27 provide further costimulation, and is believed to be regulated by class I costimulatory signals.

There is some debate on what roles the different subsets of DCs. Conflicting evidence suggest that they may contribute to T-cell lineage and differentiation, while other data suggests that each may initiate either an acute or central memory response [82-85]. Briefly, CD11b+ cDCs are suspected to have a Th2 or Th17 bias when stimulated with an allergic or fungal antigen, respectively, while CD103+ cDCs bias towards Th1 or Th2. In the context of influenza,

CD103+ cDCs have been shown to have the ability to present antigens derived from apoptotic cells, and have enhanced MHC class I presentation compared to CD11b+ cDCs. Furthermore, CD103+ cDCs preferentially induce effector CD8+ T-cell responses while CD11b+ cDCs induce memory CD8+ T-cell responses. CD8α+ pDCs on the other hand have been shown to have regulatory role against harmless allergens, which may be mediated by the expression of Fas (CD95), which induces T-cell apoptosis. Conversely, CD8α- pDCs have been shown to mediate hyper-responsiveness. CD103+ cDCs have also been shown to play a role in tolerance through mediation of regulatory T-cell differentiation. DC subtype and function studies are still a relevant topic of research, with many unanswered questions currently under investigation [82-85].

Dendritic cells play an important role during *Pneumocystis* infection. Patients with dendritic cell deficiencies develop a primary immunodeficiency and may develop *Pneumocystis* pneumonia [86]. The *Pneumocystis* cell wall component, β-glucan, can directly induce dendritic cells to express costimulatory molecules such as B7-1/B7-2 and CD40 ligand (CD40L) [87]. CD4-depleted mice that receive antigen-pulsed bone marrow-derived (BM-) DCs are partially protected for *P. murina* infection. However, *Pneumocystis* is unique in the sense that DCs alone are not sufficient to induce a protective T-cell response, and that during natural infection B-cells play a critical role in antigen presentation and priming of CD4+ T-cells [88, 89]. It's still not well understood, why B-cells specifically are required to fully prime CD4+ T-cells or why DCs alone are not sufficient.

Macrophages also play a major role in lung immunity and can be divided into at least three different categories based on their localization. These include alveolar macrophages (AM) located in the luminal space of the alveoli, interstitial macrophages (IM) located in the parenchymal space between two adjacent alveoli, and bronchial macrophages located within the

**Table 2. Dendritic cell and macrophage surface marker expression**

| Surface Marker | Macrophages | | Dendritic Cells | | | |
|---|---|---|---|---|---|---|
| | Alveolar | Interstitial | Conventional | | Monocyte-derived | Plasmacytoid |
| | | | CD103+ | CD11b+ | | |
| **CD103** | + | + | +++ | + | - | - |
| **CD11b** | + | + | + | +++ | +++ | + |
| **CD11c** | +++ | + | +++ | +++ | +++ | + |
| **CD207** | - | unclear | + | - | - | - |
| **CD24** | + | + | +++ | ++ | + | + |
| **CD64** | + | - | - | - | + | - |
| **CLEC9A** | - | - | +++ | - | - | - |
| **F4/80** | +++ | ++ | + | ++ | +++ | + |
| **Ly6C** | + | + | - | - | + | + |
| **MerTK** | ++ | - | - | + | ++ | - |
| **MHC class II** | + | +++ | +++ | +++ | +++ | + |
| **PDCA-1** | + | - | - | - | - | +++ |
| **Siglec F** | +++ | - | - | - | - | - |
| **Siglec H** | - | - | - | - | - | +++ |
| **SIRPα** | + | + | - | + | + | - |

Expression levels indicated from high (+++) to low (+) and absent (-).

branches of the bronchi and bronchioles. In steady state, AMs comprise greater than 90% of the cellular compartment in alveolar spaces. However, with their low number, only a single AM can be detected for approximately every three alveoli. To fully monitor the alveolar spaces, AM

travel between alveoli through the connecting pores of Kohn [74, 90, 91]. AMs can be distinguished from IMs through their unique expression of Siglec-F. For complete description of markers defining macrophage and dendritic cell subsets refer to **(Table 2)** [74, 77, 82, 92-101].

Interstitial macrophages are believed to function as antigen presenting cells to interstitial lymphocytes, but there is evidence that they play an important role in tolerance by promoting T regulatory cell responses. AMs can also modulate immune responses by blocking DC-mediated T-cell activation and producing transforming growth factor-beta (TGF-β) in conjunction with retinol precursors. This process is dependent on antigen presentation by AMs, and occurs specifically in the lung. Stimulation of pattern recognition receptors such as TLR-4 can initiate the switch to an inflammatory response by the induction of IL-1, IL-6, and tumor necrosis factor (TNF) [102]. Numerous reports and publications have confirmed the importance of AMs in the host response to viral, bacterial, and fungal infections. AMs have been demonstrated to be able to phagocytose a variety of pathogens including *Streptococcus, Mycobacterium, Pseudomonas,* and *Pneumocystis*.

AMs are currently believed to be the major player for clearance of *Pneumocystis* infection through phagocytosis of both the trophic **(Figure 4)** and cystic forms. AMs express Dectin-1, which allows them to recognize the β-1,3-glucan rich cell wall on the ascus. Dectin-1 deficient mice are more susceptible to *Pneumocystis* infection than wild-type mice, while mice treated with recombinant Dectin-1-FC protein have reduced burden [103-106]. Macrophages are generally categorized as classically activated (M1) or alternatively activate (M2). Type-1 cytokines such as IFN-γ are believed to promote the M1 phenotype while type-2 cytokines such as IL-4, IL-13, and IL-33 promote an M2 phenotype. They differ in the both their cytokine profiles and mode for bactericidal/fungicidal activity; M1 macrophages function through nitric

oxide synthase while M2 macrophages use arginase. Clearance of *P. murina* appears to be driven by alternatively activate macrophages, and data from this thesis corroborate those finding [107, 108].

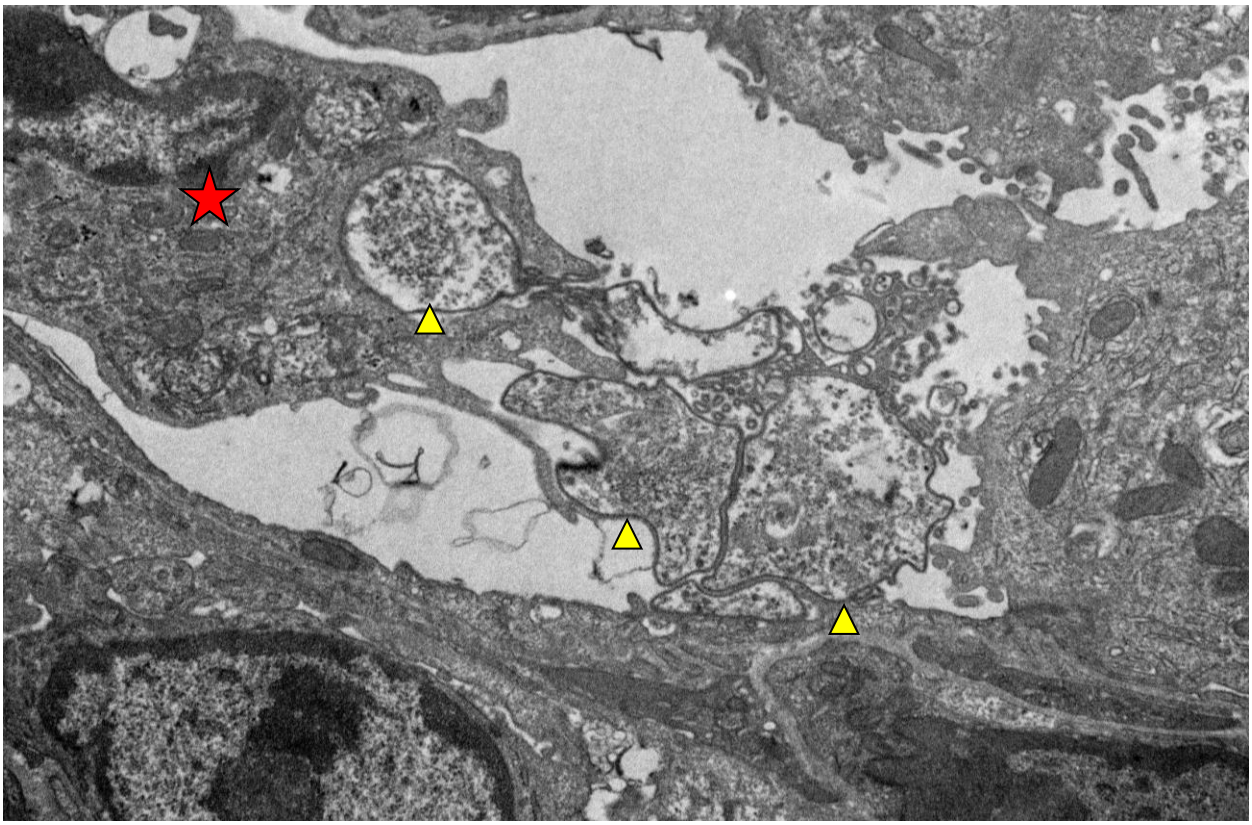

**Figure 4. Macrophage phagocytosis of *Pneumocystis***

Transmission Electron Microscopy (TEM) of an alveolar macrophage (red star) in the process of phagocytosis of a *Pneumocystis* trophozoites (yellow arrows).

### 1.3.3 T-Cell Mediated Immunity in the Lung

*Pneumocystis* is an organism that requires an intact adaptive immune system involving both humoral and cellular responses to mediate clearance. Many cell types and immunological factors have been implicated in the protective and/or the pathological responses to infection, including T-cells, B-cells, macrophages, dendritic cells, eosinophils, neutrophils, and the cytokine and

chemokine signals that coordinate their specific roles. T helper cells, CD4+ T-cells, are the most associated with immunity to *Pneumocystis* infection. As previously mentioned, reduction in frequency below 200 cells per microliter blood is the threshold for risk. This correlation has been validated in numerous animal models from mouse to macaque, by means of CD4-depletion and genetic knockout studies. Upon infection, antigen presenting cells (APCs), typically DCs, bridge adaptive and innate immunity by migrating from the lung to the draining lymph nodes where they present the antigen to naïve T-cells. Based on the DC's MHC class restriction, CD4+ or CD8+ T-cells are activated and primed to perform specific immunological functions. Migration to the lymph node is not critical to prime the immune response as demonstrated by Lymphotoxin-α-/- and Ccr7-/- mice which are deficient in lymph node formation and DC migration to lymph nodes, respectively [109, 110].

Activated CD4+ T-cells can be subdivided based on transcriptional regulation and effector cytokines, these classically include: T helper 1 (Th1), T helper 2 (Th2), and T helper 17 (Th17). Each of these subsets have unique differentiation signals, transcriptional regulation and effector cytokines **(Table 3)**. Th1 cells are classified by their production of interferon-gamma (IFNγ), and differentiate in the presence of IL-12p40. Th1 cells are transcriptionally controlled by T-box transcription factor (T-BET) and signal transducer activator of transcription-4 (STAT4), and are generally induced in response to intracellular pathogens such as viruses and *Mycobacterium* [111-116]. IFNγ can stimulate macrophages to induce nitric oxide synthesis and generate reactive oxygen species (ROS), which in part mediate clearance of pathogens. IFNγ can also act as an inhibitor to other T-cell lineage development and reduce superfluous pathological responses. Th2 cells are classified and differentiated by the primary cytokine they produce, IL-4. Transcriptionally regulated by GATA3 and STAT6, and are typically induced in response to

extracellular parasites such as helminths and house-dust-mites (HDMs). IL-4 not only acts as an autocrine for Th2 differentiation but also inhibits Th1 and Th17 differentiation, and promotes B cell maturation into plasma cells. Th2 cells also produce IL-13 which works which has many

**Table 3. CD4+ T-cell Subtypes**

| T helper cell subset | Transcriptional Regulation | Differentiation Signals | | Effector Cytokine(s) |
|---|---|---|---|---|
| | | Activation | Inhibition | |
| T helper 1 | Tbx21<br>Stat1 • Stat4 | IL12 • IFNγ | IL4 | IFNγ |
| T helper 2 | Gata3<br>Stat5 • Stat6 | IL33 • IL4 | IFNγ, TGFβ | IL4 • IL5<br>IL6 • IL13 |
| T helper 17 | Rorc • Rorα<br>Stat3 | IL6 • IL1β<br>TGFβ • IL21 | IFNγ • IL4 | IL17 (a/f)<br>IL22 |
| T follicular helper | Bcl6<br>Stat3 | IL6 • IL21<br>CXCL13 | N/A | IFNγ • IL4<br>IL17 (a/f) • IL21 |
| T regulatory | Foxp3<br>Stat5 | IL2 • TGFβ | IL21 • IL23 | IL10 • TGFβ |

overlapping functions as IL-4, but is critical for the induction of airway hyper-responsiveness, goblet cell metaplasia, and mucus hypersecretion. IL-5 is also involved in important Th2 functions by mediating eosinopoiesis and function. Eosinophils, as well as mast cells, basophils, and macrophages can produce copious amounts of IL-4 and IL-13 further enhancing the Th2 responses. However, an overreaction of Th2 signals can cause pathological conditions such as asthma and allergy. Epithelial-derived cytokines, such as thymic stromal lymphopoietin (TSLP), IL-25 (IL-17E), and IL-33, are also believe to play in important role in Th2 protective and pathological responses.

Th17 cells, cleverly named, are classified by their signature cytokine, IL-17. Transcriptionally regulated by RAR-related orphan receptor-C (RORc) and STAT3, Th17 cells

differentiate in the absence of Th1 and Th2 cytokines and presence of IL-1, IL-6, IL21, IL-23, and TGF-β. IL-17 has an important role in immunity against extracellular microbes such as gram-negative bacteria and fungi. IL-17 receptor signaling is also important for G-CSF production, granulopoiesis, and neutrophil recruitment in response to bacterial infection. Th17 cells also produce IL-22, which has also been shown to play important role on epithelial responses and recovery, during and post-infection.

Another class of T helper cells are regulator T cells (Treg), which can dampen the immune response through the production of IL-10. Tregs can be derived thymically and are referred to as natural (nTregs), but they can also be induced (iTregs) under the stimulation of TGFβ, retinoic acid, and high levels of IL-2. They have a transcription upregulation of forkhead box P3 (FOXP3) and STAT5 transcription factors. Defects in Treg function can lead to development of autoimmune disorders such as IPEX (immunodysregulation, polyendocrinopathy, enteropathy, X-linked syndrome), while certain cancers and pathogens may stimulate Tregs to evade the immune response [117, 118]. Tregs play a crucial role in lung immunity in order to ensure maintenance respiratory function during immunological responses to allergens and pathogens. Another, somewhat controversial, subset of T helper cells is the T follicular helper cell (Tfh), named after its localization to germinal centers. Expression of Cxcr5 on CD4+ T-cells draws them toward Cxcl13 expressing germinal centers which are composed of T-cells, B-cells, macrophages, and dendritic cells. Tfh cells help with B-cell activation and class-switched antibody production, primarily through the production of IL-21. However, Tfh cells have also been characterized to mimic Th1, Th2, and Th17 responses. Whether Tfh cells are a unique lineage or a phenotypic state of Th1, Th2, and Th17 cells is still under debate [119].

In the context of *Pneumocystis* infection, it is still unknown which T helper cell subset and effector function mediates protection. Various studies have shown recruitment of all three T helper cell subsets during *Pneumocystis* infection in various models [120]. Macaques infected with simian HIV (SHIV) upregulated Th2 cytokines upon *Pneumocystis* colonization [121]. Some studies have shown worsened *Pneumocystis* pneumonia in IFNγ-deficient mice, while other studies have shown neutralization of IL-17 and IL-23 leads to worsened infection [122]. In many of these studies, mice merely display transient or delayed clearance, so there is speculation whether *Pneumocystis* is a true opportunist that can be clear with any individual subset, or perhaps a unique unidentified subset is involved.

On the other hand, CD8+ T-cells have a more questionable role during infection. Also referred to as cytotoxic T-cells, from their release of cytotoxic molecules such as granzyme and perforin, CD8+ T-cells are key producers of IL-2, IFNγ, and TNF-α. Although, CD8+ T-cells do accumulate in the long run during *Pneumocystis* infection, however, CD8+ T-cell deficiency does not lead to susceptibility [123]. Several other studies have shown that CD8+ T-cells influx in the long does not impact severity of disease [124-126]. However, few studies have shown that CD8+ T-cells may have a protective role, such as depletion of CD8+ T-cells in addition to CD4-depletion exacerbates burden. Also, IFNγ treatment showed enhanced protection that was conferred by type 1 cytotoxic CD8+ T-cells through macrophage-mediated clearance [127, 128]. Although γδ T-cells are not implicated in clearance, some research suggest that they may play a role in managing the inflammatory pathology [129].

## STATEMENT OF PURPOSE

*Pneumocystis* is an opportunistic fungal pathogen that is considered a global health issue to HIV-positive and non-HIV immunocompromised populations. It has been shown that prophylaxis of at risk patients can reduce the incidence of infection, severity of disease, and mortality rate in immunocompromised patients. However, TMP/SMX, the primary prophylactic drug, is relatively toxic, and only prescribed to defined at risk populations. Anti-CD20 monoclonal antibodies were originally used in treatment of chemotherapy-resistant B-cell non-Hodgkin lymphomas, but since then it's also used therapeutically against hematological malignancies, autoimmune diseases, and post-transplant lymphoproliferative disease. Studies have shown that up to 30% of patients receiving Rituximab develop *Pneumocystis* pneumonia, however, there is debate as to the precise role anti-CD20 has in conferring risk. Many of these patients are also on concomitant immunosuppressive drugs, thus complicating any analyses of clinical studies. The first aim of this dissertation is to demonstrate that anti-CD20 therapy induces susceptibility to *Pneumocystis* infection, and that patients receiving this treatment should be categorized as an at-risk population.

The predominant factor required for immunity against *Pneumocystis* infection is the presence of CD4+ T-cells. This has been validated several times over by clinical data and experimental animal models. Early on, studies have examined the role of T helper 1 (Th1), T helper 2 (Th2), and T helper 17 (Th17). To briefly summarize these studies, Th1, Th2, and Th17

cells can all be detected in the lung during infection, however, removal of their classically defined effector molecules, at most, only delayed clearance. Our goal in the second part of this study is to dissect the exact CD4+ T-cell signals that are required initiate a protective immune response, and identify the factors that mediate clearance. Understanding the exact immunological response will aid in the development of safer and more effective prophylaxis and treatments against *Pneumocystis* infection.

# 2.0 CHAPTER TWO: ANTI-CD20 THERAPY AND SUSCEPTIBILITY TO *PNEUMOCYSTIS* PNEUMONIA

Work described in this section was partly published in the Infection and Immunity (Infect Immun. 2015 May; 83(5): 2043-52. doi: 10. 1128/IAI.03099-14) by authors Waleed A Elsegeiny, Taylor Eddens, Kong Chen, and Jay K Kolls

## 2.1 INTRODUCTION

### 2.1.1 Anti-CD20 Therapy

CD20 is a B-lymphocyte antigen encoded by a membrane-spanning 4A family member, MS4A1. There is no known ligand for CD20; however it is believed to play a role in B-cell development and differentiation into plasma cells and T-cell independent antibody responses [130]. In 1997, anti-CD20 monoclonal antibodies were shown to be efficacious in treatment of chemotherapy-resistant B-cell non-Hodgkin lymphomas [131, 132]. Since then the use of anti-CD20 has been used therapeutically against a broad range of conditions, including hematological malignancies such as lymphatic leukemia, autoimmune diseases such as rheumatoid arthritis, and post-transplant lymphoproliferative disease. With the increased use of anti-CD20 as treatment over the years, there have been a number of reports of patients who have received anti-CD20 therapy that have subsequently developed a potential fatal pneumonia by *Pneumocystis jirovecii* [133]. In a study, Martin-Garrido found that *Pneumocystis* pneumonia developed in approximately 30% of patients receiving Rituximab (human anti-CD20 antibody), with a mortality rate as high as 30% [134]. However, there is debate as to the precise role anti-CD20 has in conferring risk to *Pneumocystis* infection as many of these patients are also on concomitant immunosuppressive drugs, thus complicating any analyses of clinical studies [134-136]

### 2.1.2 B-cells and *Pneumocystis* Infection

The importance of B-cells was first observed when it was demonstrated that B-cell deficient mice (μMT-/-) were susceptible to *Pneumocystis* infection. At the time, this effect was suggested to be due to the lack of serum immunoglobulins, however, mice deficient in Fcγ receptor can clear infection [137]. Subsequent studies demonstrated that B-cells play a larger role than just antibody generation, as Lund *et al*. showed that B-cells were required for priming of CD4+ T-cells and generating protective effector and memory CD4+ T-cells in response to *Pneumocystis* infection in mice [88]. This was demonstrated in both μMT-/- mice and MHC class II/μMT chimeras. Briefly, irradiated μMT mice received a 3:1 ratio of μMT:WT, μMT:MHCII-/-, or μMT:μMT bone marrow which forms a largely WT hematopoietic compartment with wild-type B-cells, MHC class II knockout B-cells, or B-cell deficient, respectively [88, 89]. They demonstrated that mice with MHC class II deficient B-cells were susceptible to infection, and this was attributed to a CD4 intrinsic defect. This suggests that depletion of CD20+ B-cells would also lead to CD4+ T-cell dysfunction and susceptibility to *Pneumocystis* infection. To experimentally test this hypothesis, we administered a murine anti-CD20 depleting antibody (5D2) followed by subsequent infection with *P. murina.* We found that administration of anti-CD20 conferred susceptibility to primary *Pneumocystis* infection.

### 2.1.3 Anti-CD20 Therapy and Immune Reconstitution Inflammatory Syndrome

It has been reported that some patients receiving an anti-CD20 containing treatment regimens for lymphoma developed immune reconstitution inflammatory syndrome (IRIS) after receiving the last regimen of treatment [138]. Thus we next investigated the effects of CD20 depletion on the

development of IRIS in our murine model. We concluded that although the pathology/lung injury associated with CD4+ T-cell reconstitution was not influenced by the presence or absence of B-cells, the ability of the CD4+ T-cells to mount a protective immune response against *Pneumocystis murina* was in fact dependent on CD20+ B-cells. CD20 depletion does not affect the recruitment of CD4 cells to the lung, but infected lungs have a reduced type II immune responses. This study sheds some light on how anti-CD20 treatment in patients may affect their ability to mount a defense against *Pneumocystis*, and it may be critical to monitor these patients for *Pneumocystis jirovecii*.

## 2.2 MATERIALS AND METHODS

### 2.2.1 Mice

Six- to Eight- week-old wild-type C57BL/6J (WT), immunodeficient B6.129S7-Rag1tm1Mom/J (Rag1-/-), and B6.CB17-Prkdcscid/SzJ (SCID) mice were obtained from The Jackson Laboratory (Bar Harbor, ME). Immunodeficient B10:B6-Rag2tm1FwaIl2rgtm1Wjl (Rag2-/-Il2rγ-/-) were originally obtained from Taconic (Hudson, NY) then bred and maintained at the University of Pittsburgh Division of Laboratory Animal Resources (DLAR) Facility at Rangos Research Building of Children's Hospital of Pittsburgh of UPMC. Animals were housed in a pathogen-free environment and given food and water by the DLAR ad libitum. All experiments were approved by the University of Pittsburgh Institutional Animal Care and Use Committee.

### 2.2.2 *Pneumocystis* Isolation, Inoculum and Antigen Preparation

*Pneumocystis murina* organisms were administered by oral-pharyngeal delivery into $Rag2^{-/-}$ $IL2r\gamma^{-/-}$ mice, propagated for 10-12 weeks *in vivo*, and isolated from mouse lung tissue, as previously described [139]. Briefly, $Rag2^{-/-}IL2r\gamma^{-/-}$ with *Pneumocystis* pneumonia were sacrificed, and the lungs were aseptically harvested and frozen in 1ml of sterile Dulbecco's phosphate buffered saline (PBS) at $^{-}$80°C. Too process the inoculum, frozen lungs were thawed and strained through a 70μm filter and pelleted by centrifugation (800xg, 10min, and 4°C). The pellet was resuspended in 1ml of PBS. A 5μl aliquot was diluted 1:10 and heat-fixed on a slide, and stain with Hema-3 modified Wright-Giemsa stain (Fisher Scientific Pittsburgh, PA) followed by asci counting. *Pneumocystis murina* asci were quantified microscopically, and the inoculum is adjusted to $2x10^6$ asci per ml. Mice are administered 100μl ($2x10^5$ asci) of the inoculum by oral pharyngeal aspiration as previously described [140]. *Pneumocystis* protein antigen was prepared by differential centrifugation of the inoculum as previously described, followed by sonication of 1mg of inoculum per ml for 5 minutes [120].

### 2.2.3 Whole Lung Cell Preparation and Antigen Stimulation

Mice were infected with an inoculum of *P. murina* for 2 weeks. At the time of euthanasia, mice were anesthetized by intraperitoneal injection of ketamine/xylazine cocktail and euthanized by exsanguination. Immediately after mice were perfused vascularly by 5ml of heparinized PBS injection into the right ventricle. The right superior and inferior lobes are then harvested, minced with razorblades, and digested in 5ml serum-free media with 2mg/ml collagenase for 90 minutes

in a 37°C shaking incubator. Cell suspension is then strained through a 70μm filter, then washed and resuspended in complete DMEM media. Red blood cells were then lysed with ammonium chloride solution, washed, resuspended in 5mls, and counted. $10^6$ cells per well are plated on a 96-well round bottom plate in complete DMEM media with 1μg/ml PC antigen and 20U/ml IL-2. An aliquot from each group is taken for cell analysis by flow cytometry. Plated cells are stimulated at 37°C at 5% CO2 for 72 hours. Finally, supernatants are harvested for multiplex (Millipore) cytokine analysis on a Bioplex reader (Bio-Rad).

### 2.2.4 Flow Cytometric Analysis

$10^6$ single cells from mouse lung were stimulated with 50ng/ml PMA (Sigma) and 750ng/ml ionomycin (Sigma) for 5-6 hours. After 1 hour from the start of stimulation cell were given 1μl/mL GolgiStop (BD Pharmingen, San Diego, CA) to block cytokine secretion. Cells were surface stained with TCRβ (PerCP-Cy5.5), CD4 (E450), CD8 (PE-Cy7), and B220 (APC-Cy7) for 15-30 minutes in PBS supplemented with 1% BSA. Cells were then fixed in 1% Formalin, and acquired for flow cytometry by an LSR-II (BD Biosciences, San Jose, CA) and data was analyzed using FlowJo (Treestar).

### 2.2.5 RNA Isolation and *Pneumocystis* Quantification by RT-PCR

The right middle lobe of the lung is harvest in 1ml of Trizol and homogenized. RNA is purified and quantified has previously described [139]. Briefly, cDNA was synthesized from 1μg whole

lung RNA via iScript reverse transcription reagents (Bio-Rad, Hercules, CA), and real-time PCR was performed using primers and probes for *Pneumocystis murina* large-subunit rRNA (LSU) transcript with SsoFast/SsoAdvanced Probes Supermix (Bio-Rad). The threshold cycle values were converted to copy number using a premade standard of known *Pneumocystis* LSU rRNA, as previously described [141].

### 2.2.6 Serum Collection and *Pneumocystis murina* Antigen ELISA

Blood was collected either periodically by tail-bleed and/or at time of sacrifice by syringe from the vena cava. Coagulated blood was then centrifuged for 10 minutes at 10,000xg. The serum supernatant was collected and stored at -80°C. Maxisorb plates are coated with 1µg *P. murina* antigen in 100µl bicarbonate coating buffer per well overnight at 4°C. Plates were blocked with 5% blotting grade blocker (Bio-Rad) and 1% BSA. Plates were first primary stained with sample serum in a dilution series from 26 to 213 overnight at 4°C, then secondary stained with murine Ig-specific-HRP antibodies. Plates were then developed with TMB substrate for 5-30 minutes depending on control serum, and reaction stopped with equal volume 2N H2SO4. OD450 is read using Synergy H1 Hybrid Reader (BioTek Winooski, VT).

### 2.2.7 Antibody Mediated Cell Depletion

CD4+ cells were depleted using an anti-CD4 monoclonal antibody, GK1.5, as previously described [139]. Mice were injected in the intraperitoneal space weekly with 0.3mg dose of Ab in 200µl sterile PBS. CD4+ cell depletion efficiency is assessed by flow cytometry with anti-

CD4, clone RM4-5, which does not compete with GK1.5. CD20+ cells are depleted using a mouse anti-mouse CD20 monoclonal antibody (Genentech, clone 5D2, isotype murine IgG2a). Mice were given intraperitoneal injections with 0.1mg doses of Ab every 5 days. CD20+ cell depletion efficiency is assessed by flow cytometry with anti-B220.

### 2.2.8 Preparation of Splenocyte, Purified-CD4, and Purified-B220 Cells for Adoptive Transfer

Spleens are harvested from C57BL/6J mice were harvested, diced, and strained through a 70μm filter for a single cell splenocyte suspension. CD4+ cells and B220 cells were purified using Stem Cell EasySep Negative Selection- Mouse CD4+ T-cell Isolation Kit and Mouse B220 B-cell Isolation Kit, respectively. Cells were enumerated and resuspended in sterile PBS. Cells were resuspended at 2.5x106 cells/ml, and each mouse received 5x105 cells (200μl) via intravenous (tail-vein) injection. In testing CD4 capacity for clearance, mice were adoptively transferred 2 weeks prior to infection and sacrificed 4-6 weeks after infection with *Pneumocystis murina*. To induce immune reconstitution syndrome, mice were originally infected for 21 days prior to cell adoptive transfer, and then sacrificed 10 days after transfer.

### 2.2.9 Pulse Oximetry and Lung Injury Qualification from BALF

CD4+ cells were depleted using an anti-CD4 monoclonal antibody, GK1.5, as previously described [140]. Mice were injected in the intraperitoneal space weekly with 0.3mg dose of Ab

in 200µl sterile PBS. CD4+ cell depletion efficiency is assessed by flow cytometry with anti-CD4, clone RM4-5, which does not compete with GK1.5. CD20+ cells are depleted using a mouse anti-mouse CD20 monoclonal antibody (Genentech, clone 5D2, isotype murine IgG2a). Mice were given intraperitoneal injections with 0.1mg doses of Ab every 5 days. CD20+ cell depletion efficiency is assessed by flow cytometry with anti-B220.

### 2.2.10 Statistical Analysis

Graphpad Prism (GraphPad Software, La Jolla, CA) one-way analysis of variance (ANOVA) with a HolmSidak multiple comparison post-test to calculate P values. Nonparametric data with three or more groups were analyzed with Kruskal-Wallis test with Dunn multiple comparison post-test. Two group comparisons were done with multiple t test. P values are annotated as follows (*) ≤0.05, (**) ≤0.01, (***) ≤0.001, and (****) ≤0.0001.

## 2.3 RESULTS

### 2.3.1 Anti-CD20 Treatment Induces Susceptibility To *Pneumocystis*

First, we independently validated that 5D2 (murine anti-CD20) was capable of depleting B-cells in mice. Prior to depletion (Day 0), over half of the splenocytes are IgM+, and the majority of which are also CD23+. By Day 6 post depletion, this population of cells is reduced by approximately 90% **(Figure 5A)**. To investigate if anti-CD20 conferred susceptibility to primary *Pneumocystis* infection, we administered anti-CD20 to mice followed by *Pneumocystis murina*

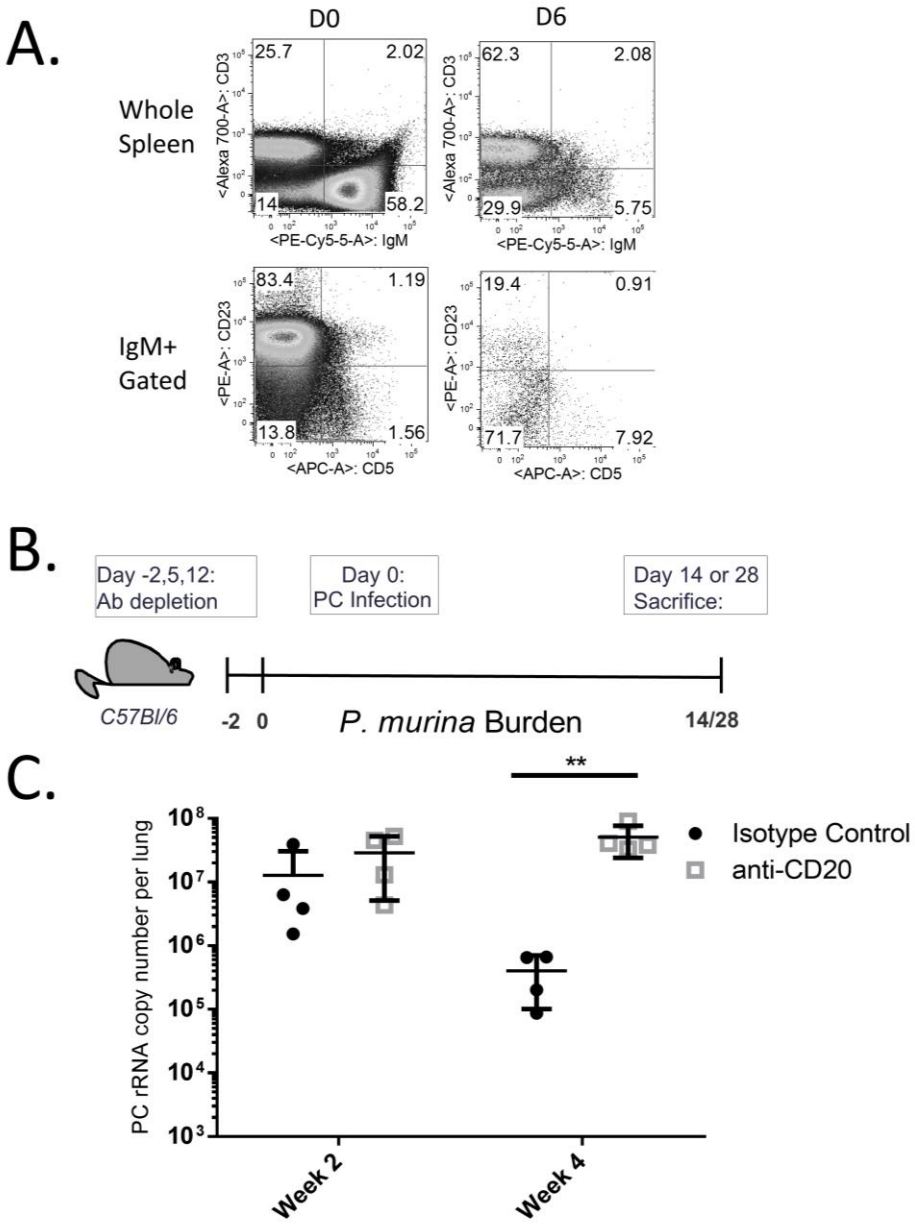


**Figure 5. Anti-CD20 treatment during *Pneumocystis* infection**

(A) Flow cytometry of whole splenocytes from untreated mice (left panels) and mice 6 days post treatment (right panels). Upper panels Y-axis (CD3) and X-axis (IgM). Lower panels are gated on the IgM+ and CD3- quadrant of upper panels; Y-axis (CD23) and X-axis (CD5). Representative images of n=3 per treatment were shown. (B) C57Bl/6 mice were depleted 2 days prior to infection and were treated with 5D2 every 7 days. Mice were sacrificed 2 and 4 weeks post infection. (C) Total lung RNA was isolated and *Pneumocystis* burden was measured by real-time

PCR of the mitochondrial Large Subunit rRNA copy number. Burden is reported as means + SEM for n = 4 per group. P values are annotated as follows (*) ≤0.05, (**) ≤0.01, (***) ≤0.001, and (****) ≤0.0001. Contributors: W. Elsegeiny and K. Chen.

infection **(Figure 5B)**. We measured P *murina* burden at both two and four weeks after infection, and at two weeks, 5D2 treated mice and isotype control mice had no differences in infectious burden. However, 4 weeks after infection, control mice began clearing infection whereas 5D2 treated mice had approximately a two log greater P *murina* burden in the lung **(Figure 5C)**. Thus, CD20+ cells are crucial for a protective immune response and depletion results in high susceptibility to primary *Pneumocystis* infection.

### 2.3.2 CD20 depletion blocks type 2 immune responses in the lung.

To determine mechanisms by which anti-CD20 was permissive for sustained *Pneumocystis* infection, we assessed cellular immune responses in whole lung cells (WLC). We harvested lungs from 5D2 treated, GK1.5 treated (CD4 depleted), and isotype control mice 2 weeks after infection. We chose two weeks because the infection load is approximately equal among all the groups, so any difference in immune responses could not be attributed to the presence of more antigen *in vivo* **(Figure 6A)**. The lungs were digested and strained to generate WLC cultures that were analyzed by flow cytometry or stimulated with *P. murina* antigen. Total WLCs were counted so that absolute lymphocyte count could be calculated. There was no difference in the number of recovered WLCs; however, there was a significant reduction in the total lymphocyte count in CD20 depleted animals **(Figure 6B,C)**. Furthermore, flow cytometry analysis showed

that there was 98% CD4 depletion with GK1.5 administration and approximately 90% B220 depletion with 5D2 **(Figure 6D)**.

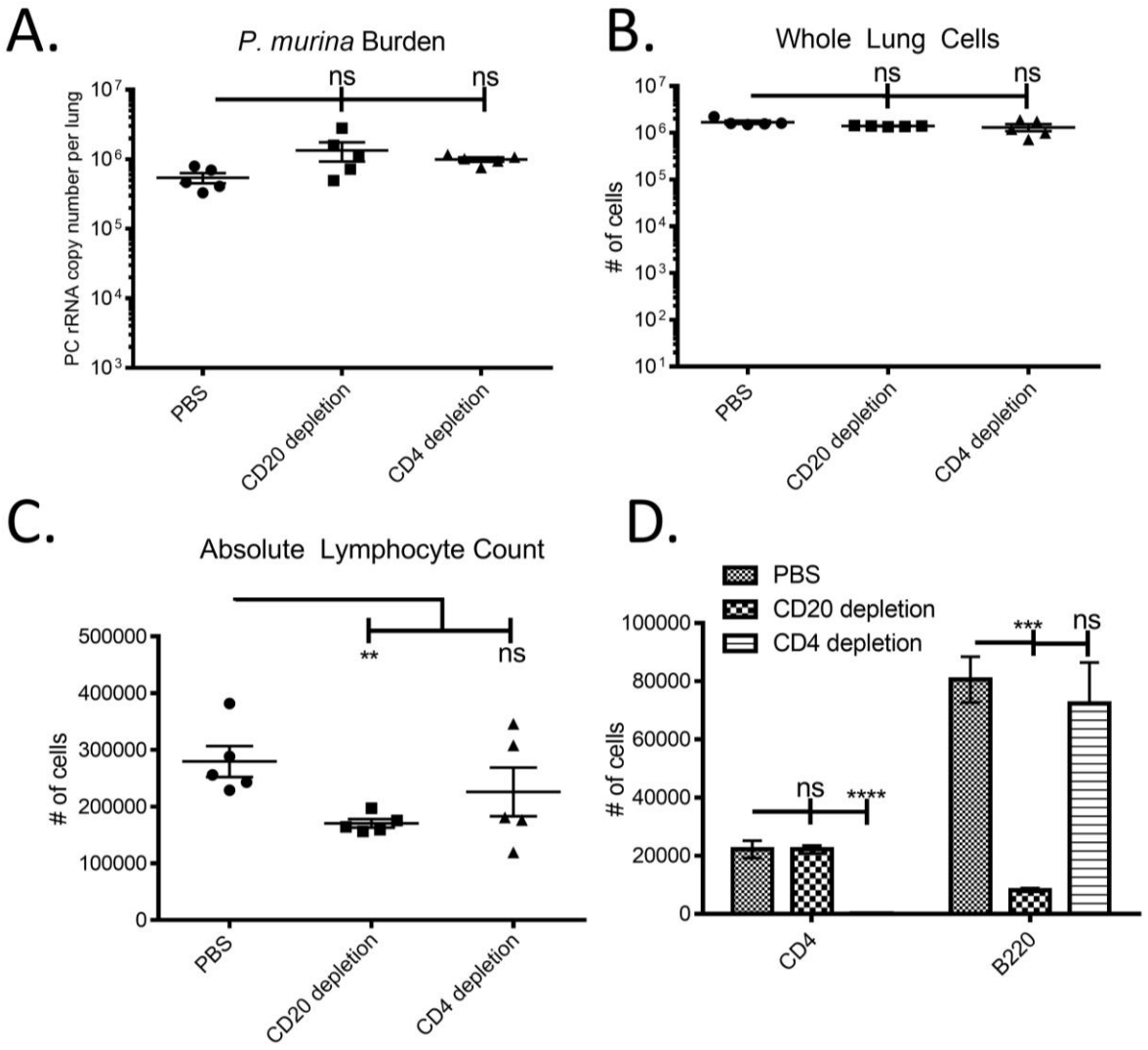


**Figure 6. CD4 and B220 cell assessment post anti-CD20 treatment**

(A) C57Bl/6 mice were administered anti-CD20 or control and infected with *Pneumocystis* for 2 weeks. Total lung RNA was isolated and *Pneumocystis* burden was measured by real-time PCR of the mitochondrial Large Subunit rRNA copy number. (B) Whole lung cells (WLCs) were counted from right superior and inferior lobes. The absolute lymphocyte count was determined from the % lymphocyte gate (based on FSC and SSC) and the total lung WLC count. (C) Similarly, CD4 and B220 absolute counts were calculated by % positive cells and the absolute

lymphocyte count. All data are reported as means + SEM for n = 5 per group. P values are annotated as follows (*) ≤0.05, (**) ≤0.01, (***) ≤0.001, and (****) ≤0.0001. Contributors: W. Elsegeiny.

After stimulation of WLCs with *P. murina* antigen for 72 hours, we analyzed effector cytokines in cell supernatants by Luminex. IFNγ production by WLCs did not differ across the groups **(Figure 7A)**. IL17a was not highly produced and although there was trend to have higher levels in control mice, this was not statistically significant different between the groups **(Figure 7B)**. However, the vehicle control group had a strong type II signature, which was substantially reduced in both CD4 and CD20 depleted groups. Briefly, IL-4 and IL-13 were substantially reduced in both CD4 and CD20 depleted samples. Although IL-5 expression was also reduced after CD20 depletion, levels were still significantly higher than the CD4 depleted samples **(Figure 7C)**. However, depleting CD4+ cells from CD20 depleted mice further reduced type II responses, and were equivalent to levels of CD4 depletion alone. These data show that CD20 depletion leads to a defect in effector immune responses in the lung, and that the decrease is primarily in type II immunity of whole lung cells.

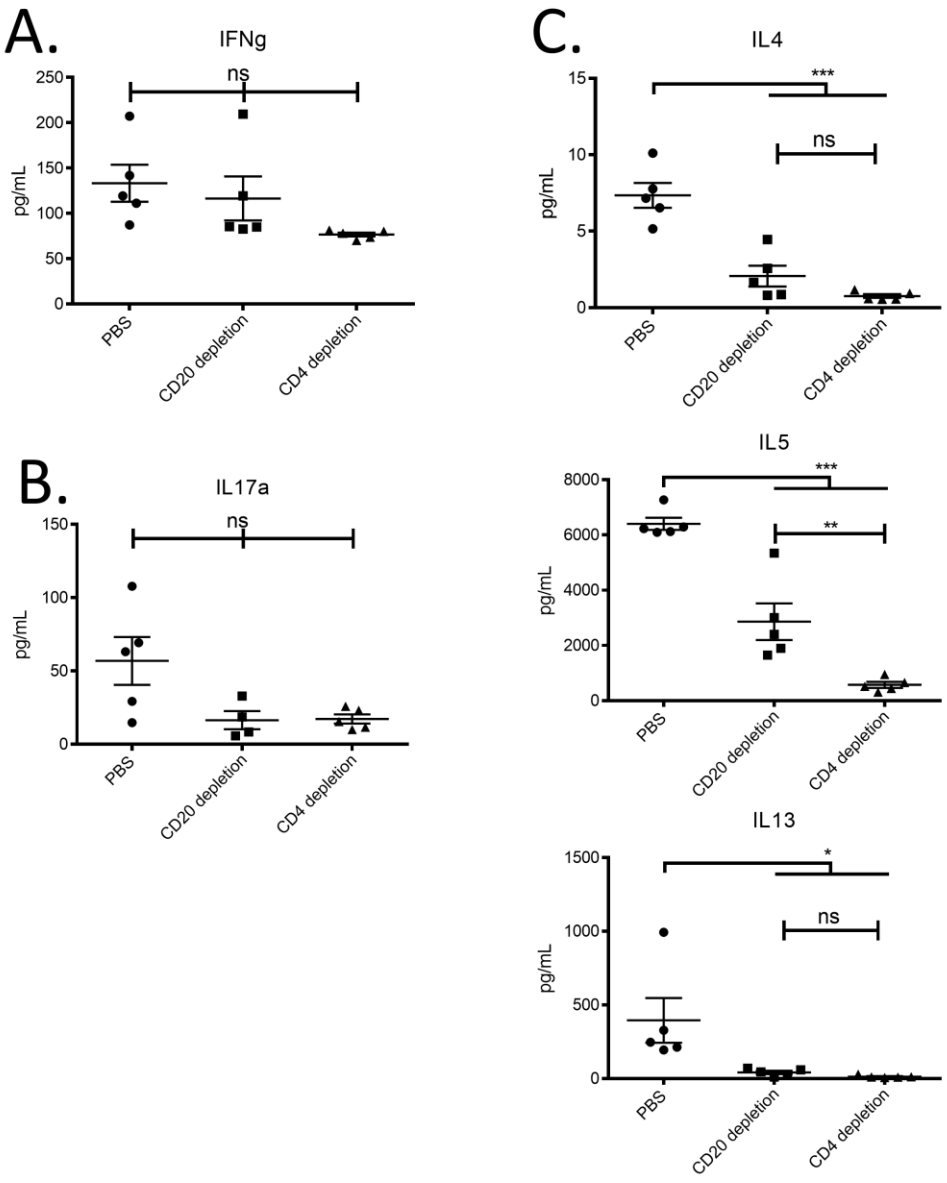


**Figure 7. Cytokine analysis of supernatants from *Pneumocystis* antigen stimulated WLCs**

WLCs were cultured in the presence of *P. murina* antigen and IL-2 for 72 hours. (A-C) All cytokines were analyzed simultaneously by Millipore multiplex on a bioplex reader. All data are reported as means + SEM for n = 5 per group. P values are annotated as follows (*) ≤0.05, (**) ≤0.01, (***) ≤0.001, and (****) ≤0.0001. Contributors: W. Elsegeiny

### 2.3.3 Anti-CD20 treatment eliminates CD4+ T-cell protective responses.

To address whether CD20 depletion alters specifically CD4 effector function, we then examined whether adoptively transferring purified CD4+ T-cells from naïve C57BL/6J WT mice into Rag1-/- had any protective effects against *Pneumocystis*. Adoptive transfer of purified CD4+ T-cells resulted in significant reductions in *P. murina* lung burden compared to vehicle control mice **(Figure 8)**.

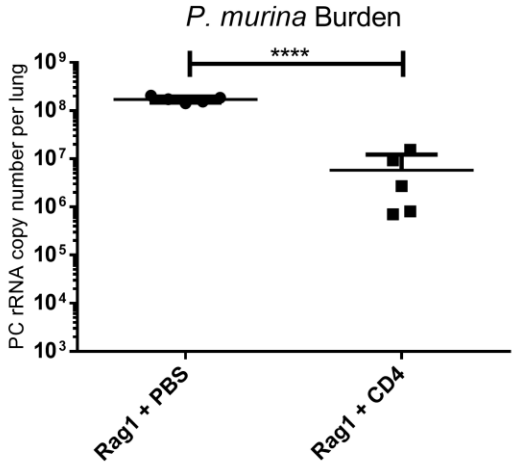


**Figure 8. Adoptive transfer of naïve CD4+ cells protects Rag1-/- from *P. murina* infection**

Naïve CD4+ cells were adoptively transferred into Rag1-/- mice. After homeostatic proliferation, mice were infected with *P. murina* for 4 weeks Total lung RNA was isolated and *Pneumocystis* burden was measured by real-time PCR of the mitochondrial Small Subunit rRNA copy number. Burden is reported as means + SEM for n = 4/5 per group. Contributors: W. Elsegeiny.

We next examined if CD4+ T-cells from 5D2 treated mice or isotype control mice could clear *Pneumocystis*. Briefly, 5D2 treated C57BL/6J WT mice were infected with the standard inoculum of *Pneumocystis murina* for 2 weeks. After which, CD4+ cells from these mice were purified and adoptively transferred to Rag1-/- mice **(Figure 9A)**. Splenic CD4+ T-cells were also tested for their capacity to respond to CD3/CD28 bead stimulation ex vivo. CD4+ T-cells from CD20 depleted mice had significantly less IFNγ production and a trend for decreased IL-5

**(Figure 9B)**. The cells were given 14 days to homeostatically proliferate in Rag1-/- mice before infecting with *Pneumocystis murina*. Lungs were harvested at four weeks after infection and analyzed for *P. murina* burden. Adoptive transfer of lung CD4+ T-cells from control mice again resulted in control of *P. murina* infection whereas lung CD4+ T-cells from CD20 depleted mice were defective in clearing *P. murina* **(Figure 9C)**. This could be result of clonal deletion or anergy to *Pneumocystis* antigen during infection of CD20-depelted mice.

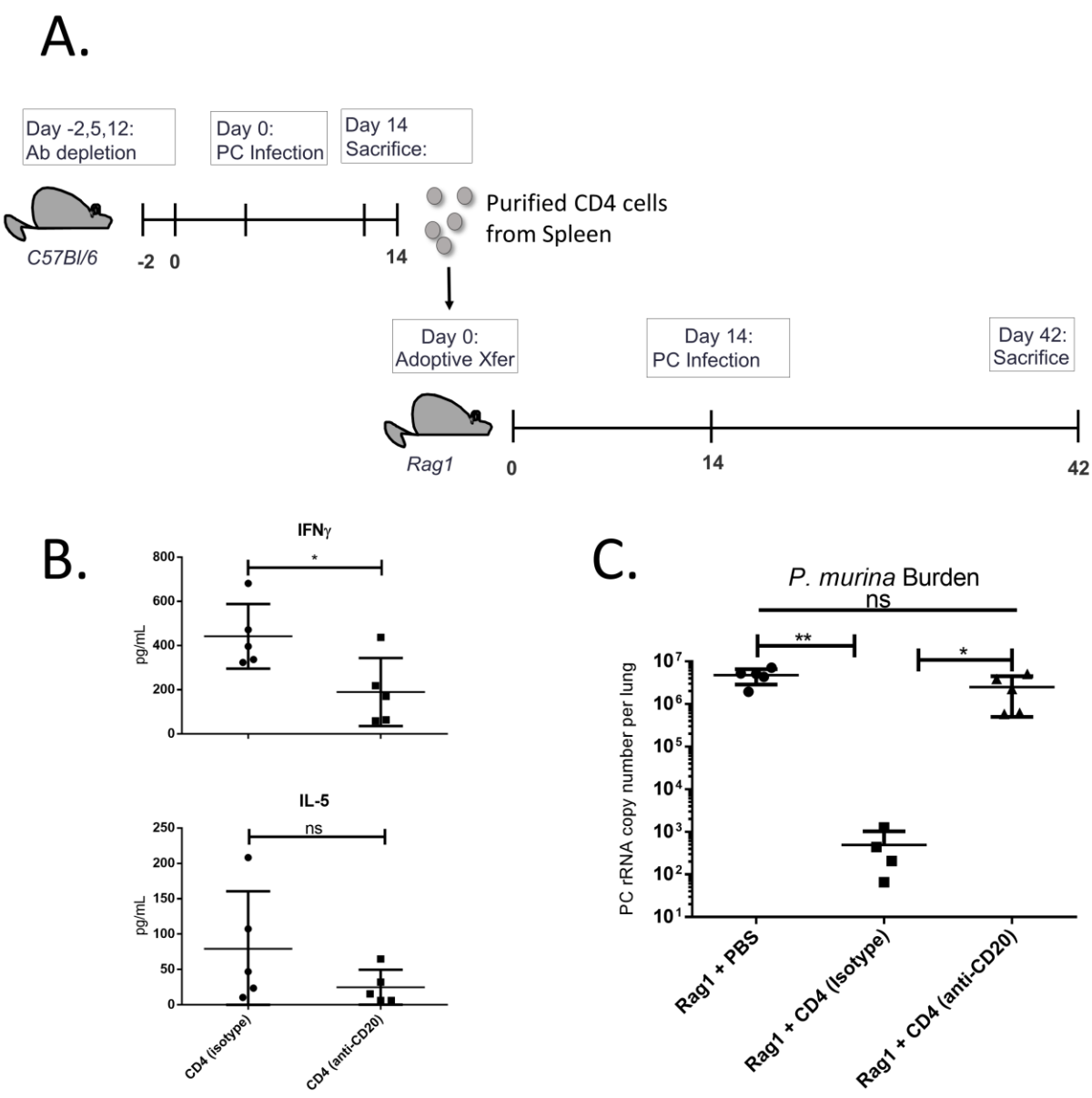


**Figure 9. Loss of CD4+ cell specific protection after anti-CD20 treatment**

(A) Mice were CD20 depleted and infected for two weeks with *P. murina*. Splenic CD4+ cells were then purified and adoptively transferred into Rag1-/- mice. After homeostatic proliferation, mice were infected with *P. murina* for 4 weeks. (B) Purified splenic CD4+ cells from CD20 depleted mice were stimulated with CD3/CD28 beads. Cytokines in the supernatants were analyzed simultaneously by Millipore multiplex on a bioplex reader. (C) Total lung RNA was isolated and *Pneumocystis* burden was measured by real-time PCR of the mitochondrial Large

Subunit rRNA copy number. Burden is reported as means + SEM for n = 5 per group. P values are annotated as follows (*) ≤0.05, (**) ≤0.01, (***) ≤0.001, and (****) ≤0.0001. Contributors: W. Elsegeiny.

### 2.3.4 Mice with convalescent immunity are resistant to anti-CD20 mediated susceptibility.

We next determined if anti-CD20 conferred risk to a secondary infection with *P. murina*. To examine this, we generated convalescent mice by infecting them with *P. murina* and allowing them 8 weeks to clear and recover from the infection. After the recovery period, one group was given 5D2, another group received GK1.5, and another group received carrier control (sterile PBS). All groups were then reinfected with the same inoculum of *P. murina*, and fungal burden was measured 2 weeks after the second infection **(Figure 10A)**. All groups, including the CD4 and CD20 depleted groups completely eradicated the infection **(Figure 10B)**. We wanted to discern the method of clearance, so we assessed the level of *Pneumocystis murina* specific antibodies in the serum. All groups had approximately equal levels anti-P *murina* IgG **(Figure 10C)**. We attributed the clearance to the presence of anti-*Pneumocystis* IgG. To formally test this we examined the effector activity of these antibodies by adoptively transferring 200µl of either naïve or convalescent serum, from WT C57Bl/6 mice infected with *P. murina*, to Rag1-/- mice which lack T and B-cells **(Figure 10D)**. Rag1-/- mice that receive convalescent serum were protected from infection **(Figure 10E)**. These studies show that anti-CD20 does not confer susceptibility to infection in the presence of pre-existing *Pneumocystis* immunity.

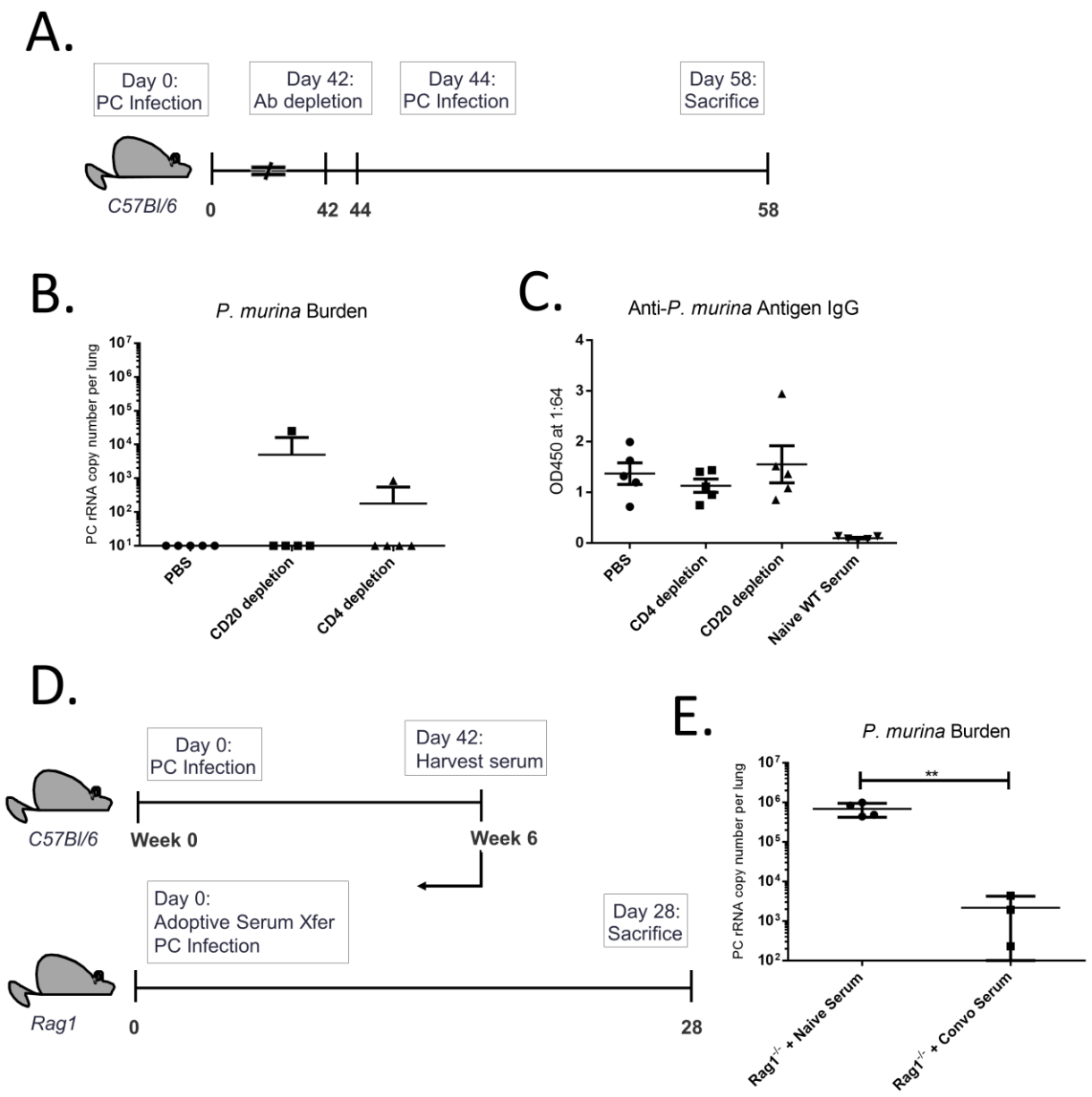


**Figure 10. Humoral immunity is sufficient for protection against *Pneumocystis***

(A) Wild-type C57Bl/6 mice were infected with *P. murina* and allowed to convalesce for 6 weeks. They were then CD20 depleted and infected with *P. murina* for 2 weeks. (B) Total lung RNA was isolated and *Pneumocystis* burden was measured by real-time PCR of the mitochondrial Large Subunit rRNA copy number. (C) Total *P. murina* antigen specific IgGs were measured by direct ELISA of a 1 to 64 dilution of serum as primary and anti-mouse IgG-HRP secondary. (D) Serum harvested from convalescent mice were adoptively transferred into Rag1-/- at time of infection with *P. murina*. (E) *Pneumocystis* burden following transfer of convalescent serum as measured by real-

time PCR as described above. All data are reported as means + SEM for n = 3 to 5 per group. P values are annotated as follows (*) ≤0.05, (**) ≤0.01, (***) ≤0.001, and (****) ≤0.0001. Contributors: W. Elsegeiny.

### 2.3.5 B-cells are dispensable during T-cell immune reconstitution inflammatory syndrome (IRIS).

We next determined if CD20+ cells may contribute to IRIS. The first model we used to test this experiment was using severe combined immune deficient (SCID) mice infected with *Pneumocystis murina* followed by adoptive transfer of whole splenocytes to induce IRIS [142]. As a negative control for IRIS in this experiment, a group of SCID mice received whole splenocytes and were depleted of CD4+ T-cells *in vivo*. We then examined whether or not anti-CD20 reduced or prevented tissue pathology **(Figure 11A)**. We first measured weight and found that mice that received anti-CD20 lost approximately the same percent of total body weight as the non-depleted **(Figure 11B)**. However depletion of CD4+ T-cells prevented weight loss. Total protein in the BAL, a measure of lung damage, was also significantly reduced in mice that received anti-CD4 antibodies but increased in control and anti-CD20 treated mice **(Figure 11C)**. Lactate dehydrogenase activity in the BAL, a measure of cell death in the lung, was elevated in mice that received whole splenocytes but was significantly abrogated in mice that received anti-CD4 **(Figure 11D).** However there was slightly greater LDH activity in mice that received anti-CD20. These data show that IRIS requires CD4+ T-cells but anti-CD20 had little effect on the development of IRIS in this model.

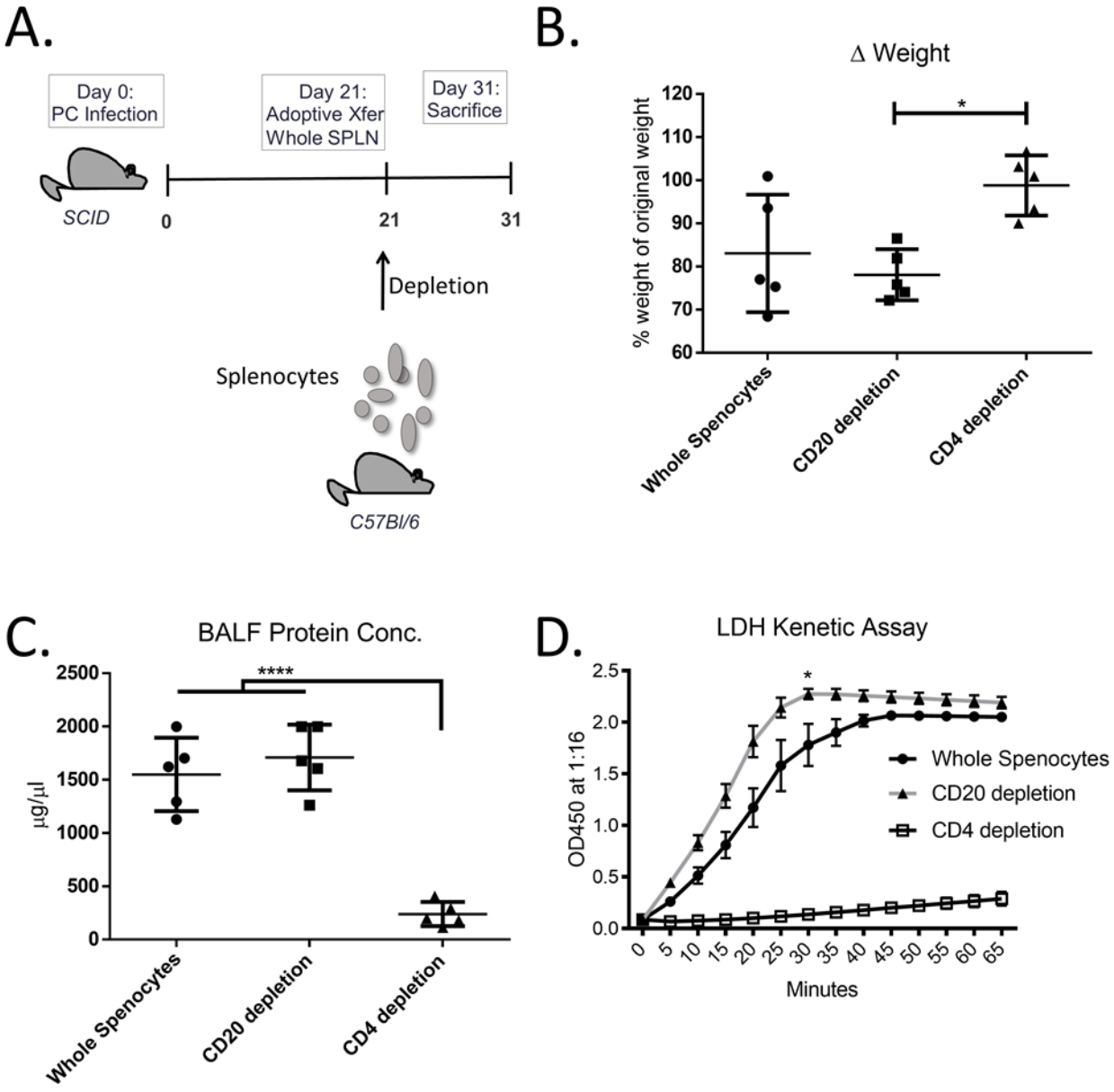


**Figure 11. Influence of CD20 depletion on Immune Reconstitution Inflammatory Syndrome**

(A) Balb/c SCID mice are infected with *P. murina* for 3 weeks, then reconstituted with WT splenocytes + CD20 or CD4 depletion for 10 days. (B) Mice were weighed before and after reconstitution to determine percent weight loss. (C) Total protein from BALF was measured by BCA assay. (D) Lactate dehydrogenase in the BAL was measured

by a kinetic assay of LDH activity. All data are reported as means + SEM for n = 5 per group. P values are annotated as follows (*) ≤0.05, (**) ≤0.01, (***) ≤0.001, and (****) ≤0.0001. Contributors: W. Elsegeiny and T. Eddens.

We next examined if CD20+ cells in conjunction with CD4+ T-cells affected IRIS. We also tested the hypothesis that *Pneumocystis*-experienced B-cells or plasma cells would provide a protective effect and mitigate IRIS. Briefly, we adoptively transferred CD4+ T-cells alone, CD4+ T-cells plus B220 cells from naïve mice, or CD4+ T-cells plus B220 cells from antigen experienced (Ag Exp) mice into *P. murina* infected Rag1-/-. Ag Exp cells were from mice infected with *Pneumocystis murina* for 14 days. We sacrificed mice at day 10 post transfer, as at this time point *Pneumocystis* burden is still equal between all the groups **(Figure 12A)** but is the peak day of lung injury. By day 10 we could detect anti-chitin IgM levels in the serum of the naïve and antigen experience B220 cell transferred mice, and anti-*Pneumocystis* IgG levels only in the Ag Exp B220 cell transfer **(Figure 12B,C)**. Like the previous experiment, adding B220 cells, naïve or Ag Exp, did not affect weight loss, blood oxygen saturation, or BALF lactate dehydrogenase **(Figure 12D-F)**. These data show that B-cells are dispensable for CD4+ T-cell mediated IRIS in this model.

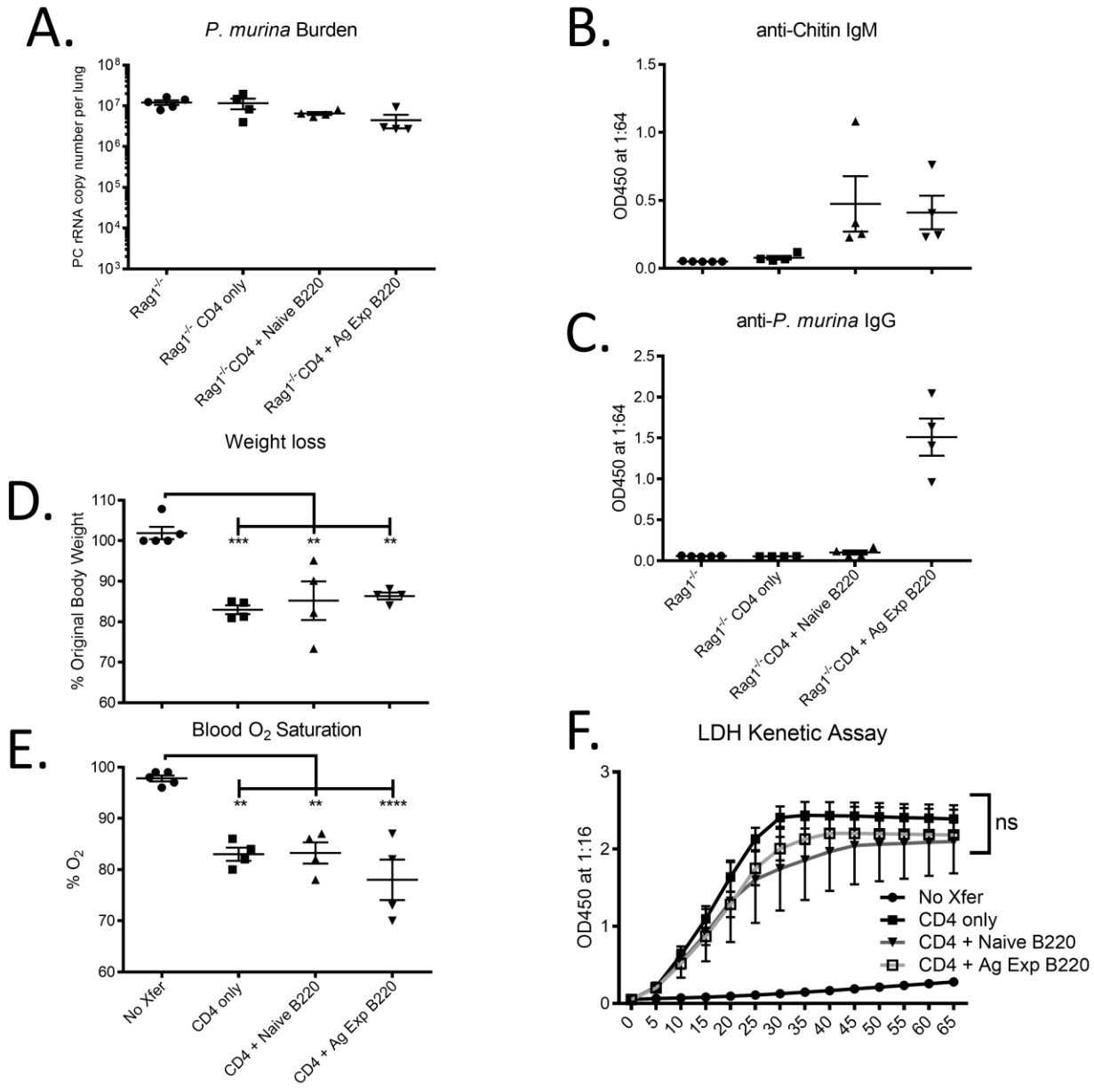


**Figure 12. Influence of naïve and antigen-experienced B220 cells on IRIS**

(A) Total lung RNA from mice reconstituted with a combination of CD4+ T-cells plus naïve or antigen experienced B220 cells were isolated and *Pneumocystis* burden was measured by real-time PCR of the mitochondrial Large Subunit rRNA copy number. (B and C) Anti-Chitin-IgM and anti-*P. murina*-IgG in serum were assessed by direct ELISA with anti-IgM and anti-IgG secondary HRP antibodies, respectively. (D) Mice were weighed before and after reconstitution to determine percent weight loss. (E) Mouse blood oxygenation was measured immediately prior to sacrifice, by pulse-oximeter. (F) Lactate dehydrogenase in the BAL was measured by a kinetic assay of LDH

activity. All data are reported as means + SEM for n = 4 or 5 per group. P values are annotated as follows (*) ≤0.05, (**) ≤0.01, (***) ≤0.001, and (****) ≤0.0001. Contributors: W. Elsegeiny and T. Eddens

## 2.4 DISCUSSION

As there is an increase in the number of incidents of opportunistic infections involving patients receiving anti-CD20-containing treatment regimens, there is a need to understand the effects of anti-CD20 on the immune response to infection. We pursued this question by developing an *in vivo* mouse model of CD20-depletion in an attempt to recapitulate the clinical scenario of anti-CD20 treatment. We were first able to observe that anti-CD20 alone was capable of inducing susceptibility to *Pneumocystis* infection by diminishing the immune response to *Pneumocystis* in the lung. WLCs showed reduced type 2 responses and CD4+ T-cells specifically were not capable of providing protective responses in an adoptive transfer model. These data suggest that anti-CD20 inhibits T-cell priming to *P. murina.* [143]. As such, $CD4^+$ T-cells appear to recruit eosinophils early in infection while B cells are undergoing and provide preliminary control of *Pneumocystis* burden. Importantly, IL-5 transcription and eosinophil recruitment appears to be dependent on $CD4^+$ T-cells in this model, as such markers do not appear until after activation of the adaptive immune response at day 7 post-infection (refer to Appendix A).

Eosinophils, classically recognized as mediators of immunity against helminths, have recently been implicated in host defense against a variety of pathogens, including bacterial and viral infections [144]. Recently, we have demonstrated that eosinophils contribute to host defense against the fungal pathogen *Aspergillus fumigatus* through a secretory factor, as eosinophils could mediate fungal killing when separated using transwells [145]. The study in

Appendix A extends these findings by demonstrating that eosinophil-deficient mice are more susceptible to *Pneumocystis* infection and that eosinophils display antifungal activity *in vitro*. Additionally, treatment of bone marrow derived eosinophils with IL-4 and IL-13 greatly enhanced killing of *Pneumocystis*, suggesting that Th2 cytokines in the lung may augment eosinophil-dependent antifungal activity (refer to Appendix A).

It is still not known why specifically CD20+ B-cells are required to prime CD4+ cell responses to *Pneumocystis*. Previous studies that have shown that both CD40 and MHC class II on B-cells are critical for the CD4+ T -cell priming; however, why other antigen presenting cells were not capable is still a question that needs addressing [89]. Interestingly, the absence of CD20+ cells during *Pneumocystis* infection may lead to clonal deletion of *Pneumocystis* specific CD4+ cells since they are not as capable of clearing *Pneumocystis* as CD4+ cells from naïve mice. This may be due to a lack of CD4+ T-cell costimulation by B-cells during *Pneumocystis* infection.

While the previous experiments were conducted in naïve mice, anti-CD20-treated patients are likely not naïve to *Pneumocystis jirovecii*, as most individuals are seropositive for anti-*Pneumocystis* antibodies [120, 146]. It is still unknown what the potential reservoirs are for *Pneumocystis*, but some research indicates the possibility that many diseased and healthy patients may be colonized with *Pneumocystis*. Some studies also suggest that hosts may be transiently exposed or asymptomatically carry *Pneumocystis* throughout their lives [147]. We observed that convalescent mice were capable of clearing *Pneumocystis* without the aid of CD4 or CD20+ cells, most likely through antibody mediated protection. Since memory CD4+ cells and antibodies are enough to clear *Pneumocystis*, these data raise a question as to why immunosuppressed patients acquire *Pneumocystis jirovecii* infections. Anti-CD20 antibody

therapy in patients alone has not been shown to decrease immunoglobulin levels, however, when combined with other immunosuppressive therapies hypogammaglobulinaemia can occur [148]. It has also been demonstrated that *Pneumocystis spp* have a dynamic extracellular proteome by varying their major surface glycoproteins, which may be used to evade the host immune response [149, 150]. Reports of large genetic variability between *Pneumocystis jirovecii* isolates also suggests the possibility that patients are simply being exposed to a new strain of *Pneumocystis* [143, 151].

Immune Reconstitution Inflammatory Syndrome (IRIS) is a condition that was first observed with the advent of highly active antiretroviral therapy (HAART), which dramatically suppresses HIV replication [152]. This suppression leads to an expedient reconstitution of CD4+ T-cells, which then react to an accumulation of viable infection and/or residual microbial antigens acquired during immunosuppression. As a result, the host can experience a massive amount of inflammation in multiple organs, primarily the lungs and CNS [153, 154]. This immunopathology is mediated through CD4+ T-cells [155], but it has been previously shown that other cell types such as CD8 cells modulate the pathology by increasing the $T_{reg}$:$T_{effecor}$ ratio [156]. Previous studies have shown that natural antibodies may reduce pathology [140]; however, the direct role of B-cells during IRIS has yet to be studied. Thus, as B-cells are required for T cell effector function in protection, we hypothesized that CD20+ cells may also play a role in the inflammatory pathology of T cell mediated IRIS. We observed that the absence or presence of CD20+ cells does not exacerbate the pathology in the model studied here. We hypothesize that this is due to CD4+ T-cell nonspecific activation through homeostatic proliferation. Thus we conclude that CD20+ cells are dispensable in CD4 mediated IRIS.

Thus, in conclusion, anti-CD20 confers risk to primary infection with *P. murina* but we did not observe risk of secondary infection in mice that had pre-existing humoral immunity. In addition, mice treated with anti-CD20 had reduced whole lung cell type II responses to *Pneumocystis*, and CD4 cells from depleted mice had an intrinsic impairment in their ability to clear *Pneumocystis* in our adoptive transfer model. These data suggest that clinical *Pneumocystis jirovecii* pneumonia could be due to concomitant immunosuppression or patients are requiring antigenically distinct strains of *Pneumocystis* that pre-existing humoral immunity is ineffective in preventing. Lastly anti-CD20 did not affect the severity of CD4 T-cell mediated IRIS in this model.

# 3.0 CHAPTER 3: CD4+ T-CELL INTRINSIC IL-21R SIGNALING AND THE FACTORS THAT MEDIATE *PNEUMOCYSTIS* CLEARANCE

Work described in this section is in preparation for publication

by authors

Waleed A Elsegeiny, Mingquan Zheng, Taylor Eddens, Leticia Monin, Radha Gopal, Derek Pociask, William Horne, John Alcorn, and Jay Kolls

## 3.1 INTRODUCTION

The predominant factor required for immunity against *Pneumocystis* infection is the presence of CD4+ T-cells. The emergence of *Pneumocystis* pneumonia as an AIDS-defining infection established the direct correlation of CD4+ T-cell loss with susceptibility to infection. This role has been validated numerous times in a variety of animal models from murine to macaque. Restoration of CD4+ T-cells in otherwise deficient patients or animals also restores the immunity against *Pneumocystis* infection, which further demonstrating the importance of CD4+ T-cells. However, the exact mechanism in which CD4+ T-cells mediate clearance is still unclear.

Early on, studies have examined the role of T helper 1 (Th1) and T helper 2 (Th2) lymphocyte subsets in murine and SHIV-macaque models of *Pneumocystis* infection, and concluded that both subsets could be observed in the lungs. Particularly, Th2 cytokines, such as interleukin-4 (IL-4), IL-5, and IL13, were found to be upregulated in the BAL of macaques colonized with *Pneumocystis* [120, 157]. Th1 cytokines, such as interferon gamma (IFN-γ) and tumor necrosis factor alpha (TNF-α), were increased only when macaques began to develop active infection. Later, as T helper 17 (Th17) lymphocytes emerged as a unique subset, they were also characterized in the context of *Pneumocystis* infection. Interestingly, Th17 cells are also detectable in the lungs during *Pneumocystis* infection, however, mice deficient in Th17 responses, such as IL-17 and IL-23, only have delayed clearance [158]. Our goal in the following study is to dissect the exact CD4+ T-cell signals that are required initiate a protective immune response, and identify the factors that mediate clearance.

## 3.2 MATERIALS AND METHODS

### 3.2.1 Mice.

Six- to Eight- week-old wild-type C57BL/6J (WT), Balb/C (WT), BALB/c-Il4ra$^{tm1Sz}$/J (Il4ra-/-), C.129S1-*Il12b*$^{tm1Jm}$/J (Il12b-/-), B6.129S7-Rag1$^{tm1Mom}$/J (Rag1-/-), B6.CB17-Prkdc$^{scid}$/SzJ (SCID), B6.129S2(C)-Stat6$^{tm1Gru}$/J (Stat6), B6N.129-Il21r$^{tm1Kopf}$/J, and B6.129S2(Cg)-*Cxcr5*$^{tm1Lipp}$/J (CXCR5-/-) mice were obtained from The Jackson Laboratory (Bar Harbor, ME). B10:B6-Rag2$^{tm1Fwa}$Il2rg$^{tm1Wjl}$ (Rag2-/-Il2rγ-/-), Il17ra$^{tm1Koll}$ (Il17ra−/−), B6.129-IL23p19$^{tm1}$N12 (Il23a-/-), and B6.IL22$^{tm1}$ (IL22), B6.Cg-Tg(CD4-cre)$^{1Cwi}$N9 (CD4-Cre) mice on C57BL/6 background were originally obtained from Taconic (Hudson, NY). Stat4-/- mice and Stat3fl/fl mice on C57BL/6 background were obtained from M.H. Kaplan. We also cross Stat4 to Stat6 to get Stat4/6 double KO mice and then crossed to Stat3fl/fl/CD4Cre mice to get Stat3/4/6 triple KO mice. B6.IL21-/- mice were obtained from Dr. Khader at University of Pittsburgh School of Medicine. Mice were then bred and maintained at the University of Pittsburgh Division of Laboratory Animal Resources (DLAR) Facility at Rangos Research Building of Children's Hospital of Pittsburgh of UPMC. GM-CSF-/- splenocytes were provided by Dr. Z.C. Chroneos at PSU. Animals were housed in a pathogen-free environment and given food and water by the DLAR ad libitum. All experiments were approved by the University of Pittsburgh Institutional Animal Care and Use Committee.

### 3.2.2 *Pneumocystis* Isolation, Inoculum and Antigen Preparation.

*Pneumocystis murina* organisms were administered by oral-pharyngeal delivery into $Rag2^{-/-}$ $IL2r\gamma^{-/-}$ mice, propagated for 10-12 weeks *in vivo*, and isolated from mouse lung tissue, as previously described [139]. Briefly, $Rag2^{-/-}IL2r\gamma^{-/-}$ with *Pneumocystis* pneumonia were sacrificed, and the lungs were aseptically harvested and frozen in 1ml of sterile Dulbecco's phosphate buffered saline (PBS) at $^{-}$80°C. To process the inoculum, frozen lungs were thawed and strained through a 70μm filter and pelleted by centrifugation (800xg, 10min, and 4°C). The pellet was resuspended in 1ml of PBS. A 5μl aliquot was diluted 1:10 and heat-fixed on a slide, and stain with Hema-3 modified Wright-Giemsa stain (Fisher Scientific Pittsburgh, PA) followed by asci counting. *Pneumocystis murina* asci were quantified microscopically, and the inoculum is adjusted to $2x10^6$ asci per ml. Mice are administered 100μl ($2x10^5$ asci) of the inoculum by oral pharyngeal aspiration as previously described [140]. *Pneumocystis* protein antigen was prepared by differential centrifugation of the inoculum as previously described, followed by sonication of 1mg of inoculum per ml for 5 minutes [120].

### 3.2.3 Whole Lung Cell Preparation and Antigen Stimulation.

Mice were infected with an inoculum of *P. murina* for 2 weeks. At the time of euthanasia, mice were anesthetized by intraperitoneal injection of ketamine/xylazine cocktail and euthanized by exsanguination. Immediately after mice were perfused vascularly by 5ml of heparinized PBS injection into the right ventricle. The right superior and inferior lobes are then harvested, minced with razorblades, and digested in 5ml serum-free media with 2mg/ml collagenase for 90 minutes in a 37°C shaking incubator. Cell suspension is then strained through a 70μm filter, then washed

and resuspended in complete DMEM media. Red blood cells were then lysed with ammonium chloride solution, washed, resuspended in 5mls, and counted. 106 cells per well are plated on a 96-well round bottom plate in complete DMEM media with 1μg/ml PC antigen and 20U/ml IL-2. An aliquot from each group is taken for cell analysis by flow cytometry. Plated cells are stimulated at 37°C at 5% CO2 for 72 hours. Finally, supernatants are harvested for multiplex (Millipore) cytokine analysis on a Bioplex reader (Bio-Rad).

### 3.2.4 RNA sequencing

Total RNA from mouse whole lung was used to perform RNA sequencing. Each sample was assessed using Qubit 2.0 fluorometer and Agilent Bioanalyzer TapeStation 2200 for RNA quantity and quality. Library preparation was done using Illumina TruSeq Stranded mRNA sample prep kit. The first step in the workflow involves purifying the poly-A containing mRNA molecules using poly-T oligo attached magnetic beads. Following purification, the mRNA is fragmented into small pieces using divalent cations. The cleaved RNA fragments are copied into first strand cDNA using reverse transcriptase and random primers. Strand specificity is achieved by using dUTP in the Second Strand Marking Mix, followed by second strand cDNA synthesis using DNA polymerase I and RNase H. These cDNA fragments then have the addition of a single 'A' base and subsequent ligation of the adapter. The products are then purified and enriched with PCR to create the final cDNA library. The cDNA libraries are validated using KAPA Biosystems primer premix kit with Illumina-compatible DNA primers and Qubit 2.0 fluorometer. Quality is examined using Agilent Bioanalyzer Tapestation 2200.The cDNA libraries will be pooled at a final concentration 1.8pM. Cluster generation and 75bp paired read single-indexed sequencing was performed on Illumina NextSeq 500's.

### 3.2.5 Flow Cytometric Analysis.

$10^6$ single cells from mouse lung were surface stained with a combination of TCRβ (PerCP-Cy5.5), CD3 (Pacific Blue), CD4 (PE or Pacific Blue), CD44 (APC-Cy7), CD62l (APC), CD69 (Pe-Cy7), and CD127 (PE) for T-cell phenotyping; CD11b (PerCP-Cy5.5), CD11c (PE-Cy7), F4/80 (APC-Cy7), MHCII (APC), SiglecF (PE), Ly6G (FITC), and CD103 (Pacific Blue) for APC phenotyping. Cells were stained for 15-30 minutes in PBS supplemented with 1% BSA. Cells were then fixed in 1% Formalin, and acquired for flow cytometry by an LSR-II (BD Biosciences, San Jose, CA) and data was analyzed using FlowJo (Treestar).

### 3.2.6 RNA Isolation and *Pneumocystis* Quantification by RT-PCR.

The right middle lobe of the lung was harvested in 1ml of Trizol and homogenized. RNA was purified and quantified as previously described [139]. Briefly, cDNA was synthesized from 1μg whole lung RNA via iScript reverse transcription reagents (Bio-Rad, Hercules, CA), and real-time PCR was performed using primers and probes for *Pneumocystis murina* large-subunit rRNA (LSU) transcript with SsoFast/SsoAdvanced Probes Supermix (Bio-Rad). The threshold cycle values were converted to copy number using a premade standard of known *Pneumocystis* LSU rRNA, as previously described [141]. Quantification was also performed using primers and a probe specific for *Pneumocystis murina* small subunit (SSU) rRNA with a standard curve of known *Pneumocystis* SSU rRNA concentrations. SSU primer and probe sequences are as follows: Forward: 5'-CATTCCGAGAACGAACGCAATCCT; Reverse: 5'-TCGGACTTGGATCTTTGCTTCCCA; FAM-Probe: 5'- TCATGACCCTTATGGAGTGGG CTACA.

### 3.2.7 Serum Collection and Direct ELISA.

Blood was collected either periodically by tail-bleed and/or at time of sacrifice by syringe from the vena cava. Coagulated blood was then centrifuged for 10 minutes at 10,000xg. The serum supernatant was collected and stored at -80°C. Maxisorb plates are coated with 1µg/well of *P. murina* antigen, chitin, or GSC-1 in 100µl bicarbonate coating buffer per well overnight at 4°C. Plates were blocked with 5% blotting grade blocker (Bio-Rad) and 1% BSA. Plates were first primary stained with sample serum in a dilution series from 26 to 213 overnight at 4°C, then secondary stained with murine Ig-specific-HRP antibodies. Plates were then developed with TMB substrate for 5-30 minutes depending on control serum, and reaction stopped with equal volume 2N H2SO4. OD450 is read using Synergy H1 Hybrid Reader (BioTek Winooski, VT).

### 3.2.8 Antibody Mediated Cell Depletion.

CD4+ cells were depleted using an anti-CD4 monoclonal antibody, GK1.5, as previously described [139]. Mice were injected in the intraperitoneal space weekly with 0.3mg dose of Ab in 200µl sterile PBS. CD4+ cell depletion efficiency is assessed by flow cytometry with anti-CD4, clone RM4-5, which does not compete with GK1.5.

### 3.2.9 Preparation of Purified-CD4+ T-cells for Adoptive Transfer.

Spleens from control or experimental mice were harvested, diced, and strained through a 70μm filter for a single cell splenocyte suspension. CD4+ cells were purified using Stem Cell EasySep Negative Selection- Mouse CD4+ T-cell Isolation Kit. Cells were enumerated and resuspended in sterile PBS. Cells were resuspended at $2.5x10^6$ cells/ml, and each mouse received $5x10^5$ cells (200μl) via intravenous (tail-vein) injection. In testing CD4 capacity for clearance, mice were adoptively transferred 2 weeks prior to infection and sacrificed at 2, 4, or 6 weeks after infection with *Pneumocystis murina*.

### 3.2.10 Histology

The left main bronchus was clamped using forceps and 250μL of 10% formalin was injected into the bronchus. The lung tissue was then submerged in 10% formalin, paraffin-embedded, and processed by the Children's Hospital of Pittsburgh Histology Core. Sections were then stained from H&E and PAS.

### 3.2.11 Statistical Analysis.

Graphpad Prism (GraphPad Software, La Jolla, CA) one-way analysis of variance (ANOVA) with a HolmSidak multiple comparison post-test to calculate P values. Nonparametric data with three or more groups were analyzed with Kruskal-Wallis test with Dunn multiple comparison post-test. Two group comparisons were done with multiple t test. *P* values are annotated as follows (*) ≤0.05, (**) ≤0.01, (***) ≤0.001, and (****) ≤0.0001.

## 3.3 RESULTS

### 3.3.1 Classical Th1, Th2, and Th17 effector cytokine signals are not required for *Pneumocystis* clearance.

Initially, to understand which effector CD4+ T-cell signals are important for clearance of *Pneumocystis* during infection, we measured *P. murina* burden in wild-type and numerous different cytokine/receptor knockout mice. In a standard infection model, mice are infected with an inoculum of $2x10^5$ asci for 4 weeks **(Figure 13A)**. To assess the role of Th1 cells, IL-12p40 knockout mice, which are deficient in IFN-γ production, were used, and IL4 receptor-α knockout mice were used as a model of impaired Th2 signaling. Both of these mice were able to completely clear infection comparable to wild type mice **(Figure 13B)**. Next we examined the importance of Th17 cells by infecting IL-23α and IL-17 receptor-α knock out mice, and similar to the Th1 and Th2 deficient mice, Th17 effector responses also appeared to be dispensable **(Figure 13C)**. However, these T helper cells can function through various non-classical signals, thus we decided to target the signal transducers and activators of transcription (STATs) of these subsets; Stat4, Stat6, and Stat3 which are critical for Th1, Th2, and Th17 differentiation, respectively. Global Stat4 and Stat6 knockout mice were acquired, and CD4-driven Cre+, Stat3 floxed transgenic mice were used since global Stat3-deficiency is embryonically lethal. We also infected these mice with *P. murina* as previously described and examined burden. Stat4 and Stat6 knockout mice had delayed clearance of *P. murina* infection, however, $Stat3^{fl/fl}$ | CD4-Cre+

mice were susceptible **(Figure 13D)**. These data show that although the classical Th17 cytokines, IL-17 and IL-23, are not critical for clearance, the key transcriptional activator for Th17 cells, Stat3, is required.

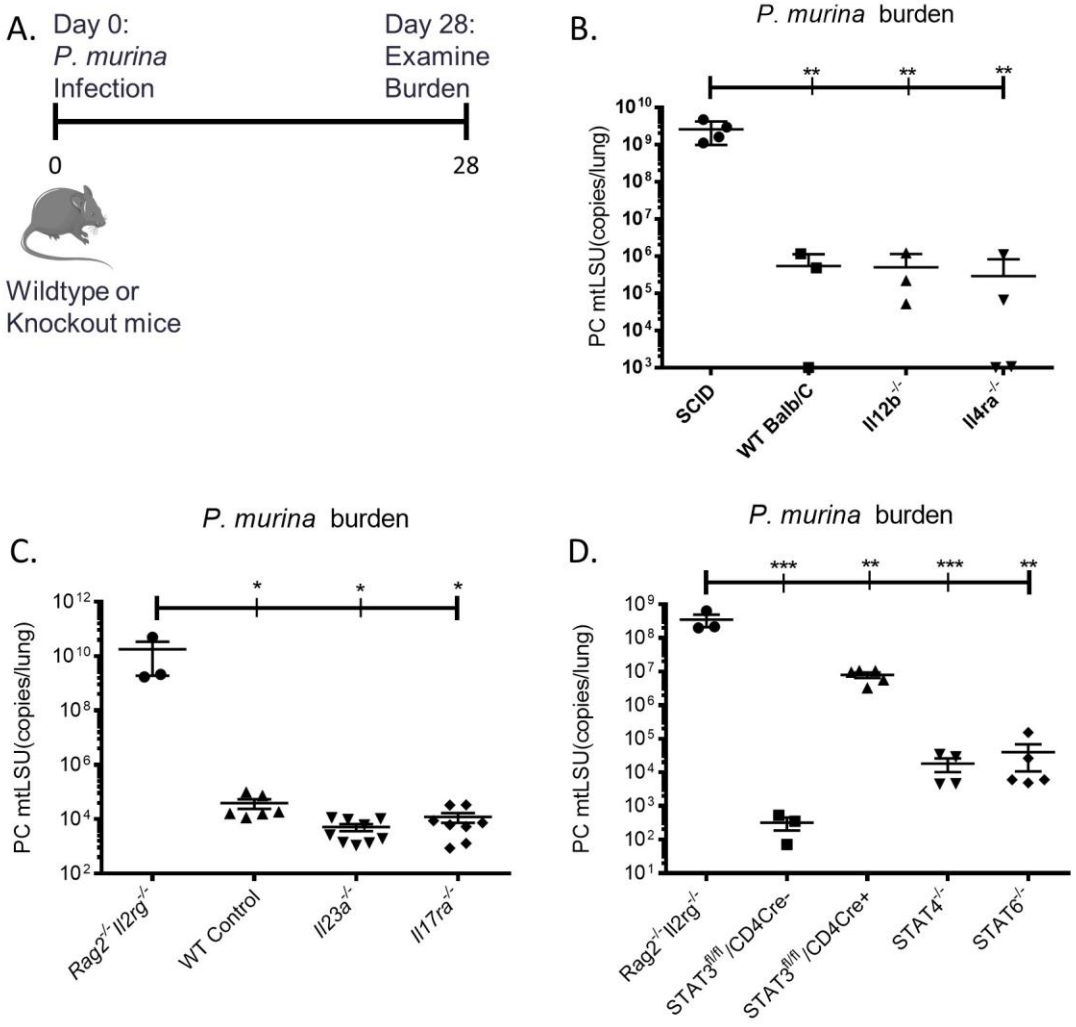


**Figure 13. Classical Th1, Th2, and Th17 factors are dispensable during *P. murina* infection**

(A) Diagram depicting the standard infection timeline with inoculation of *P. murina* defined as Day 0, and burden examined on Day 28. (B-D) Total lung RNA was isolated and *Pneumocystis* burden was measured by real-time PCR of the mitochondrial Large Subunit rRNA copy number. Burden is reported as means + SEM for n ≥3 per group. P values are annotated as follows (*) ≤0.05, (**) ≤0.01, (***) ≤0.001, and (****) ≤0.0001. Contributors: W. Elsegeiny, M. Zheng, and J. Alcorn.

We next were interested in examining the STAT knockouts in a CD4+ T-cell intrinsic model. To do so, we examined whether we could rescue Rag1 knockout mice through reconstitution of CD4+ T-cells. Rag1-/- mice have ablated T- and B-cell development, and are susceptible to *P. murina* infection. We purified splenic CD4+ T-cells from *wild-type* mice, and intravenously administered $5x10^5$ cells into Rag1-/- mice, 2 weeks prior to infection **(Figure 14A).** Mice that received wild-type CD4+ T-cells had approximately a log reduction in burden, while mice that received CD4+ T-cells from an OTII transgenic Rag1-/- mice showed no protection **(Figure 14B)**. CD4+ T-cells from OTII transgenic Rag1-/- mice express can only express an OVA peptide specific TCR, thus are incapable of mounting an antigen specific response against any other epitope. Using this model, we verified that Stat3 knockout CD4+ T-cells are intrinsically defective in generating a protective immune response to infection **(Figure 14C)**. However, to determine if Stat3 was exclusively required for clearance, we also generated Stat4/Stat6 double knockout (DKO) mice, and adoptively transferred DKO CD4+ T-cells into Rag1-/-. Surprisingly, these cells demonstrated enhanced clearance of *Pneumocystis*. The enhancement correlated directly to increased Stat3 function, assessed by a measured increase in IL-17a, IL-17f, and IL-22. Furthermore, when Stat3 was additionally knocked out, forming triple knockout (TKO), CD4+ T-cells lost the ability to control infection, showing that this enhancement is dependent on Stat3 signaling **(Figure 14D)**.

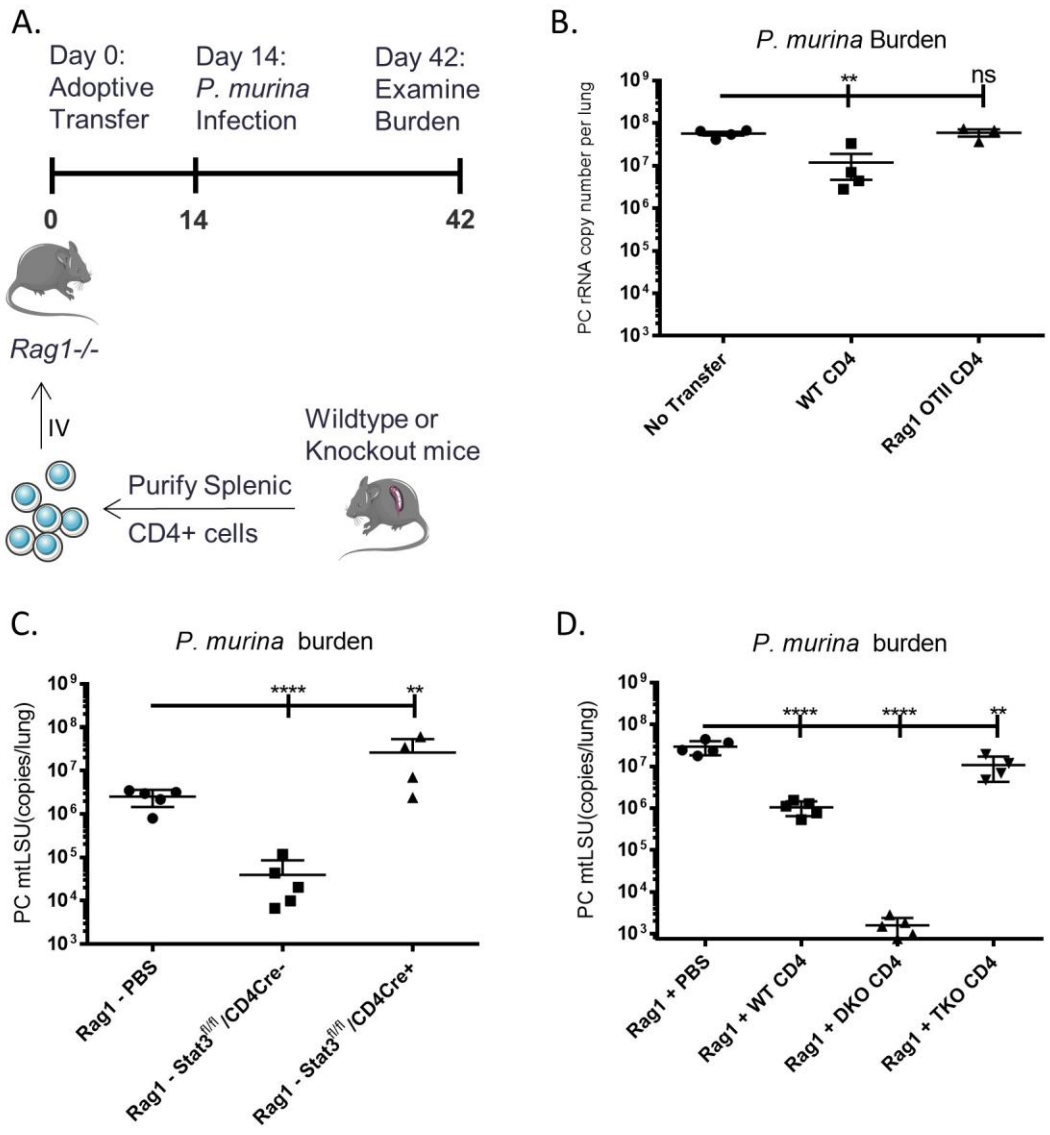


**Figure 14. CD4 intrinsic Stat3 required for clearance**

(A) Diagram depicting standard adoptive transfer protocol. Briefly, splenic CD4+ cells are purified from control and experimental mice, then adoptively transferred intravenously signifying Day 0. Mice are rested as cells homeostatically proliferate for 2 weeks. Mice are then infected for 4 weeks prior to endpoint readouts. (B-D) Total lung RNA was isolated and *Pneumocystis* burden was measured by real-time PCR of the mitochondrial Large Subunit rRNA copy number. Burden is reported as means + SEM for n ≥4 per group. P values are annotated as follows (*) ≤0.05, (**) ≤0.01, (***) ≤0.001, and (****) ≤0.0001. DKO- double knockout (Stat4/Stat6). TKO- triple knockout (Stat4/Stat6/Stat3$^{fl/fl}$|CD4-Cre+). Contributors: W. Elsegeiny; S. Khader provide IL-21-/- mice. Contributors: W. Elsegeiny and M. Zheng.

### 3.3.2 IL-21R signaling is necessary for control of *Pneumocystis* infection.

Many cytokines and factors activate Stat3, such as interferons, growth factors, and various interleukins. IL-6 and IL-21 are considered two important immunological activators of Stat3 in CD4+ T-cells. IL-21 is also the signature molecule for T follicular helper cells, so we next examined the importance of IL-21 signaling during *P. murina* infection. We infected and measured burden in IL-21 and IL-21 receptor knockout mice at 2 and/or 4 weeks after infection **(Figure 15A)**. At 4 weeks, both IL-21 and its receptor were shown to be critical for clearance **(Figure 15B)**. We followed up by examining burden and other markers at both 2 and 4 weeks of infection. The adaptive immune response against *Pneumocystis* starts at two weeks of infection, so burdens are still equivalent. However, by week, 4 WT mice cleared 90 to 99 percent of the infection, while IL21 receptor knockout mice remained heavily burdened **(Figure 15C)**. Furthermore, IL-21 receptor knockout mice showed no defect in Th1 transcription factor expression, Tbx21, or cytokine expression of IFN-γ **(Figure 15D,E)**. They also had no defect in Th2 transcription factor expression, Gata3, or cytokine expression of IL-13 **(Figure 15F,G)**. There was, however, a significant reduction the Th17 transcription factor expression, such as RORc and RORα expression **(Figure 15H,I)**.

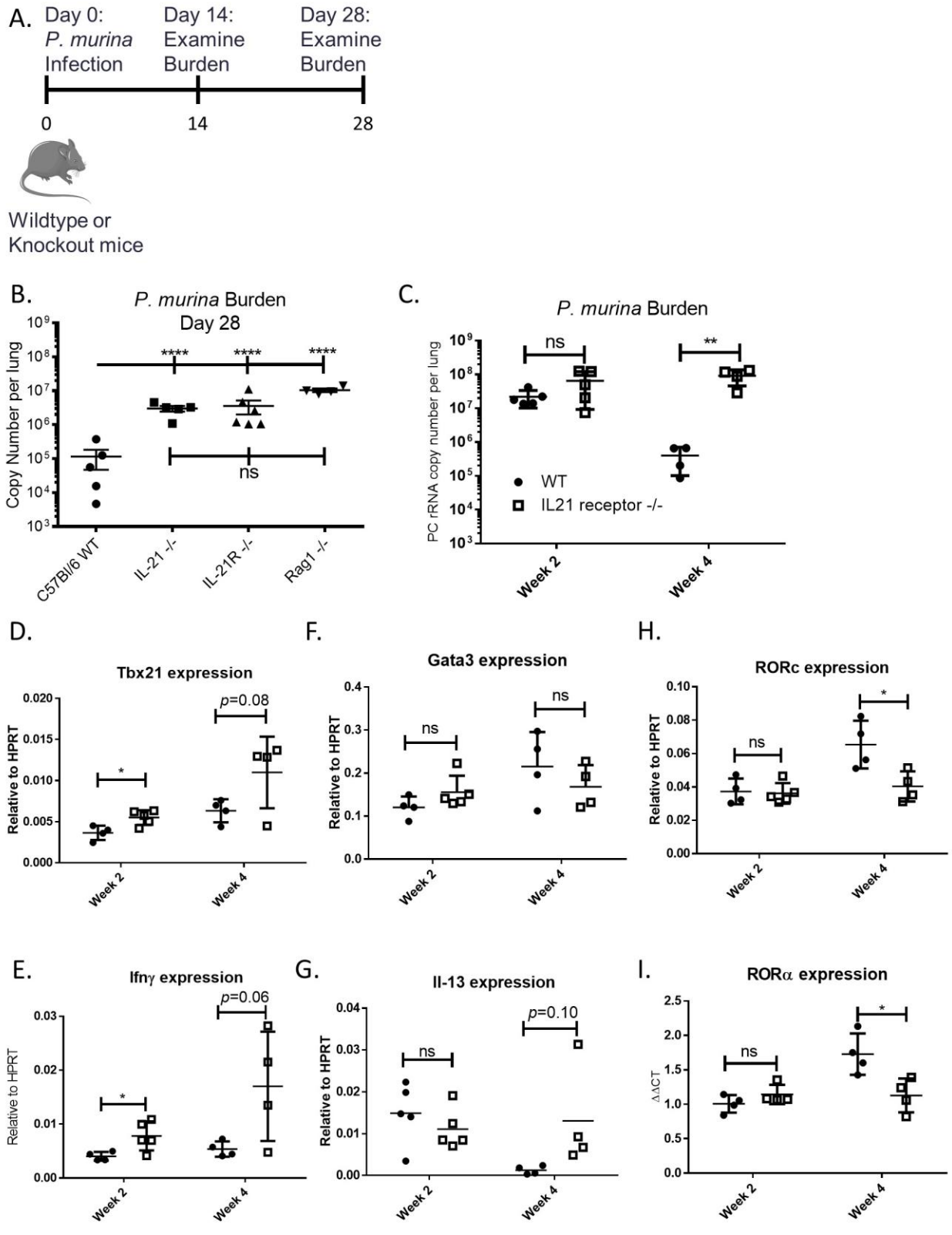


**Figure 15. IL-21 signaling required for *P. murina* clearance**

(A) Diagram depicting time-course infection model with inoculation of *P. murina* defined as Day 0, and burden examined on Day 14 and 28. Total lung RNA was isolated. (B-C) *Pneumocystis* burden was measured by real-time PCR of the mitochondrial Small Subunit rRNA copy number. (D-I) Gene expression was measured by real-time PCR, normalized to paired HPRT expression. Burden and gene expression are reported as means + SD for n ≥4 per group. P values are annotated as follows (*) ≤0.05, (**) ≤0.01, (***) ≤0.001, and (****) ≤0.0001. Contributors: W. Elsegeiny; S. Khader provided IL-21-/- mice.

### 3.3.3 IL-21 signaling is required for protective B- and T-cell responses.

We also took a close look at the B cell responses in mice deficient of IL21 signaling. Although IL21 and IL21 receptor deficient mice have normal levels of natural antibodies, as measured by anti-Chitin IgM titers **(Figure 16A)**, they have decreased IgG antibodies against whole *Pneumocystis* antigen **(Figure 16B)**. This was confirmed against a purified cyst-specific recombinant protein, Gsc1 **(Figure 16C)**. It is still unclear as to whether this decrease is due to antibody titer, affinity, or epitope differences, so we performed western with reduced and non-reduced *Pneumocystis* antigen, and with serum from *wild-type* or IL21r-/- mice. Mice deficient in IL21 signaling not only had weaker overall signal by western, but they also had different banding patterns **(Figure 16D)**. These data suggests that IL21r-/- mice may have a defect in antigen recognition, presentation, and/or immunogenicity. We then tested the functionality of the serum antibodies in an *in vitro* killing assay of *P. murina*, and as expected, serum from IL21r-/- mice had impaired complement-mediated killing **(Figure 16E)**. We next wanted to demonstrate this loss of functionality in an *in vivo* model, and as proof of concept, showed that adoptive transfer of ultra-convalescent serum (wild-type mice with multiple exposure to *Pneumocystis*) is enough to reduce burden by 2 to 3 logs **(Figure 16F,** left panel**)**. Standard wild-type convalescent serum only reduced burden by half a log, however, IL21r-/- serum was not able to

significantly reduce burden in vivo **(Figure 16F,** right panel**)**. Finally, we wanted to determine whether this immunodeficiency is associated with a defect in T follicular helper cell function, so we infected Cxcr5-/- mice with *Pneumocystis*. These mice, however, were fully capable of clearing infection, similar to the WT controls **(Figure 16G)**.

The ability for Cxcr5-/- mice to clear *Pneumocystis* suggests that the IL-21r-/- mice may also have additionally a T-cell defect, thus we examined whether intrinsic IL21 signaling on CD4+ T-cells is required for clearance. We adoptively transferred wild-type or receptor knockout CD4+ T-cells into Rag1-/- mice prior to infection **(Figure 17A)**. Unlike the wild-type controls, IL21r-/- CD4+ T-cells provided no protection against *Pneumocystis* **(Figure 17B)**. Although, IL21r-/- CD4+ T-cells were capable of infiltrating the lung **(Figure 17C)**, there was a slight reduction in recruitment **(Figure 17D,** upper panel**)**. Both wild-type and IL21r-/- CD4+ cells harvested from Rag1-/- mice were phenotypically similar, except, there was a small decrease in percentage of CD69+ CD127- CD4+ T-cells **(Figure 17D,** lower panel**)**. Since activated IL21r-/- CD4+ T-cells are capable of being recruited to the lung, we next tried dissect differences in the effector signals produced by each. We observed no significant difference in most analytes including IFNγ, TNFα, IL-5, IL1β, and GM-CSF. Although, there was a slight reduction in IL-17, levels were still high compared to the no transfer controls **(Figure 17E)**.

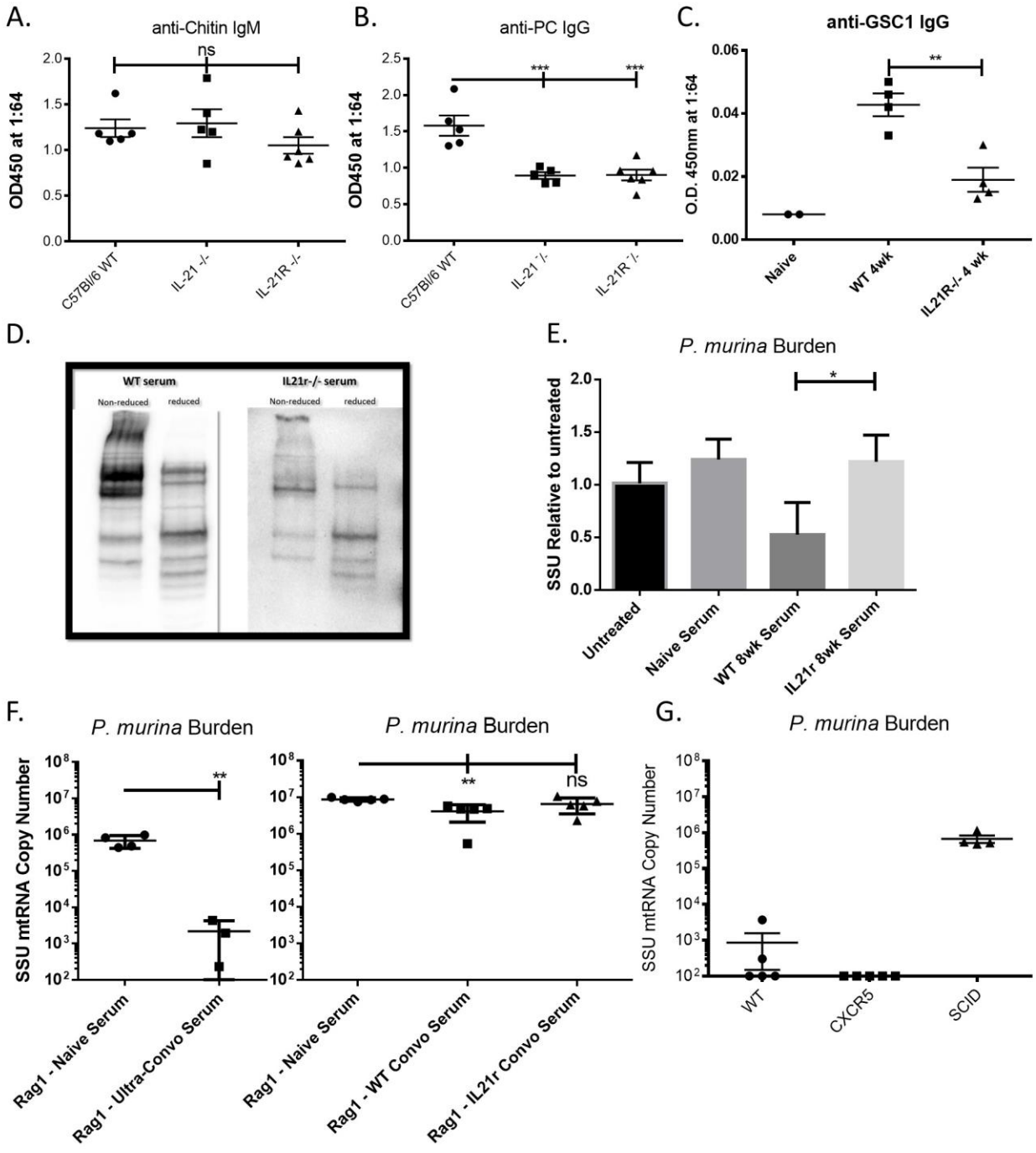


**Figure 16. IL-21 signaling required for B-cell mediated clearance against *P. murina* infection**

(A) Total Chitin specific IgMs, (B) total *P. murina* antigen specific IgGs, and (C) total GSC-1 specific IgGs were measured by direct ELISA of a 1 to 64 dilution of serum as primary and anti-mouse IgG-HRP secondary. (D) Western blots of 10μg (non-reduced or reduced) *Pneumocystis* antigen were stained directly with 1:500 dilution of serum as primary and anti-mouse IgG HRP secondary. Images acquired by chemiluminescence. (E) In vitro killing

assay with non-heat-inactivated serum. *Pneumocystis* burden was measured by real-time PCR of the mitochondrial Small Subunit rRNA normalized to untreated control. (F) Rag1-/- mice treated with a single dose of serum prior to 4 week infection. (G) Standard infection model. *Pneumocystis* burden was measured by real-time PCR of the mitochondrial Small Subunit rRNA copy number. Readouts are reported as means + SD for n ≥4 per group. P values are annotated as follows (*) ≤0.05, (**) ≤0.01, (***) ≤0.001, and (****) ≤0.0001. Contributors: W. Elsegeiny and T. Eddens.

### 3.3.4 Defining a role for IL-22 during *Pneumocystis* infection.

In order to identify the CD4 signals required for clearance, we differentiated naïve wild-type, Stat3-deficient, and IL21r-/- CD4+ T-cells in vitro under Th1, Th2 and Th17 conditions. We then analyzed the cytokine and chemokine profiles of each, and targeted factors that were impaired in both Stat3-deficient and IL21r-/- CD4+ T-cells. Stat3-deficient CD4+ T-cells had impaired production of many cytokines including IL-2, IL-13, IL-17A/F, IL-22, GM-CSF, CD40L, Mip3α, and TNFα/β. However, the IL-21r-/- CD4+ T-cells were only impaired in IL-22 production **(Figure 18A)**. To validate this in vivo, we transferred WT and IL-21r-/- CD4+ T-cells into Rag1-/- mice, followed by *P. murina* infection for 2 weeks, and finally assayed purified CD4+ cells by RNAseq **(Figure 18B)**. RNAseq analysis verified results from the T-cell differentiation assay, and revealed IL-22 expression during *P. murina* infection in wild-type mice, which was absent in IL-21r-/- mice **(Figure 18C)**.

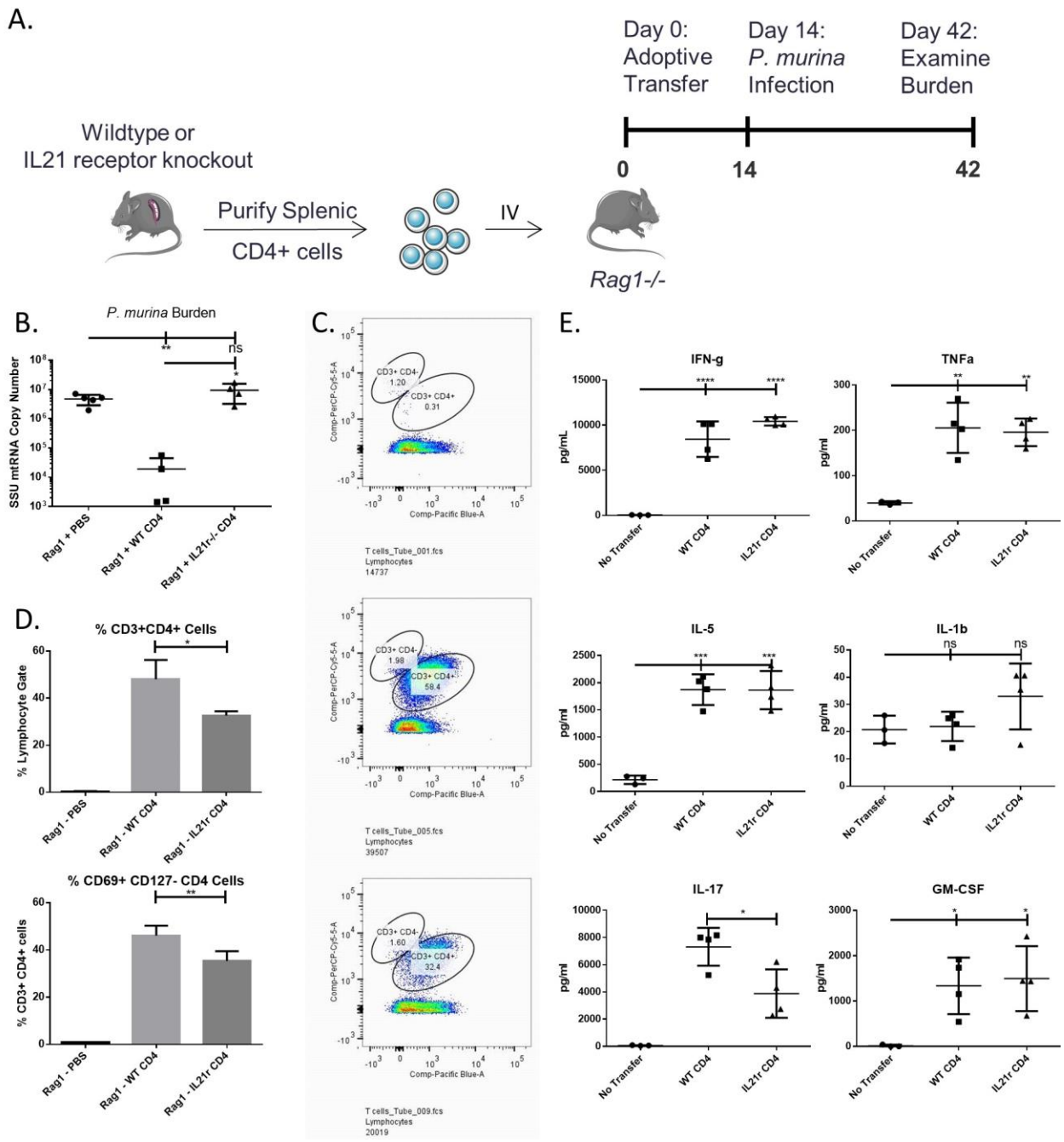


**Figure 17. CD4 intrinsic IL21r signaling is required for protection**

(A) Diagram depicting standard adoptive transfer protocol. Briefly, splenic CD4+ cells are purified from control and experimental mice, then adoptively transferred intravenously signifying Day 0. Mice are rested as cells homeostatically proliferate for 2 weeks. Mice are then infected for 4 weeks prior to RNA, Protein, and cellular endpoint readouts. (B) *Pneumocystis* burden was measured by real-time PCR of the mitochondrial Small Subunit rRNA copy number. (C) Flow cytometry of whole lung from Rag1-/- mice without CD4 transfer (upper panel), with

WT CD4+ cell transfer (middle panel) and IL-21r-/- CD4+ cell transfer (lower panel). Panels are gated on lymphocyte FSC/SSC, and stained with Y-axis (CD3) and X-axis (CD4). Representative images of n ≥3 per group. (D) Cumulative percentage values from FACS panels (upper panel). (Lower panel) gated on CD3+CD4+, cumulative percentages of CD69+CD127- cells. (E) WLCs were cultured in the presence of *P. murina* antigen for 72 hours. All cytokines were analyzed simultaneously by Millipore multiplex on a bioplex reader. All data are reported as means + SD for n ≥3 per group. P values are annotated as follows (*) ≤0.05, (**) ≤0.01, (***) ≤0.001, and (****) ≤0.0001. Contributors: W. Elsegeiny and T. Eddens.

To determine the physiological relevancy of IL-22 during *Pneumocystis* infection, we stained naïve and *Pneumocystis* infected lung tissue for IL-22 receptor (IL-22rα1). Naïve lungs do not stain for IL-22rα1 **(Figure 18D)**, however, *Pneumocystis* infected lungs have intense staining throughout the alveolar space **(Figure 18E)**. Upon closer inspection, the alveolar epithelial cells are surprisingly not the most intensely stained cell type, but instead large, globular, mononuclear cells **(Figure 18E,** red arrows**)**. Interestingly, Rag1-/- mice infected with *Pneumocystis* lack these macrophage-like cells, which also revealed apparent staining of the trophic form of *Pneumocystis* **(Figure 18F)**.

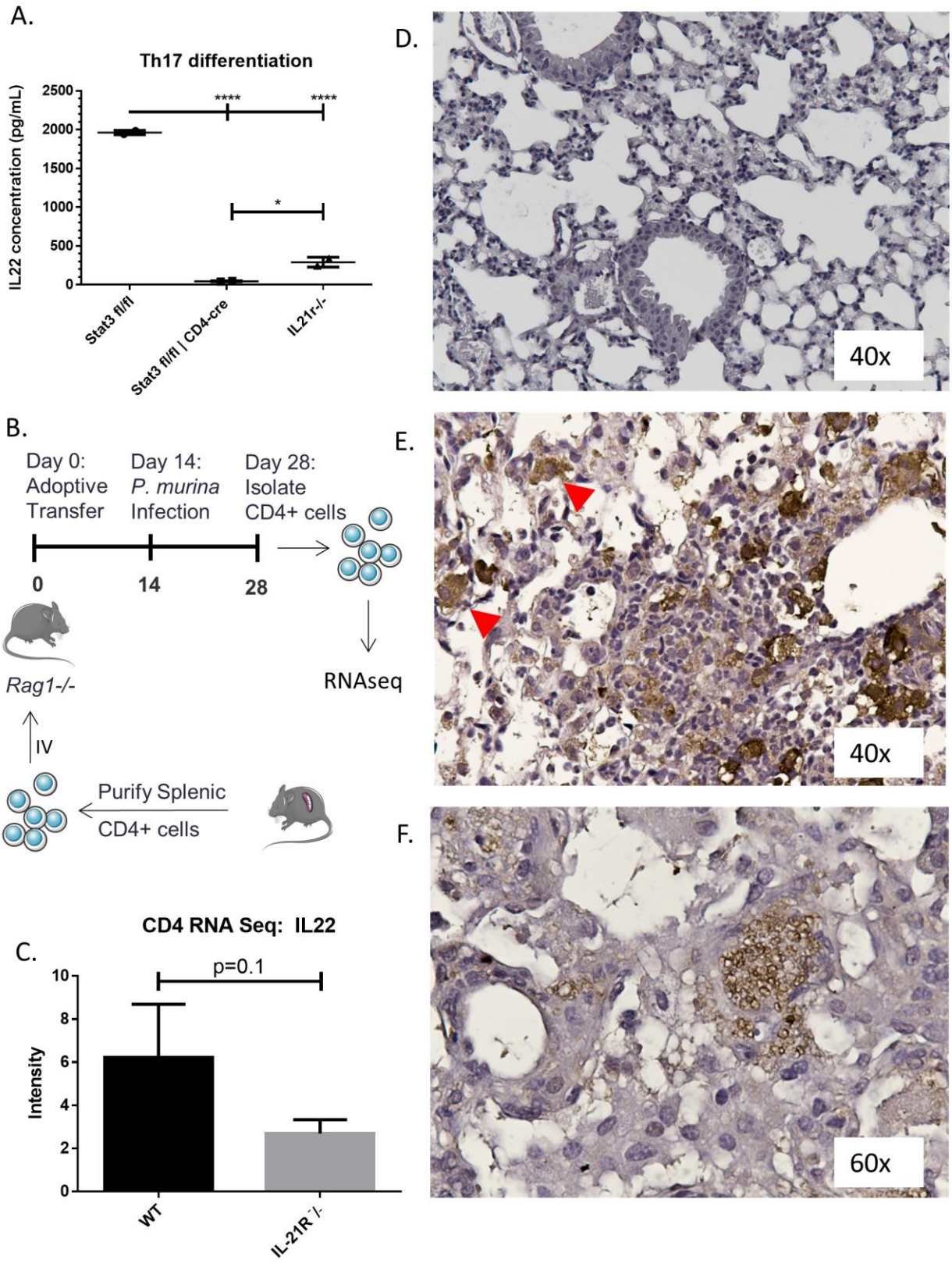


**Figure 18. IL-22 signaling is increased during *Pneumocystis* infection**

(A) Purified naïve CD4+ cells were cultured in Th17 conditions. IL-22 was one of a panel of cytokines that were analyzed simultaneously by multiplex analysis, n =2. (B) Diagram depicting *in vivo* T-cell phenotyping. Briefly, splenic CD4+ cells are purified, then adoptively transferred intravenously at Day 0. Mice are rested as cells homeostatically proliferate for 2 weeks. Mice are then infected for 2 weeks prior to retrieving CD4+ T-cells for RNA extraction and sequencing. (C) RNAseq intensity values for IL-22 gene expression in WT and IL21r-/- CD4+ T-cells, n ≥2. (D) Naïve WT, (E) 2 week *P. murina* infected WT, and (F) 4 week infected Rag1-/- representative images of mouse lung tissue, stained with anti-IL-22ra1 immunohistochemistry, n=3. All data are reported as means + SD. Contributors: W. Elsegeiny, D. Pociask, Radha Gopal, and W. Horne.

### 3.3.5 IL-22 supports the clearance of *Pneumocystis*

To test whether IL-22 is required for clearance, we once again used the adoptive transfer model. Briefly, splenic CD4+ cells were purified from IL-22-/- mice and transferred into Rag1-/- mice. Mice were given two weeks for homeostatic proliferation and infected with *P. murina* for 4 weeks **(Figure 19A)**. At the end of week 4, IL-22-/- mice had significantly higher burden than wild-type controls **(Figure 19B)**. Degree of clearance in wild-type CD4 recipients, was directly correlated with the expression of IL-22 and associated genes such as S100a8 **(Figure 19C&D)**. However, during a 6 week infection, IL-22-/- CD4 recipients begin to clear infection, suggesting IL-22 may only play a supportive role **(Figure 19E)**. It is also possible that there are multiple modes for clearance. Next we examined whether IL-22 was sufficient to mediate clearance. Briefly, IL-21r-/- mice were infected with *P. murina* for 2 weeks, followed by 4 doses of recombinant IL-22-FC over the following two weeks. Burden was examined at the end of the 4$^{th}$ week of infection **(Figure 19F)**, and the IL21r-/- mice that received treatment had approximately a 10-fold reduction in burden **(Figure 19G)**. Next we performed the same experiment with CD4-depleted mice, however, IL-22 treatment had no effect **(Figure 19H)**.

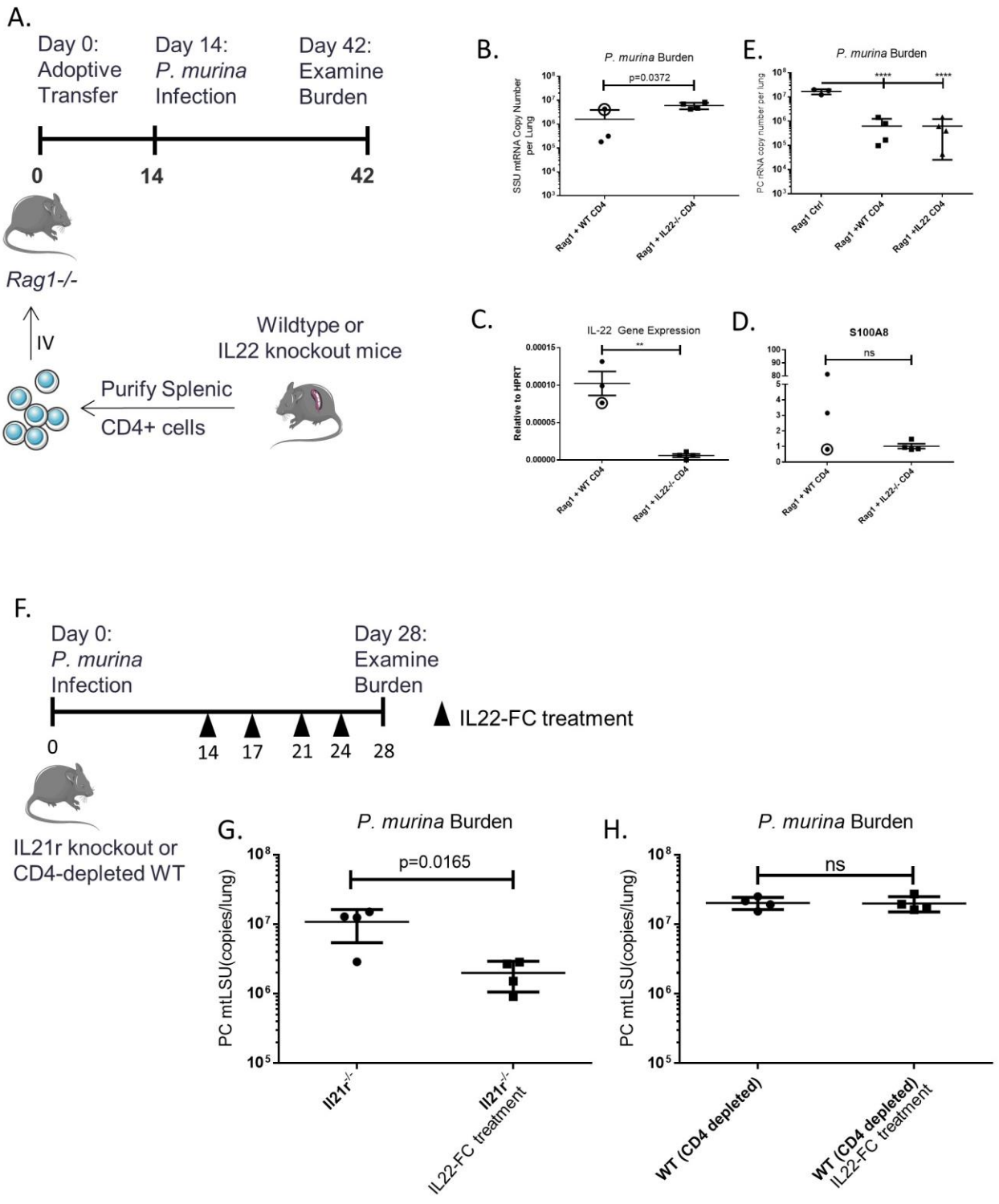


**Figure 19. IL-22 supports clearance of *P. murina* infection**

(A) Diagram depicting standard adoptive transfer protocol. Briefly, splenic CD4+ cells are purified from control and experimental mice, then adoptively transferred intravenously signifying Day 0. Mice are rested as cells

homeostatically proliferate for 2 weeks. Mice are then infected for 4 weeks prior to endpoint readouts. (B) *Pneumocystis* burden was measured by real-time PCR of the mitochondrial Small Subunit rRNA copy number. (C.D) Gene expression was measured by real-time PCR, normalized to paired HPRT expression. (E) Diagram depicting IL22 treatment model. Briefly, IL21r-/- or CD4-depleted WT mice are infected with *P. murina* for 2 weeks, followed by 2 weeks of IL-22-FC treatment at 2 doses per week. (F-G) *Pneumocystis* burden was measured by real-time PCR of the mitochondrial Small Subunit rRNA copy number. Burden and gene expression are reported as means + SD for n ≥3 per group. P values are annotated as follows (*) ≤0.05, (**) ≤0.01, (***) ≤0.001, and (****) ≤0.0001. Contributors: W. Elsegeiny and L. Monin.

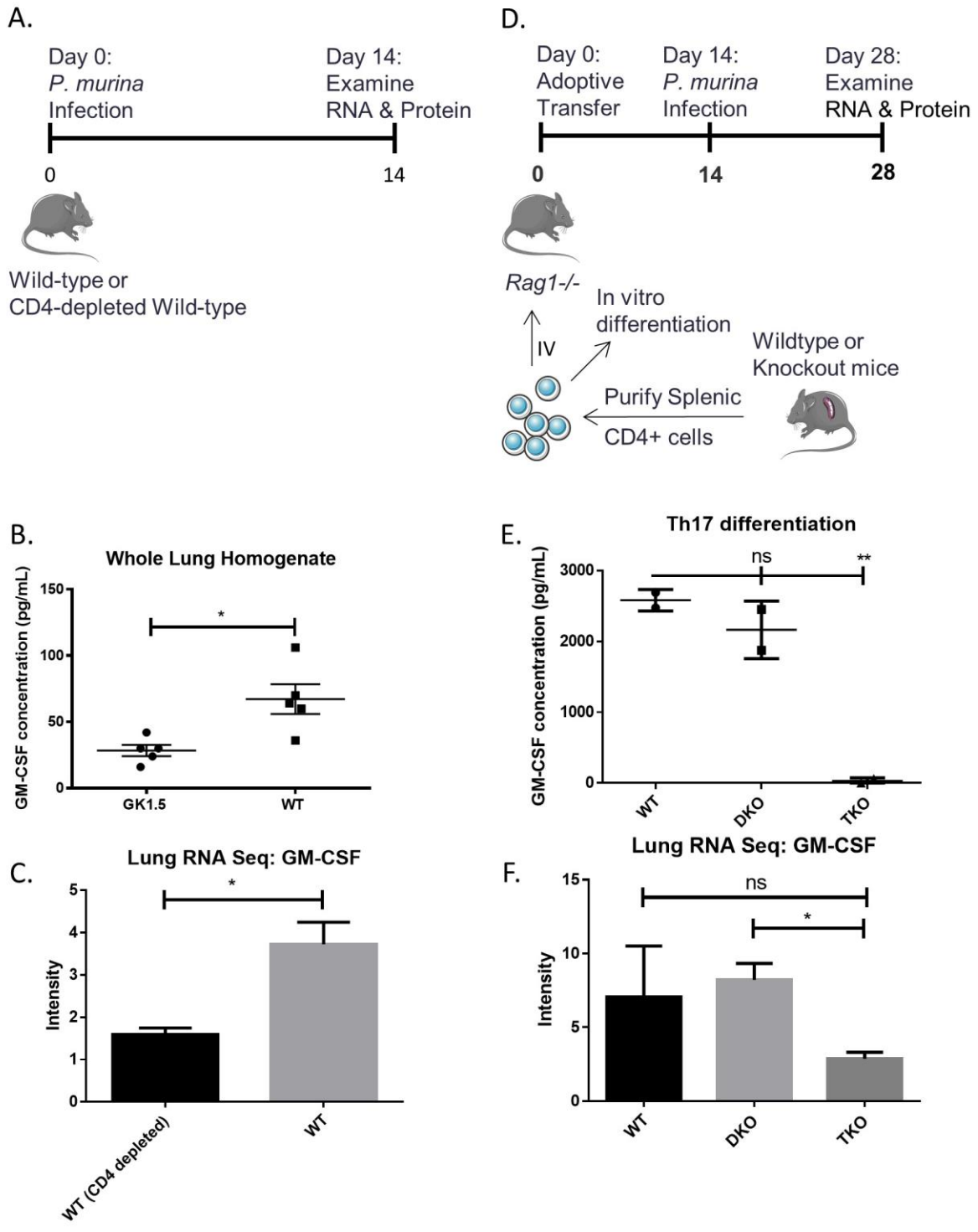


**Figure 20. CD4+ T-cells produce GM-CSF during infection**

(A) Diagram depicting the CD4-phenotyping infection model with inoculation of *P. murina* defined as Day 0, followed by RNA and protein isolation at Day14. (B) An indirect GM-CSF ELISA using 25ul of whole lung protein

homogenate. n=5. (C) RNAseq intensity values for GM-CSF expression in WT control and CD4-depleted mice, n =3. (D) Diagram depicting standard adoptive transfer protocol. Briefly, splenic CD4+ cells are purified from control and experimental mice, then adoptively transferred intravenously signifying Day 0. Mice are rested as cells homeostatically proliferate for 2 weeks. Mice are then infected for 2 weeks prior to endpoint readouts. (E) Naïve CD4+ cells were stimulated under Th17 conditions. GM-CSF was one of a panel of cytokines that were analyzed simultaneously by Millipore multiplex on a bioplex reader, n =2. (C) RNAseq intensity values for GM-CSF expression in WT, DKO, and TKO adoptively transferred Rag1-/- lung RNA. Values are reported as means + SD. P values are annotated as follows (*) ≤0.05, (**) ≤0.01, (***) ≤0.001, and (****) ≤0.0001. Contributors: W. Elsegeiny, T. Eddens, and W. Horne.

### 3.3.6 GM-CSF-producing CD4+ T-cells are required for clearance of *P. murina* infection.

Since IL-22 alone was not sufficient to rescue CD4-depleted mice, we reexamined RNA and protein for factors expressed in IL-21r-/- mice that are absent in CD4-depleted mice. At 2 weeks of infection, wild-type mice have detectable levels of GM-CSF by ELISA and RNAseq, and this is diminished during CD4-depletion **(Figure 20A-C).** Similarly, Stat3-deficient CD4+ T-cells have ablated GM-CSF production during Th17 differentiation **(Figure 20D&E)**. Also, upon adoptive transfer, Stat3-deficient CD4+ T-cells have diminished expression of Csf2 **(Figure 20D&F)**.

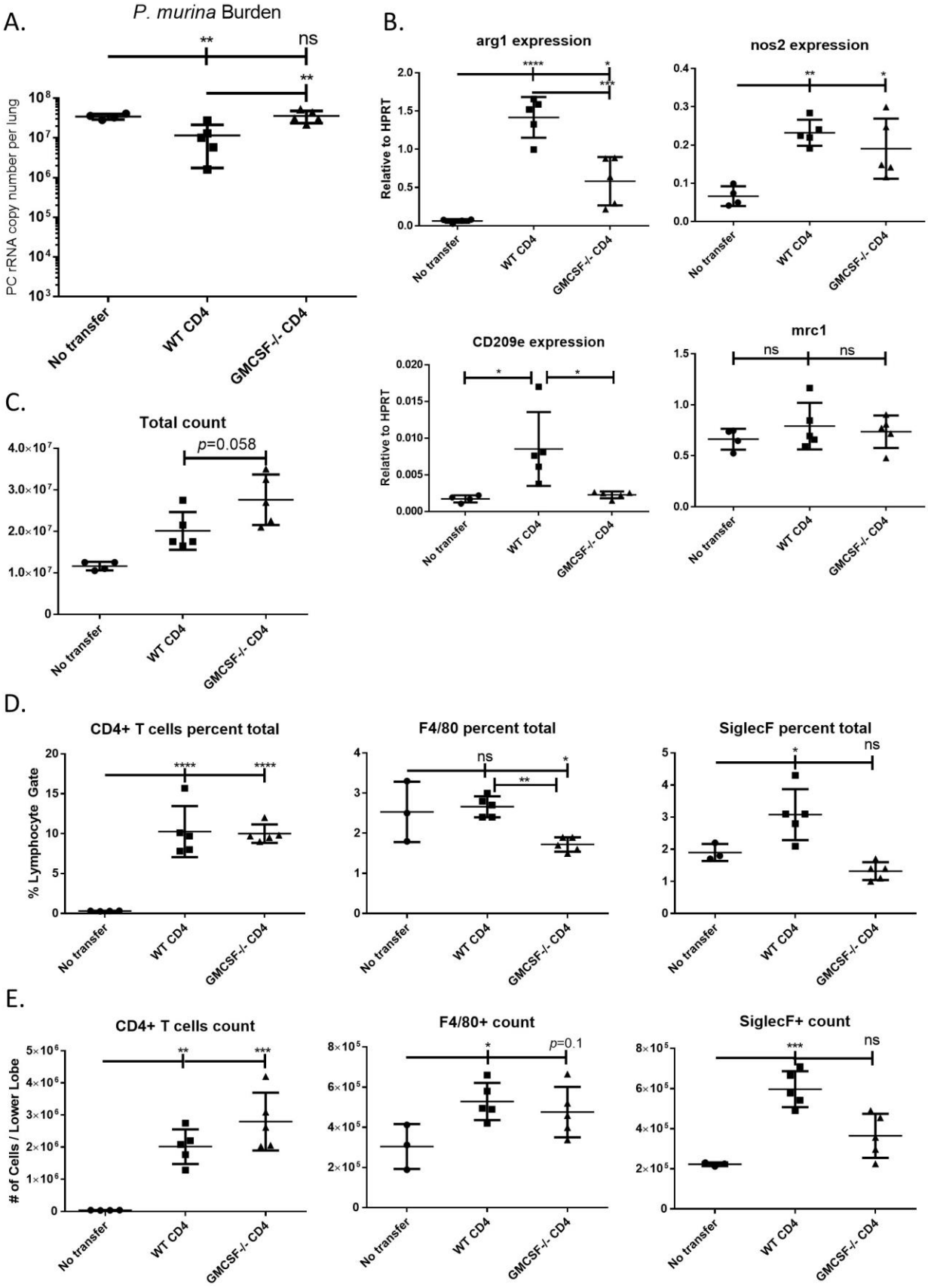
A.
P. murina Burden
PC rRNA copy number per lung
No transfer
WT CD4
GMCSF-/- CD4
B.
arg1 expression
Relative to HPRT
nos2 expression
CD209e expression
mrc1
C.
Total count
p=0.058
D.
CD4+ T cells percent total
% Lymphocyte Gate
F4/80 percent total
SiglecF percent total
E.
CD4+ T cells count
# of Cells / Lower Lobe
F4/80+ count
SiglecF+ count

**Figure 21. GM-CSF is required for *P. murina* clearance**

(A) Adoptive transfer model using WT or GM-CSF-/- CD4+ T-cells. *Pneumocystis* burden was measured by real-time PCR of the mitochondrial Small Subunit rRNA copy number. (B) Gene expression was measured by real-time PCR, normalized to paired HPRT expression. (C) Total cells counts are estimated live cell numbers, calculated by Life technologies countess. (D) Cumulative percentages of whole lung flow cytometry from Rag1-/- mice, and (E) calculated total numbers. Left panels is gated on CD3+CD4+ cells, middle panel is gated on F4/80+MHCII+, and right panel is gated on SiglecF+CD11b+. All readouts are reported as means + SD for n ≥4 per group. P values are annotated as follows (*) ≤0.05, (**) ≤0.01, (***) ≤0.001, and (****) ≤0.0001. Contributors: W. Elsegeiny and T. Eddens; Z. Chroneos provides GM-CSF-/- splenocytes.

Using the adoptive transfer model, we tested whether GM-CSF was required for *P. murina* clearance. GM-CSF-/- CD4+ T-cells did not provide protection when adoptively transferred into Rag1-/- mice **(Figure 21A)**. Whole lung quantitative RNA analysis revealed that GM-CSF-/- CD4+ T-cell recipients had reduced arginase (Arg1) expression, but equivalent inos (Nos2). Also, unlike their wild-type controls, GM-CSF-/- CD4+ T-cell recipients have no upregulation of the C-type lectin receptor (CD209e), but have equivalent levels of mannose receptor C type 1 (Mrc1) **(Figure 21B)**. GM-CSF-/- CD4+ T-cell recipients had equivalent counts of total cells **(Figure 21C)**, CD4+ T-cells, and F4/80+ macrophages per lobe **(Figure 21D&E,** left and middle panels**)**. However, they did have significantly fewer recruited SiglecF+ eosinophils **(Figure 21D&E,** right panels**)**.

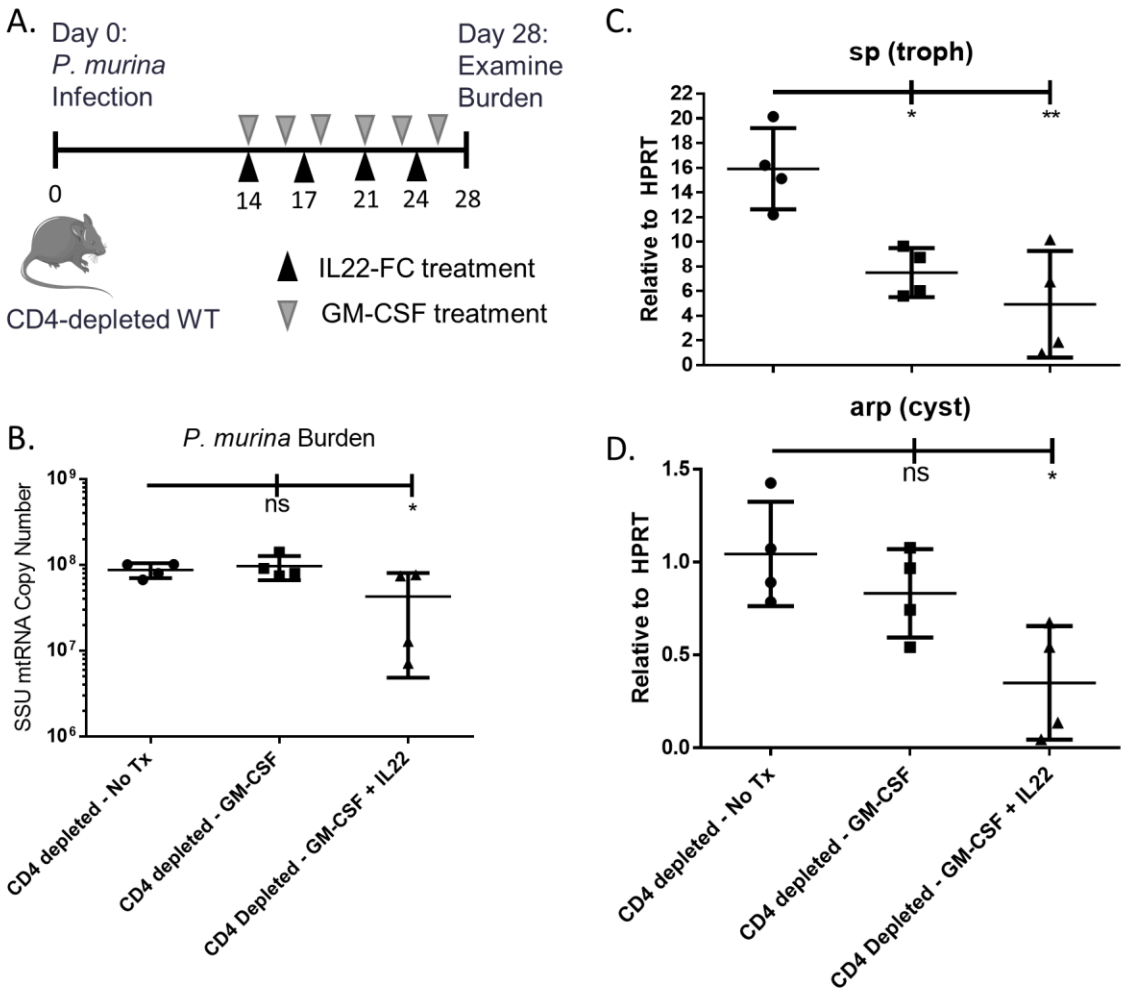


**Figure 22. GM-CSF and IL-22 work cooperatively to clear *Pneumocystis* infection**

(A) Diagram depicting GM-CSF +/- IL-22-FC treatment model. Briefly CD4-depleted WT mice are infected with *P. murina* for 2 weeks, followed by 2 weeks of recombinant GM-CSF treatment at 3 doses per week with or without IL-22-FC at 2 doses per week. (B) *Pneumocystis* burden was measured by real-time PCR of the mitochondrial Small Subunit rRNA copy number. (C,D) *Pneumocystis* cyst and troph specific gene expressions were measured by real-time PCR, and normalized to paired HPRT expression. Burden and gene expressions are reported as means + SD for n =4 per group. P values are annotated as follows (*) ≤0.05, (**) ≤0.01, (***) ≤0.001, and (****) ≤0.0001. Contributors: W. Elsegeiny and T. Eddens.

Finally, we wanted to determine if GM-CSF and IL-22 functioned cooperatively to mediate clearance of *Pneumocystis* infection. CD4-depleted wild-type mice were infected with *P. murina* for 2 weeks then were given 6 doses of recombinant GM-CSF +/- 4 doses of IL-22-FC over the following 2 weeks **(Figure 22A)**. Mice treated with GM-CSF alone showed no reduction in overall burden as measured by SSU, however, mice that received a combination of GM-CSF and IL-22 had a significant reduction in burden **(Figure 22B)**. Interestingly, GM-CSF alone was capable reducing the trophic form of *Pneumocystis* **(Figure 22C)**, however, only the combination of GM-CSF and IL-22 was able to reduce the cystic form **(Figure 22D)**.

## 3.4 DISCUSSION

Since the implementation of combinational antiretroviral therapy and anti-fungal prophylaxis, *Pneumocystis* pneumonia has reemerged as a predominantly HIV-negative infection while still maintaining its rank as the leading opportunistic infection in HIV-positive patients. Although, much has been studied as to what factors may lead to susceptibility, CD4+ T-cell count below 200 cells per microliter is still considered the primary indicator. However, the exact CD4+ T-cell effector functions that mediate clearance is still unknown. We initially attempted to address this question by infecting mice deficient in Th1, Th2, or Th17 immunity through the use of cytokine and cytokine receptor knockout mice. IL-12p40-/- mice have a defect in Th1 differentiation, thus are deficient in IFNγ production, while IL-4rα-/- mice are unable to signal through the Th2 signature cytokine, IL-4. Finally, IL-23α-/- and IL-17rα-/- are incapable of mounting a Th17 response. Surprisingly, none of these knockout mice were susceptible to *Pneumocystis* infection.

At this point, it could be speculated that more than one subset could mediate clearance, or that less conventional T helper signals are required.

Thus, we took a broader approach and targeted the Stat transcription factors for each T helper subset. Stat4 and Stat6, which are involved in the differentiation of Th1 and Th2 cells, respectively, were not required for clearance of *Pneumocystis* infection. However, Stat3-deficient T-cells, that are completely deficient in mounting Th17 responses, could not clear infection. This was also verified using adoptive transfer of Stat3-deficient CD4+ T-cells into Rag1-/- mice. Interestingly, Stat4/Stat6 double knockout CD4+ T-cells have enhanced Stat3 function, which is correlated with improved clearance of *Pneumocystis* infection. Additionally removing Stat3 from Stat4/Stat6 DKO CD4+ T-cells leads to a loss of their protective capacity. Although Stat3 is required, RORc-/- CD4+ T-cells which are completely deficient in Th17 responses, are capable of clearing infection. In short, a Th17-independent Stat3 response is required for CD4 mediated clearance of *Pneumocystis*.

Stat3 plays a role in many cell types and is involved numerous functions from immunity to embryogenesis. In CD4+ T-cells, Stat3 can be activated by IL-6, but more recent literature suggests that IL-21 can activate Stat3 through a distinct route. In exploring the potential role of IL-21 signaling, we observed that IL-21 and IL-21 receptor knockout mice are susceptible to *Pneumocystis* infection. Patients with loss-of-function IL-21 receptor mutations suffer from a primary immunodeficiency syndrome, presenting with multiple infections including, *Pneumocystis jirovecii* [159]. IL-21r-/- mice have impaired antibody responses to *Pneumocystis* infection, particularly in the generation of effective IgG class-switched antibody responses. To rule out impaired T follicular helper functions as cause for this immunodeficiency, we demonstrated that Cxcr5-/- mice have no defect in clearance of *Pneumocystis* infection.

CD4+ T-cell responses, such as Tbx21 and Gata3, appeared to be intact in IL-21r-/- mice, though there was a slight decrease in RORc and RORα expression. Interestingly, adoptive transfer of IL-21r-/- CD4+ T-cells into Rag1-/- mice provided no protection against *Pneumocystis* infection, suggesting that IL21r-/- CD4+ T-cells have an impaired effector function. In order to define the missing signal, we performed RNA sequencing on CD4 cells purified from the Rag1-/- mice, and found a decrease of IL-22 in the IL-21r-/- mice. This was corroborated by the in ability of IL21r-/- CD4+ T-cells to produce IL-22 at the protein level, when differentiated under Th17 conditions. Additionally, it has been recently published that IL-21 signaling is important for IL-22 production in a Ahr and Stat3 dependent pathway [160]. By staining, IL-22 receptor is upregulated during *Pneumocystis* infection, and appears to be primarily on macrophages. We explored the role of IL-22 production during *P. murina* infection by adoptively transferring IL-22-/- CD4+ T-cells into Rag1-/- mice and observed a decrease in efficiency of clearance. Furthermore, treatment of IL-21r-/- mice with IL-22 was able to significantly reduce burden. However, this effect could not be observed in CD4-depleted wild-type mice, suggesting that IL-22 works in collaboration with at least one other factor to mediate clearance. GM-CSF has previously been shown to have some therapeutic effect during *Pneumocystis* infection [161], but even though IL-21r-/- mice express GM-CSF, they are not protected from infection.

Considering GM-CSF as the potential co-signal for *Pneumocystis* clearance, we tested whether GM-CSF producing CD4+ T-cells were required for clearance. As expected, GM-CSF-/- CD4+ T-cells could not provide protection in the adoptive transfer model. This was correlated with lower arginase and CD209e expression. Finally, when testing whether GM-CSF and IL-22

could synergistically reduce burden in CD4-depleted WT mice, we observed a significant decrease in burden with the combinational treatment.

To conclude, Stat3 signaling in CD4+ T-cells is required to generate a protective immune response against *Pneumocystis* infection, however, it is independent of IL-17 and IL-23 signals. We also identified IL-21 receptor as a key signaling pathway that is required to mediate clearance. Using a variety of approaches, we determined that GM-CSF and IL-22 play important roles during *Pneumocystis* infection. GM-CSF+ CD4+ T-cells are required for T-cell mediated clearance, however, it alone is not sufficient. While IL-22, although not required, is sufficient to reduce burden in IL-21 receptor knockout mice. These data suggest a model of clearance that requires non-classical T helper cell function may explain the discrepancies observed in previous studies.

# 4.0 CHAPTER 4: CONCLUSIONS AND FUTURE PERSPECTIVES

*Pneumocystis jirovecii* pneumonia (PJP) has remained a major opportunistic infection in HIV-positive patients, but in the last decade has reemerged as a primarily HIV-negative infection [162]. Patients that receive prophylaxis have lower risk of acquiring infection, and reduced disease severity and mortality. However, TMP-SMX, a relatively toxic drug, is the primary medication for prophylaxis, and is generally only prescribed to established at-risk populations. Identifying these at-risk populations can be complicated due to the combinational drug nature of patients that acquire infection. To determine if patients receiving anti-CD20 therapy are at risk for developing PJP, we developed an *in vivo* murine model of CD20-depletion. Our results confirmed that anti-CD20 alone is capable of inducing susceptibility to *Pneumocystis* infection by diminishing the immune response to *Pneumocystis* in the lung. We deduce that patients receiving anti-CD20 therapy should be considered as a risk group for *Pneumocystis* infection and be carefully monitored.

However, it is important to consider that these experiments were conducted with naïve mice, and that most individuals are seropositive for anti-*Pneumocystis* antibodies [120, 146]. Experimentally, we observed that convalescent mice are capable of clearing *Pneumocystis* without the aid of CD4 or CD20+ cells. Since memory CD4+ cells and antibodies are sufficient to clear *Pneumocystis*, these data raise a question as to why immunosuppressed patients acquire *Pneumocystis jirovecii* infections. Anti-CD20 antibody therapy in patients alone has not been

shown to decrease immunoglobulin levels, however, when combined with other immunosuppressive therapies hypogammaglobulinaemia can occur [148]. It has also been demonstrated that *Pneumocystis* can alter their major surface glycoproteins creating dynamic extracellular epitopes, which is implicated as a mechanism in evading the host immune response [149, 150]. Furthermore, reports of large genetic variability between *Pneumocystis jirovecii* isolates also suggests the possibility that patients are simply being exposed to a new strain or special form of *Pneumocystis* [143, 151].

We explored the underlying cause for susceptibility and found a general decrease in immune response, particularly type 2, in mice treated with anti-CD20. CD4+ T-cells specifically were not capable of providing protective responses in an adoptive transfer model, thus suggesting that anti-CD20 inhibits T-cell priming to *P. murina.* Interestingly, the absence of CD20+ B-cells during *Pneumocystis* infection may also lead to clonal deletion of *Pneumocystis* specific CD4+ cells. CD4+ T-cells from anti-CD20 treated mice are not as capable of clearing *Pneumocystis* as CD4+ T-cells cells from naïve mice. This may be due to a lack of CD4+ T-cell costimulation by B-cells during *Pneumocystis* infection, which would lead to cell death or anergy. It is still not understood why other antigen presenting cells (APCs) beside CD20+ B-cells are not sufficient to compensate for the loss of CD20+ B-cells. CD40 and MHC class II on B-cells have been shown to be critical for the CD4+ T -cell priming, but these are not exclusively expressed on B cells. [89]. We hypothesize that a B-cell specific costimulatory molecule would be a plausible explanation for these results.

To examine the role of Th2 responses during *Pneumocystis* infection, we first analyzed type 2 responses in an infection time-course model with WT and CD4-depleted mice. We found that IL-5 transcription levels peaked by day 7 post infection. This production was lost in CD4-

depleted animals, suggesting an early adaptive immune response to infection. This led us to ask the question whether eosinophils play a role in *Pneumocystis* infection.

Classically recognized as mediators of immunity against helminths, Eosinophils have recently been shown to play a role against a variety of pathogens, including bacterial, viral, and even fungal infections. For example, eosinophils contribute to host defense against *Aspergillus fumigatus*, a fungal pathogen, through a secretory factor. [144, 145]. In our studies, Gata1$^{tm6Sho}$/J, eosinophil-deficient, mice had delayed clearance of *P. murina* infection, while mice treated with IL-5 had an eosinophilia-mediated reduction in burden. This was observed in both CD4-depleted and Rag1-/- mice, but not in the Gata1$^{tm6Sho}$/J mice. In collaboration with Chad Steele, we also showed eosinophils display antifungal activity *in vitro*, and that addition of IL-4 and IL-13 greatly enhanced killing of *Pneumocystis*. Cumulatively, these data suggest that Th2 cytokines in the lung may mediate some degree of clearance during *Pneumocystis* infection, and that anti-CD20 therapy diminishes these responses.

However, the CD4+ T-cell factors that are absolutely required for clearance are still unknown. Exploring the role of each T helper cell subset (Th1, Th2, or Th17), we used of variety of cytokine and cytokine receptor knockout mice. For example, we used IL-12p40-/- mice which have a defect in Th1 differentiation and IFNγ production, and IL-4rα-/- mice that are unable to signal through the Th2 signature cytokine, such as IL-4. To analyze the importance of Th17 responses, we used IL-23α-/- and IL-17rα-/-. In short, none of these knockout mice are susceptible to *Pneumocystis* infection. This meant that either more than one subset could mediate clearance and compensate for the loss of another, or that less conventional T helper signals are required.

Taking a broader approach, we targeted the signal transducers and activators of transcription (Stat) for each T helper subset. Stat4, Stat6, and Stat3 are involved in the differentiation of Th1, Th2, and Th17 cells, respectively. Although, Stat4-/- and Stat6-/- mice could mediate clearance of *Pneumocystis* infection, T-cell specific Stat3-deficient mice are completely susceptible. This was confirmed by adoptively transferring of Stat3-deficient CD4+ T-cells into Rag1-/- mice. To determine whether Stat4 and Stat6 played supportive or compensatory roles, we generated Stat4/Stat6 double knockout (DKO) mice. Remarkably, DKO CD4+ T-cells have enhance clearance of *Pneumocystis* infection, which correlated with increased Stat3 function. Removing Stat3 from DKO CD4+ T-cells ablates their protective capacity, further clarifying the importance of Stat3. Rorc-/- mice and CD4+ T-cells, although also lack most Th17 cell responses, do not have the same phenotype. This indicates that Stat3 signaling in CD4+ T-cells is required for clearance of infection independent of Th17 responses.

Stat3 is involved in many functions from embryogenesis to immunity. The specific cell types, signals, receptors, and cofactors that play a large role in mediating Stat3's function are very numerous and complex. In the context of CD4+ T-cells, Stat3 is typically known to be activated by IL-6, but more recently literature suggests that IL-21 receptor on T-cells also signals through Stat3. T follicular helper cells are thought to be the primary producers of IL-21, thus we explored the role of T follicular helper cells and IL-21 during *Pneumocystis* infection. We observed that IL-21 and IL-21 receptor knockout mice were in fact susceptible to infection. This susceptibility translates clinically as patients with loss-of-function IL-21 receptor mutations present with a primary immunodeficiency syndrome complicated by multiple infections, including *Pneumocystis jirovecii* [159]. In our studies, IL-21r-/- mice have impaired antibody responses to *Pneumocystis* infection, specifically in the generation of class-switched antibody

responses, which can also be observed in patients with IL-21r mutations. This demonstrates that IL-21 is required for T helper cell function in B-cell activation. However, Cxcr5-/- mice, which are deficient in germinal centers, are capable of clearing *Pneumocystis*, suggesting that IL-21 signaling must be required for more than just B-cell responses.

Next we tested whether IL-21r-/- mice had defective CD4+ T-cell responses. *Pneumocystis*-infected lung tissue of IL21r-/- mice had normal expression of Tbx21 and Gata3, however, there was a modest decrease in RORc expression. We elucidated the CD4+ T-cell defect by adoptively transferring IL-21r-/- CD4+ T-cells to Rag1-/- mice. The IL-21r-/- CD4+ T-cells were not able to provide any protection, although they were sufficiently recruited and activated in the lung. This suggested that IL21r-/- CD4+ T-cells have an impaired effector function, so we performed RNA sequencing on CD4+ cells purified from the Rag1-/- mice in order to define the missing signal. We found modest decrease of IL-22 in the IL-21r-/- CD4+ T-cells, which was also reported in patients with loss of function IL-21 receptor mutation. Additionally, the direct connection between IL-21 receptor signaling on CD4+ T-cells and Stat3-mediated production of IL-22 has recently been established by Yeste et al. 2014 [159, 160].

To clarify the role for IL-22 during *Pneumocystis* infection, we stained for IL-22 receptor in lung tissue of *Pneumocystis* infected mice and observed a dramatic upregulation. IL-22 receptor is believed to be expressed primarily on basolateral side of epithelial cells, and regulates production of antimicrobial peptides as well as apical surface carbohydrate composition. However, during *Pneumocystis* infection, most of the staining appears to be primarily on macrophages. To determine its importance, we adoptively transferring IL-22-/- CD4+ T-cells into Rag1-/- mice, but observed only a slight decrease in clearance efficiency. Interestingly, treatment of IL-21r-/- mice with IL-22 was able to reduce burden by up to 10 fold. However, this

effect could not be observed in CD4-depleted wild-type mice, suggesting that IL-22 works in collaboration with at least one other factor to mediate clearance. Using RNA and protein expression assays of *Pneumocystis* infected mice, we identified GM-CSF as a strong candidate. It has been shown that GM-CSF has some therapeutic effect during *Pneumocystis* infection [161], so we tested whether GM-CSF producing CD4+ T-cells were required for clearance. GM-CSF-/- CD4+ T-cells could not provide protection in the adoptive transfer model, which was correlated with lower arginase and CD209e expression. However, treatment of CD4-depleted mice with GM-CSF alone did not aid in controlling infection. Finally, when testing whether GM-CSF and IL-22 functioned cooperatively to reduce burden in CD4-depleted WT mice, we observed a significant decrease in burden.

These studies have generated new insights to patient populations at risk for *Pneumocystis*, and several mechanisms that are involved in clearance. However, there are still many unanswered questions and anomalies that can be deduced from these studies. For example, different models of *Pneumocystis* infection present with different restriction. As mentioned above, anti-CD20 therapy in wild-type mice prevents the generation of primed CD4+ T-cell responses, however, naïve wild-type CD4 cells are capable of generating effector cytokines when adoptively transferred into Rag1-/- mice. Understanding the fundamental differences in antigen presentation and T-cell activation in these models could generate insights in ways to treat non-T cell associated immunodeficiency. Furthermore, we have shown that IL-5 has therapeutic effects in Rag1-/- mice, however, IL-21r-/- CD4+ T-cells, which produce wild-type levels of IL-5, do not provide protection; the same can be observed with GM-CSF. In addition, RORc-/- CD4+ T-cell, which are deficient in IL-22 production, are capable of clearing *Pneumocystis*. This suggests that IL-21r-/- CD4+ T-cells may also produce factors that inhibit clearance. Identifying all the

factors involved in susceptibility and clearance would have clinical application and provide a deep understanding of the immune response.

In summary of this and previous studies, infection is initially acquired by inhaling *Pneumocystis* ascospores or asci **(Summary Figure A)**. As the pathogen propagates, innate immune machinery such as alveolar macrophages and dendritic cells acquire and respond to *Pneumocystis* antigens **(Summary Figure B)**. Upon acquiring antigen, CD11c+ dendritic cells leave the lung and migrate to the draining lymph nodes **(Summary Figure C)**. In the germinal centers, DCs present antigen within MHC class II molecules to CD4+ T-cells. In addition to antigen presentation, the CD4+ T-cells are also costimulated with CD40 and ICOS **(Summary Figure D)**. Antigen presentation and costimulation by B-cells are also required to generate an effective CD4+ T-cells response, but it's is unknown whether this is within the lung or lymph node, or what costimulatory molecules are required. Antigen-specific CD4+ T-cells migrate to the lung and early on, primed cells generate a Th2 response to infection. Production of IL-5, IL4, and IL-13 trigger Gata1-dependent eosinopoiesis, and stimulate eosinophil-mediated control of *Pneumocystis* infection **(Summary Figure E)**. In addition, Stat3-activated CD4+ T-cells produce GM-CSF which is required for clearance. IL-21 signaling on CD4+ T-cells is also required for effector T-cell responses, which includes IL-22. Th1 and Th17 cytokines are also generated, but are not needed for clearance. We hypothesize that Stat3-mediated clearance functions by recruiting and activating macrophages, as well as altering epithelial interactions with the trophic forms of *Pneumocystis* **(Summary Figure F)**. CD4+ T-cells, in an IL-21 dependent manner, will also generate a robust antibody response which is sufficient for protection against future infections **(Summary Figure G)**.

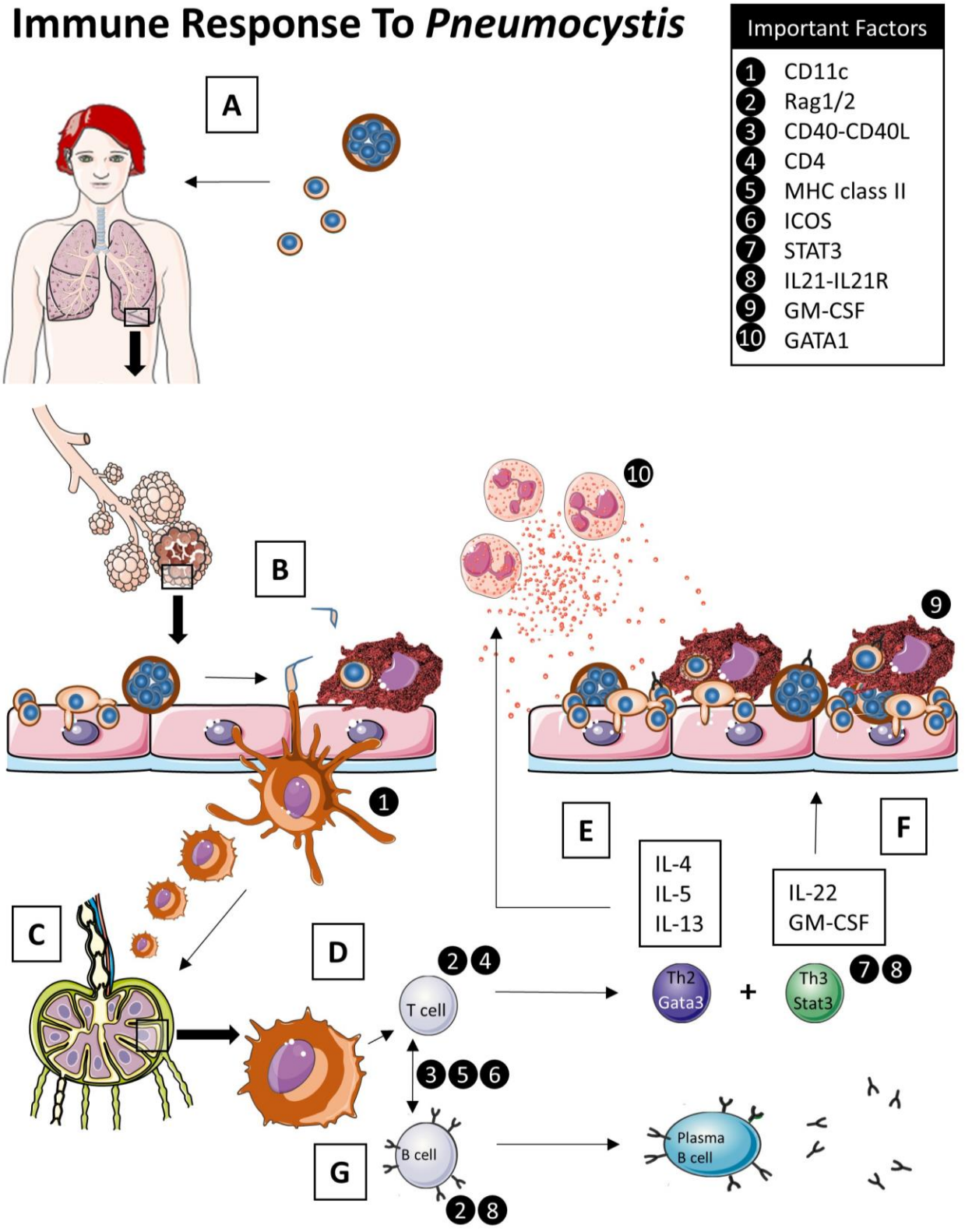


**Summary Figure. Immune Response to Pneumocystis Infection**

I would like to conclude by once again thanking my mentor Dr. Jay Kolls. “Thank you for all you’ve taught me, from molecular biology to immunology to business. The breadth of knowledge I have acquired by interacting with you over these last few years has made me a better scientist and a stronger person. I want to express my deepest gratitude for your continued patience and support. I shall be forever in your debt for all your kindness. Sincerely, Waleed”

# APPENDIX A

## EOSINOPHILS CONTRIBUTE TO EARLY CLEARANCE OF *PNEUMOCYSTIS MURINA* INFECTION

Work described in this section was partly published in the Journal of Immunology (J Immunol. 2015 Jul 1; 195(1) 185-93. doi: 10.4049/jimmunol.1403162.) by authors Taylor Eddens, Waleed Elsegeiny, Michael P. Nelson, William Horne, Brian T. Campfield, Chad Steele, and Jay K. Kolls

## A.1 INTRODUCTION

*Pneumocystis jirovecii* is a host-specific fungal pathogen that causes a diffuse interstitial pneumonia in immunocompromised individuals [41]. *Pneumocystis* remains the most common serious opportunistic infection in the HIV/AIDS population and is a frequent complication in developing countries where combination antiretroviral therapy (cART) and anti-*Pneumocystis* prophylaxis are difficult to implement [36, 37, 163-166]. In developed countries, the incidence of *Pneumocystis* infection has continued to rise due to the expansion of the immunosuppressed population [39, 40]. One study estimates that 75% of cases of *Pneumocystis* pneumonia are in non-HIV immunosuppressed individuals, such as those receiving immunosuppressive drug therapy for hematologic malignancy and post-transplantation rejection [39]. In fact, in the non-HIV infected immunosuppressed population, *Pneumocystis* tends to have increased morbidity, such as higher rates of mechanical ventilation, and increased mortality compared to the HIV-positive population [42, 43, 167].

Given the opportunistic nature of *Pneumocystis*, much can be gleaned about the host immune response required for clearance of *Pneumocystis* by examining the populations that are susceptible to infection. The HIV/AIDS population provides the strongest evidence; a clear inverse correlation exists between decreasing $CD4^+$ T-cell counts and increasing susceptibility to *Pneumocystis* [34, 168-170]. The importance of $CD4^+$ T-cells in protecting against *Pneumocystis* pneumonia has also been demonstrated in patients with a genetic immunodeficiency, such as

forms of severe combined immunodeficiency, as well as in animal models of infection [171, 172]. Although $CD4^+$ T-cells have been shown to interact with various cell types throughout the course of *Pneumocystis* infection, such as B cells and macrophages, the ability of other immune cell types to contribute to *Pneumocystis* clearance in a $CD4^+$ T-cell dependent manner is still an area of active investigation [139, 141, 173-175]. Identifying novel cell types that mediate immunity to *Pneumocystis* could potentially suggest unique pathways for targeted therapeutic development.

To investigate immunologic responses that may mediate clearance of *Pneumocystis*, we used RNA sequencing of whole lung at day 14 of *Pneumocystis murina* infection in CD4-depleted (which develop chronic progressive infection) and wild type C57Bl/6 mice (which clear by 4 weeks). This analysis revealed a prominent eosinophil signature in wild type mice compared to CD4-depleted mice. We also observed a substantial increase in recruited eosinophils in the bronchoalveolar lavage of infected CD4 replete mice compared to CD4 depleted mice. Using hydrodynamic injection of a plasmid encoding IL-5, CD4-depleted and *Rag1-/-* knockout mice receiving pIL5 demonstrated significant eosinophilia in the lung and decreased *Pneumocystis* burden 14 days post-challenge. Finally, $GATA1^{tm6Sho}$ knockout mice deficient in eosinopoiesis had no difference in burden when treated with pIL5. Taken together, this study demonstrates that one role of $CD4^+$ T-cells during *Pneumocystis* infection is to recruit eosinophils to the lung, which then contribute to clearance of *Pneumocystis*.

## A.2 METHODS

### A.2.1 MICE

C57Bl/6 mice, *Rag1-/-* knockout mice on a C57Bl/6 background, BALB/c mice, and *Gata1$^{tm6Sho}$/J* mice were all ordered from The Jackson Laboratory [176]. Mice were all 6-8 week old females and were bred in the Rangos Research Building Animal Facility. All use of laboratory animals was approved and performed in accordance with the University of Pittsburgh Institutional Care and Use Committee.

### A.2.2 *Pneumocystis* infection time course and primary infections

Twenty-five C57Bl/6 female mice were CD4-depleted using weekly intraperitoneal administration of 0.3 mg of GK1.5 monoclonal antibody per mouse and were subsequently challenged with 2.0 x $10^6$/mL *Pneumocystis murina* cysts using oropharyngeal inoculation as previously described [139, 177, 178]. Twenty-five age-matched C57Bl/6 female mice were inoculated at the same time, but were not CD4-depleted. Five mice from each group were then sacrificed at day 0, 3, 7, 10, and 14. Four BALB/c and *Gata1$^{tm6Sho}$/J* mice were also inoculated with *Pneumocystis* and sacrificed at day 14. Six uninfected BALB/c mice were used as naïve controls.

### A.2.3 RNA isolation and qRT-PCR

Lung RNA was purified using Trizol® Reagent (Life Technologies). Briefly, lungs were homogenized and following the addition of chloroform, RNA in the aqueous phase was collected and precipitated in isopropanol. Following centrifugation, the RNA was washed with 75% ethanol, centrifuged again, and then resuspended in nuclease-free water. Following incubation at 55°C, RNA was quantified using a Nanodrop and 1 μg of RNA was converted to cDNA using iScript™ cDNA synthesis kit per manufacturer's instructions (Bio-Rad). *PC* burden was then quantified using SsoAdvanced qRT-PCR universal probes supermix (Bio-Rad) using primers and a probe specific for *Pneumocystis murina* small subunit (SSU) rRNA with a standard curve of known *Pneumocystis* SSU rRNA concentrations. SSU primer and probe sequences are as follows:

Forward: 5'-CATTCCGAGAACGAACGCAATCCT;

Reverse: 5'- TCGGACTTGGATCTTTGCTTCCCA;

FAM-Probe: 5'- TCATGACCCTTATGGAGTGGGCTACA.

Other primers used include: *Prg2*, *Epx*, *Il5*, *Clca3*, *Muc5ac*, *Muc5b*, and *Il13* (Applied Biosystems). Prior to sequencing, the RNA was further purified using a Qiagen RNA cleanup kit with DNase treatment.

### A.2.4 RNA sequencing

Total RNA from mouse whole lung was used to perform RNA sequencing. Each sample was assessed using Qubit 2.0 fluorimeter and Agilent Bioanalyzer Tape Station 2200 for RNA

quantity and quality. Library preparation was done using Illumina TruSeq Stranded mRNA sample prep kit. The first step in the workflow involves purifying the poly-A containing mRNA molecules using poly-T oligo attached magnetic beads. Following purification, the mRNA is fragmented into small pieces using divalent cations. The cleaved RNA fragments are copied into first strand cDNA using reverse transcriptase and random primers. Strand specificity is achieved by using dUTP in the Second Strand Marking Mix, followed by second strand cDNA synthesis using DNA polymerase I and RNase H. These cDNA fragments then have the addition of a single 'A' base and subsequent ligation of the adapter. The products are then purified and enriched with PCR to create the final cDNA library. The cDNA libraries are validated using KAPA Biosystems primer premix kit with Illumina-compatible DNA primers and Qubit 2.0 fluorometer. Quality is examined using Agilent Bioanalyzer Tape station 2200.The cDNA libraries will be pooled at a final concentration 1.8pM. Cluster generation and 75bp paired read single-indexed sequencing was performed on Illumina NextSeq 500's.

### A.2.5 RNA Seq Data Analysis

Raw reads from an Illumina NextSeq 500 in fastq format were trimmed to remove adaptor/primer sequences. Trimmed reads were then aligned using BWA (version 0.5.9, settings aln -o 1 -e 10 -i 5 -k 2 -t 8) against the mouse genomic reference sequence. Additional alignment and post-processing were done with Picard tools (version 1.58) including local realignment and score recalibration (not duplicate marking) to generate a finale genomic aligned set of reads. Reads mapping to the genome were characterized as exon, intron, or intergenic (outside any annotated gene) using the matched annotation for the genomic reference sequence. The

remaining unmapped reads from the genomic alignment were then aligned to a splice reference created using all possible combinations of known exons (based on annotation described above) and then categorizing these as known or novel splice events. This aligned data is then used to calculate gene expression by taking the total of exon and known splice reads for each annotated gene to generate a count value per gene. For each gene there is also a normalized expression value generated in two ways: 1) Reads per Mapped Million (RPM), which is calculated by taking the count value and dividing it by the number of million mapped reads, 2) Reads per Mapped Million per Kilobase (RPKM), which is calculated by taking the RPM vale and dividing it by the kilobase length of the longest transcript for each gene. The RPM values are subsequently used for comparing gene expression across samples to remove the bias of different numbers of reads mapped per sample. RPKM values are subsequently used for comparing relative expression of genes to one another to remove the bias of different numbers of mapped reads and different transcript lengths. In addition to gene expression measurements, nucleotide variation was also detected using the GATK (version 1.3-25, -dcov 2000 -stand_call_conf 30.0 -stand_emit_conf 10.0 -A DepthOfCoverage -A BaseCounts -A AlleleBalance), which identified single nucleotide and small insertion/deletion (indel) events using default settings. Mapped exonic reads per WT sample: 44,291,011; 23,432,350; 41,004,408; and 41,308,864. Mapped exonic reads per GK1.5 sample: 23,305,058; 43,821,698; 122,834,770; and 29,805,804. Data were then filtered on a quality score of 20 and probed for eosinophil associated genes: *Ear11, Ear5, Ccl8, Ccl24, Ccr3, Prg2, Ccl11, Ccl7, Il13, Ear10, Il5ra, Ear2, Csf2rb, Ccl5, Il5, Ear1, Il4* (did not pass quality filter), and *Epx* (did not pass quality filter). Data available at http://www.ncbi.nlm.nih.gov/bioproject/.

### A.2.6 Bronchoalveolar lavage

Wild type C57BL/6, and GK1.5 treated mice infected with *Pneumocystis* were anesthetized at day 14 post-infection and a 20g Exel Safelet Catheter (Exel International Co.) was inserted in the cricoid cartilage. The needle was then removed and 1 mL aliquots were inserted and removed from the lung using a 1 mL syringe (10 mL total). Bronchoalveolar lavage (BAL) cells were then spun at 300xg for 10 minutes, resuspended in PBS, and counted using Trypan Blue stain. $1x10^6$ cells were then transferred to a round bottom 96-well plate for staining and the remainder of cells was transferred to Trizol® Reagent for RNA isolation (as described above). Naïve (uninfected) mice were also examined as a control.

### A.2.7 IL-5 and Eotaxin-1 Luminex on lung homogenate

Lung was collected in PBS containing protease inhibitors (Roche) and homogenized. We used a Bio-Plex Pro™ Assay (23-plex, Bio-Rad) according to the manufacturer's recommendations. Briefly, the plate was treated with Bio-Plex assay buffer, followed by vortexing and two washes. Lung homogenates (undiluted), standards, and blanks were then added to the plate and incubated at room temperature for one hour shaking at 850 rpm, covered. Following three washes, detection antibodies were then diluted and added to each well. The plate was incubated as above. Following three washes, diluted SA-PE was added to each well and incubated at room temperature for 20 minutes on shaker. The plate was then washed three times and resuspended in assay buffer and beads were quantified using a Bio-Plex® MAGPIX™ (Bio-Rad).

### A.2.8 Flow cytometry

BAL cells or cells from digested lung ($1x10^6$ total) were spun at 300xg for 3 minutes, resuspended in PBS, and pelleted once more. Cells were then resuspended in PBS containing 2% heat-inactivated fetal bovine serum and 0.4 μg of anti-CD16/CD32 (eBioscience, clone: 93). Following a 15 minute incubation at 4°C, cells were stained with the following antibodies: SiglecF-PE (BD Pharmigen™, clone: E50-2440), CD11b-APC (BioLegend, clone: M1/70), GR1-PE-Cy7 (BD Pharmigen™, clone: RB6-8C5), CD11c-FITC (eBioscience, clone: N418), and F4/80-APC-e780 (eBioscience, clone: BM8). Following an hour incubation at 4°C, cells were washed with PBS, pelleted, and fixed (BD CytoFix™). Cells were then analyzed using a BD LSRII Flow Cytometer with compensation via OneComp eBeads (eBioscience).

### A.2.9 Eosinophil culture and *Pneumocystis* killing assay

Bone marrow-derived eosinophils were generated using a previously described protocol [179] and per our previous work [145]. Briefly, bone marrow was isolated from naïve BALB/c mice and cells plated at 1 x $10^6$ cells/ml in RPMI 1640 containing 20% FBS (Irvine Scientific, Santa Ana, CA), 2mM Glutamine, 25mM HEPES, 1X MEM nonessential amino acids, 1mM sodium pyruvate (all from Life Technologies BRL, Rockville, MD), 50μM β-mercaptoethanol (Sigma-Aldrich, St. Louis, MO), 100 ng/ml stem cell factor and 100 ng/ml FLT3-L (both from Peprotech). After 4 days, cells were replated in the above media supplemented with 10 ng/ml IL-5. After 10 days, bone marrow cells were fully differentiated into eosinophils. As previously reported [179], samples of $1x10^5$ cells were taken for RNA analysis each time media was changed for real time PCR analysis of *Epx* for eosinophil development and *Mpo* (Applied

Biosystems) for neutrophil development. In addition, cells were cytospun onto glass slides, Giemsa stained and analyzed for morphology and purity by a murine pathologist in the Comparative Pathology Laboratory at the University of Alabama at Birmingham. On the tenth day, bone marrow-derived eosinophils were enumerated and utilized in experiments. Bone marrow-derived eosinophils ($1 \times 10^5$) were then co-cultured with $1 \times 10^3$ *Pneumocystis* cysts in 100μL for 18 h at 37°C and 5% $CO_2$ alone or in the presence of 10 ng/mL of IL-4 and IL-13. Controls included *P. murina* cultured in the absence of eosinophils as well as in the presence or absence of IL-4 and IL-13. Total RNA was isolated from the contents of each well using TRIZOL LS reagent (Invitrogen, Carlsbad, CA) and *Pneumocystis* SSU burden was calculated as above. Percent killing was defined as previously described [141].

### A.2.10 pIL5 and pCMV hydrodynamic injection

An untagged, murine IL-5 expression vector (pIL5, Origene, MC208784) and an empty vector pCMV6 control (Origene, PS100001) were grown in Mix and go *E. coli* (Zymo Research) in 200 mL of LB containing kanamycin and were prepared using an EndoFree Plasmid Maxi Kit (Qiagen) per manufacturer's instructions. Following quantification of vector, 10 μg of vector was added to 2 mL of Ringer's solution (0.9% NaCl, 0.03% KCL, and 0.016% $CaCl_2$) and injected intravenously via the tail vein within 5 seconds, as previously described [103, 180].

### A.2.11 IL-5 ELISA

Serum IL-5 was quantified using BioLegend ELISA MAX™ Mouse IL-5 ELISA kit per manufacturer's instructions. Briefly, a 96-well plate was coated with capture antibody and stored overnight at 4°C. Following washes with PBS + 0.05% Tween-20, the plate was blocked with assay diluent for 1 hour at room temperature. Serum samples (diluted 1:20) and IL-5 standard were diluted in assay diluent, added to the plate, and incubate overnight at 4°C. Detection antibody and diluted Avidin-HRP were then added to the plate, with washes in between additions, and the plate was developed with TMB substrate in the dark. Absorbance was then measured at 450 nm.

### A.2.12 Lung digestion

The right superior lobe of lung was physically digested using scissors, followed by an hour and a half incubation in collagenase/DNase in a 37°C shaker at 250 rpm. Single cell suspensions were then strained using a 70μm filter, pelleted, and then resuspended in 10 mL PBS. Following enumeration using Trypan Blue, cells were stained for flow cytometry as described above.

### A.2.13 Histology

The left main bronchus was clamped using forceps and 250μL of 10% formalin was injected into the bronchus. The lung tissue was then submerged in 10% formalin, paraffin-embedded, and processed by the Children's Hospital of Pittsburgh Histology Core. Sections were then stained from H&E and PAS.

### A.2.14 Statistics

All statistics were performed using GraphPad Prism 6. Briefly, an unpaired, two-tailed student's T test with a $p<0.05$ considered significant was used for all studies except for the BALB/c pIL-5 treatment. Given the non-Gaussian distribution for the BALB/c pIL-5 treatment, a Mann-Whitney nonparametric rank test was performed with a $p<0.05$ considered significant. For studies with three groups, a one-way ANOVA with Tukey's multiple comparisons was used with a $p<0.05$ considered significant. A Kruskal-Wallis nonparametric test with Dunn's multiple comparison's test was used for gene expression analysis in the BALB/c primary challenge experiment with a $p<0.05$ considered significant. Linear regression was also performed using Prism and Pearson's correlation coefficient calculations were performed.

## A.3 RESULTS

### A.3.1 RNA sequencing of whole lung identifies an eosinophil signature early in *Pneumocystis* infection

To further understand the role of $CD4^+$ T-cells in *Pneumocystis* infection, we examined *Pneumocystis* burden in wild type and GK1.5 treated, CD4-depleted C57/Bl6 mice. In this study, at day 14 using quantitative real time PCR, wild type mice begin to clear infection as CD4-depleted mice had a higher fungal burden at this time point (**Figure 23A**). As an unbiased approach to investigate potential mechanisms of fungal clearance, we used RNA sequencing of whole lung at this time point to examine the signatures of potential effector cells. Strikingly, several genes associated with eosinophil function and recruitment, such as *prg2* (major basic protein), *il5ra* (IL-5 receptor alpha), *ccr3*, *ccl11* (eotaxin-1), *ccl24* (eotaxin-2), were all significantly upregulated at day 14 of infection in wild type animals (**Figures 23B,C**). Another specific eosinophil marker, eosinophil-associated ribonuclease 2 (*ear2*), was also significantly upregulated in wild type animals, while less specific eosinophil-associated ribonucleases (*ear5, ear10, ear11*) also had higher expression in wild type animals. Importantly, in addition to a robust eosinophil signature at day 14 in wild type animals, IL-5 had significantly higher expression in wild type animals at the transcriptional level at day 7 and day 10 post-infection with *Pneumocystis* (**Figure 23D**). Importantly, *prg2*, an eosinophil associated gene, had a 10-fold increase in expression at day 14 by qRT-PCR, similar to that detected by RNA sequencing

(**Figure 23D**). Furthermore, protein levels of IL-5 and eotaxin-1 (CCL11) were significantly higher in wild type animals at day 14 when compared to CD4-depleted mice (**Figure 23E**).

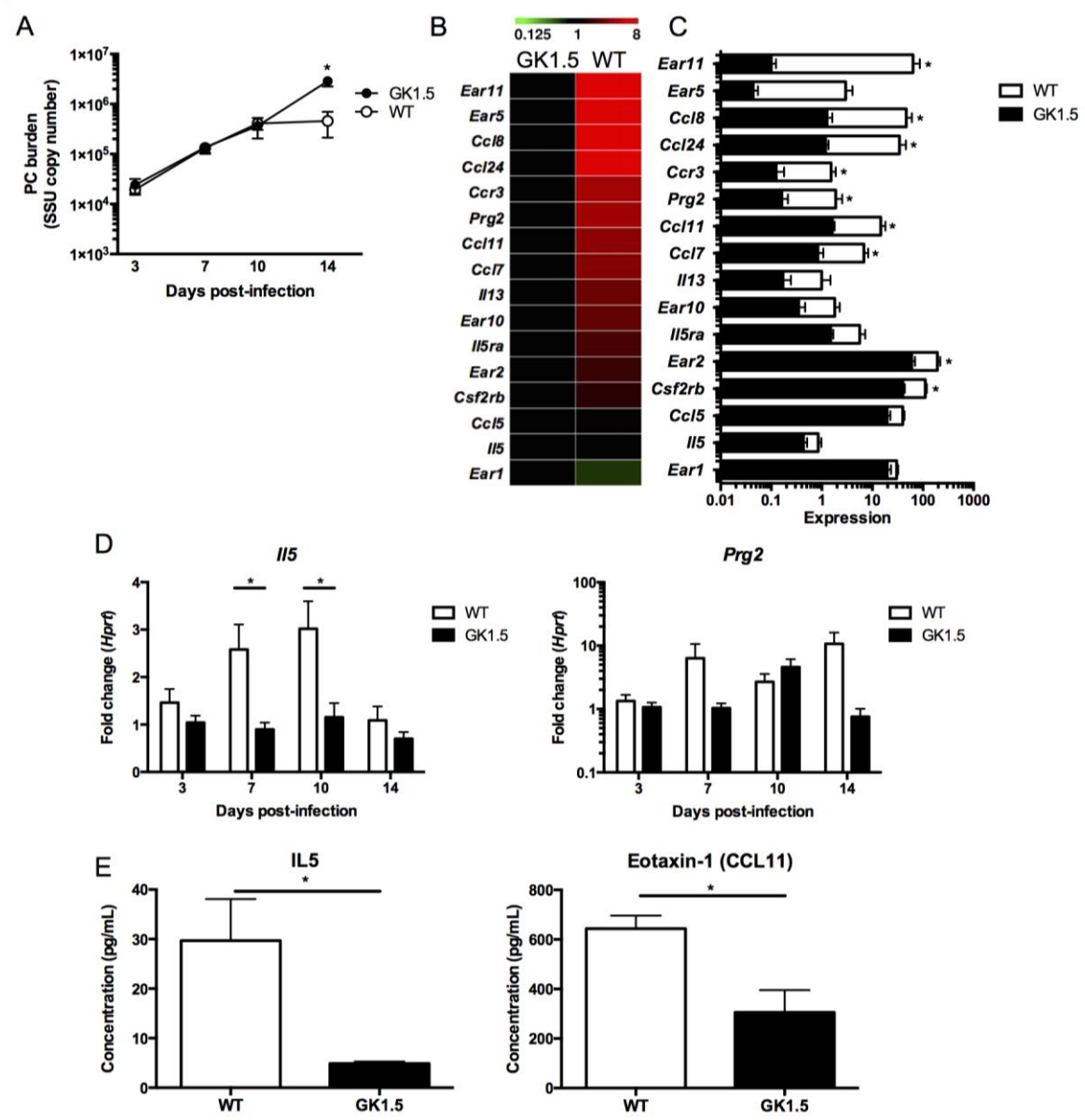


**Figure 23. RNA sequencing of whole lung shows a prominent CD4-dependent eosinophil signature at day 14 of *Pneumocystis* infection**

A. Wild type or GK1.5 treated CD4-depleted C57Bl/6 mice were infected with 2.0 x 106 cysts/ml of *Pneumocystis* and were sacrificed at day 3, 7, 10, or 14 following infection (n=5 at each time point). *Pneumocystis* burden was calculated by qRT-PCR of the small subunit ribosomal RNA and a significant decrease was seen at day 14 ($p<0.01$

by student's t-test). B. RNA sequencing of whole lung RNA at day 14 in GK1.5 treated and wild type mice shows increase in expression in genes associated with eosinophils (n=4 in each group). C. Histogram of expression values from heat map in B with * indicating $p<0.05$ by student's t-test. D. Il5 expression over the course of *Pneumocystis* infection normalized to Hprt and GK1.5 day 3 (fold change) shows increase of il5 at day 7 and 10 in wild type mice (* $p<0.05$, student's t-test). Similar to the expression pattern seen by RNA sequencing, a ten-fold increase in Prg2 is seen at day 14 by qRT-PCR ($p>0.05$). E. IL-5 and Eotaxin-1 (CCL11) protein levels in lung homogenate at day 14 as determined by Luminex (* $p<0.05$). Contributors: T. Eddens, W. Elsegeiny, and W. Horne.

### A.3.2 Eosinophils are present in bronchoalveolar lavage fluid early in infection

To further clarify the $CD4^+$ T-cell dependent eosinophil response to *Pneumocystis* infection, we sought to define the cell populations in the bronchoalveolar lavage (BAL) fluid of wild type and CD4-depleted animals at day 14. Cell populations in naïve mice were also analyzed. A population of cells with high side scatter was present in animals with intact $CD4^+$ T-cell responses, but absent in naïve and CD4-depleted animals infected with *Pneumocystis* (**Figure 24A,** *left panel*). After gating on all cells, a population of $SiglecF^+CD11b^+$ cells was noted in the wild type animals, but this population was substantially reduced back to naïve levels in animals treated with GK1.5 (**Figure 24A,** *right panel*). The $SiglecF^+CD11b^+$ population represented over 60% of cells in BAL fluid in wild type mice, while less than 2% of cells were $SiglecF^+CD11b^+$ in mice treated with GK1.5 (**Figure 24B**). Additionally, the RNA from BAL cell pellets was enriched for transcripts associated with eosinophils; *Epx* and *Prg2* expression was nearly 1000-fold higher in BAL cell pellets from wild type mice when compared to naïve and CD4-depleted mice (**Figure 24C**).

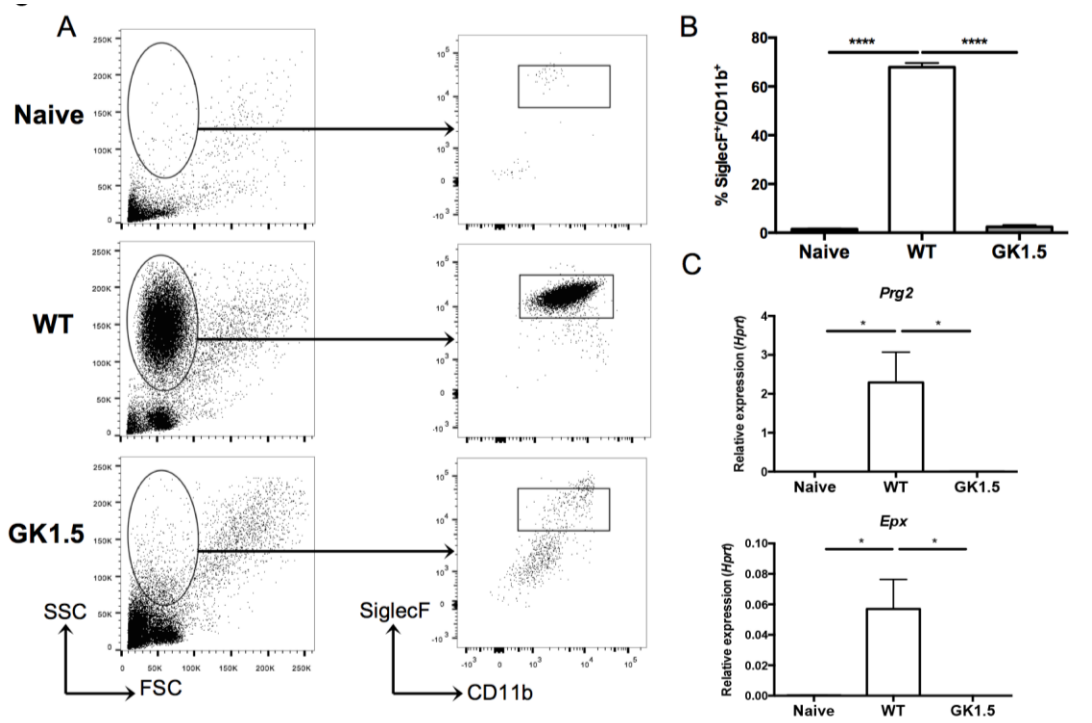


**Figure 24. CD4-dependent recruitment of eosinophils to the lung at day 14 of *Pneumocystis* infection**

A. Bronchoalveolar lavage (BAL) of naïve (uninfected), wild type, and GK1.5 treated CD4-depleted mice 14 days post-inoculation with *Pneumocystis* shows a large population of cells with high side-scatter in wild type mice (left panel). The cells were gated as shown (left panel), and a SiglecF+CD11b+ population was seen in the wild type, but not the naïve or GK1.5 treated animals (right panel). B. Significant increase in percentage of SiglecF+CD11b+ cells in wild type animals compared to naïve and GK1.5 treated animals (n=4-5, **** $p<0.0001$ by one-way ANOVA with Tukey's multiple comparisons). C. qRT-PCR for Epx (top) and Prg2 (bottom) on RNA extracted from BAL cell pellets shows significant increase in expression in wild type animals compared to naïve and GK1.5 treated animals (* $p<0.05$ by one-way ANOVA with Tukey's multiple comparisons). Contributors: W. Elsegeiny and T. Eddens.

### A.3.3 Eosinophils contribute to control of *Pneumocystis* infection both *in vitro* and *in vivo*

To determine the role of eosinophils in *Pneumocystis* infection, we used a loss-of-function approach and infected eosinopoiesis-deficient *Gata1$^{tm6Sho}$/J* mice and BALB/c controls.

*Gata1*$^{tm6Sho}$*/J* mice had an increased *Pneumocystis* burden at day 14 post infection compared to control BALB/c mice, while uninfected BALB/c had no detectable *Pneumocystis* burden (**Figure 25A**). BALB/c mice had an increase in *Epx* expression and a modest increase in *Prg2* expression compared to *Gata1*$^{tm6Sho}$*/J* mice and BALB/c uninfected controls (**Figure 25B**). Eosinophils cultured from BALB/c bone marrow also demonstrated anti-*Pneumocystis* activity *in vitro* (**Figure 25C**). Furthermore, bone marrow derived eosinophils displayed increased *Pneumocystis* killing activity when co-cultured with IL-4 and IL-13 (**Figure 25D**).

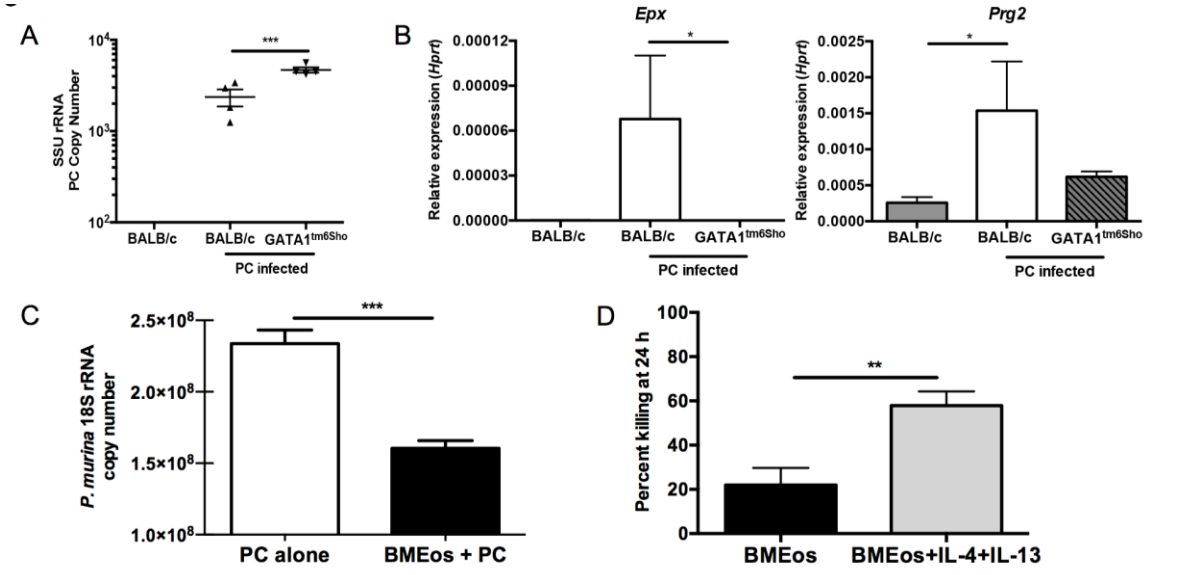


**Figure 25. Eosinophils contribute to control of *Pneumocystis* infection both *in vitro* and *in vivo***

A. BALB/c and Gata1tm6Sho/J knockout mice were infected with *Pneumocystis* and sacrificed at day 14 post-infection and SSU burden was quantified by qRT-PCR (** $p<0.01$ by student's T test). Uninfected BALB/c mice have no detectable *Pneumocystis* burden. B. qRT-PCR for Epx (left) and Prg2 (right) on RNA from whole lung shows significant increase in BALB/c mice infected with *Pneumocystis* compared to uninfected BALB/c and infected Gata1tm6Sho/J knockout mice (* $p<0.05$ by Kruskal-Wallis test w/ Dunn's multiple comparisons test). C. Bone marrow derived eosinophils from BALB/c mice demonstrate anti-*Pneumocystis* activity when co-cultured *in vitro* for 24 hours at an eosinophil to *P. murina* cyst ratio of 100:1 (*** $p<0.0001$, student's t-test). D. BM-derived eosinophils show enhanced killing activity when co-cultured with *Pneumocystis* in the presence of 10 ng/ml of IL-4 and IL-13 compared to *P. murina* alone (** $p<0.01$ by student's T-test). Contributors: T. Eddens and M. Nelson.

### A.3.4 Hydrodynamic injection of IL-5 promotes *Pneumocystis* clearance in CD4-depleted C57Bl/6 and Rag1-/- mice

To induce eosinophilia prior to *Pneumocystis* infection, we employed hydrodynamic injection with either a plasmid expressing IL-5 (pIL5) or an empty plasmid control (pCMV) in C57Bl/6 mice treated with GK1.5 or *Rag1-/-* mice three days prior to infection (**Figure 26A**). At day two following infection, mice treated with pIL5 had over a log-fold increase in serum IL-5 (**Figure 26B**). At day 14 of infection, treatment with pIL5 resulted in an increased abundance of a high side scatter population and a SiglecF$^{+}$CD11b$^{+}$ population in both CD4-depleted C57Bl/6 and *Rag1-/-* mice (**Figure 26C**). While these populations were present by flow cytometry in the groups treated with pCMV alone (**Figure 26C**, *left panel*), C57Bl/6 and *Rag1-/-* mice treated with pIL5 had significantly more SiglecF$^{+}$CD11b$^{+}$ cells as measured by both percentage and total cell number recovered from the lung (**Figure 26D**).

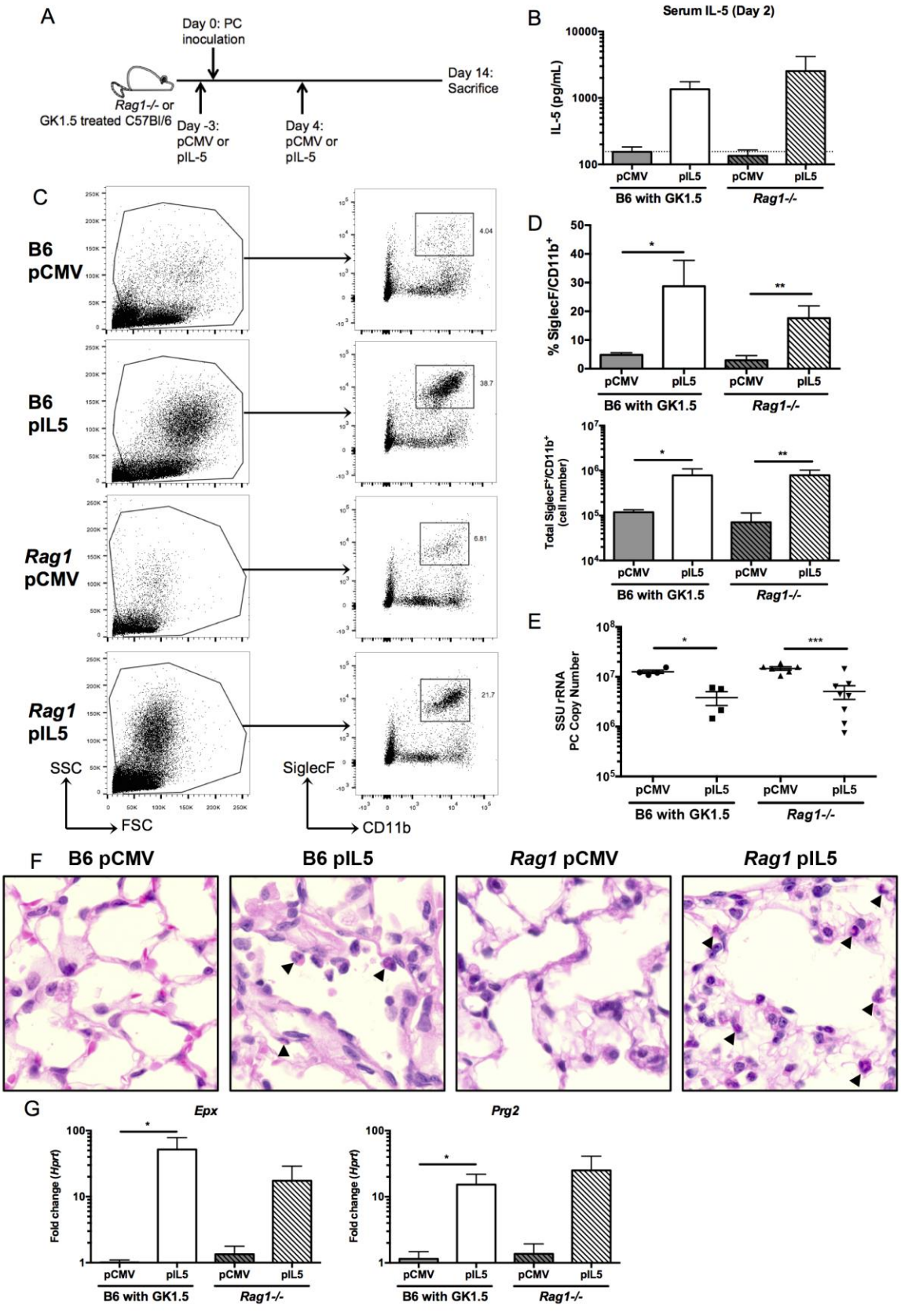
A
Day 0: PC inoculation
Day 14: Sacrifice
Rag1-/- or GK1.5 treated C57Bl/6
Day -3: pCMV or pIL-5
Day 4: pCMV or pIL-5
B
Serum IL-5 (Day 2)
IL-5 (pg/mL)
pCMV
pIL5
B6 with GK1.5
Rag1-/-
C
B6 pCMV
B6 pIL5
Rag1 pCMV
Rag1 pIL5
SSC
FSC
SiglecF
CD11b
D
% SiglecF/CD11b+
Total SiglecF+/CD11b+ (cell number)
E
SSU rRNA PC Copy Number
F
B6 pCMV
B6 pIL5
Rag1 pCMV
Rag1 pIL5
G
Epx
Prg2
Fold change (Hprt)

**Figure 26. Treatment of CD4-depleted C57Bl/6 and Rag1-/- mice with pIL5 results in eosinophilia in whole lung and decreased *Pneumocystis* burden**

A. Schematic showing timing of hydrodynamic injection of either pCMV or pIL5 (day -3 and 4) and *Pneumocystis* inoculation (day 0) into GK1.5 treated C57Bl/6 (B6) or Rag1-/- mice. B. Serum IL-5 ELISA at day 2 post infection shows log-fold increase in IL-5 in pIL5 treated animals (n=4-7, dotted line represents limit of detection). C. Digested whole lung shows a high side scatter population in the pIL5 groups compared to the pCMV treated groups (left panel). The cells were gated as shown (left panel), and a SiglecF+CD11b+ population was seen in both the B6 and Rag1-/- mice treated with pIL5 at day 14 post infection (right panel). D. pIL5 treatment resulted in a statistically significant increase in percentage (top) and total number (bottom) of SiglecF+CD11b+ cells (* $p<0.05$, ** $p<0.01$ by student's t-test). E. pIL5 treatment results in statistically significant reduction in *Pneumocystis* burden as measured by qRT-PCR of small subunit ribosomal RNA at day 14 post infection (* $p<0.05$, *** $p<0.001$ by student's t-test). F. H&E staining on paraffin-embedded lung sections demonstrating eosinophils (black arrowheads) in both the B6 and Rag1-/- mice treated with pIL5 at 60X magnification. G. qRT-PCR for Epx (left) and Prg2 (right) on RNA extracted from whole lung shows significant log-fold increase in expression in pIL5 treated animals compared to pCMV treated mice (* $p<0.05$ by student's T test). Contributors: T. Eddens and W. Elsegeiny.

Strikingly, both the CD4-depleted C57Bl/6 and *Rag1-/-* mice receiving pIL5 had a statistically significant reduction in *Pneumocystis* burden by day 14 of infection when compared to mice treated with pCMV (**Figure 26E**). While the average difference in burden was approximately a half-log in both cohorts, some individual mice had greater than a log-reduction in *Pneumocystis* burden with pIL5 treatment. A strong negative correlation existed between total number of eosinophils recruited to the lung and *Pneumocystis* burden in the C57Bl/6 treated animals (**Figure 27**, p=0.0003). Recruitment of eosinophils to the lung could also be observed by H&E staining in mice receiving pIL5 (**Figure 26F**). The pIL5 treated mice also had a ten-fold increase in expression of *Epx* and *Prg2* in whole lung RNA when compared to pCMV treated mice (**Figure 26G**). Furthermore, although pIL5 treatment increased eosinophilic lung

inflammation, this was not associated with Type 2 immune inflammation as measured by goblet cell hyperplasia or mucin expression (as measured by qRT-PCR of *Clca3*, *Muc5ac* and PAS staining) or *Il13* expression in the pIL5 treated C57Bl/6 mice.

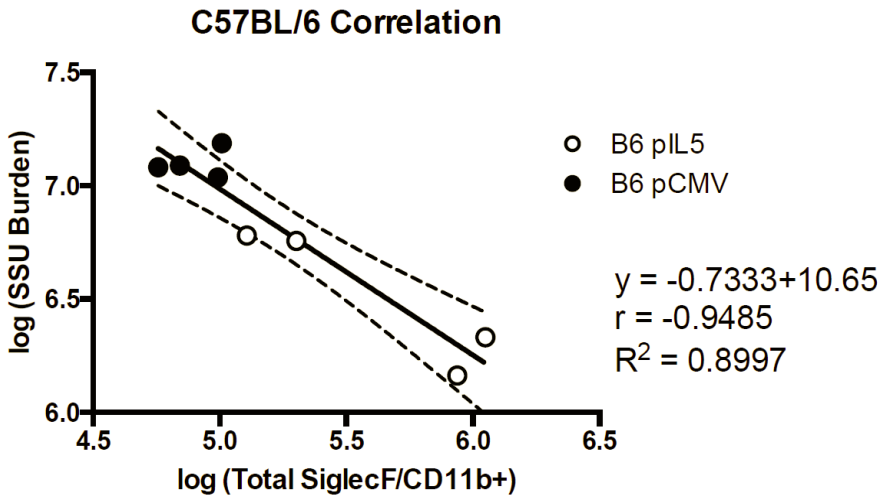


**Figure 27. Eosinophil numbers correlates with *Pneumocystis* killing in vivo**

Correlation between the log of total SiglecF+ CD11b+ cells with the log of *Pneumocystis* SSU burden demonstrates a strong negative correlation in B6 mice. Solid line represents linear regression of data points and dashed lines represent 95% confidence interval (r=-0.9485, p=0.0003 by Pearson's correlation). Contributors: T. Eddens

### A.3.5 IL-5 mediated decrease in *Pneumocystis* burden is abrogated in eosinophil-deficient Gata1tm6Sho/J mice

To verify the effect of pIL5 required eosinopoiesis, we used a genetic approach. CD4-depleted BALB/c mice were treated with pIL5 as described above and similar levels of IL-5 were induced in the serum (**Figure 28A**). Similarly, increased eosinophils were noted in the lung digest of pIL5 treated BALB/c mice (**Figure 28B**). pIL5 treated BALB/c mice had a statistically

significant increase in total number and a trend towards higher percentage of SiglecF$^{+}$/CD11b$^{+}$ cells compared to pCMV treated BALB/c mice (**Figure 28C**). Furthermore, upon sacrifice, BALB/c mice treated with pIL5 had nearly a 50% reduction in *Pneumocystis* burden when compared to pCMV treated animals (**Figure 28D**, p=0.04). Burden in this case was normalized to the pCMV group as the inoculums over three independent experiments varied; however, a similar reduction in burden was noted with C57Bl/6 and *Rag1*-/- mice (**Figure 28E**). Also noteworthy, four pIL5 treated mice had no induction of serum IL-5 and lacked eosinophils in the lung at day 14 by flow cytometry, likely due to technical variation. If only mice that responded to pIL5 treatment were included in the analysis, the mean percentage of *Pneumocystis* remaining in pIL5 treated mice would be 26% compared to 100% of pCMV treated mice ($p<0.0002$). The increased *Pneumocystis* killing in mice that recruited eosinophils to the lungs is also evident in the strong negative correlation that exists between *Pneumocystis* burden and total SiglecF$^{+}$CD11b$^{+}$ recruited cells. Hydrodynamic IL5 treatment was also associated with significant increases in eosinophil associated genes such as *Epx* and *Prg2* (**Figure 28E**).

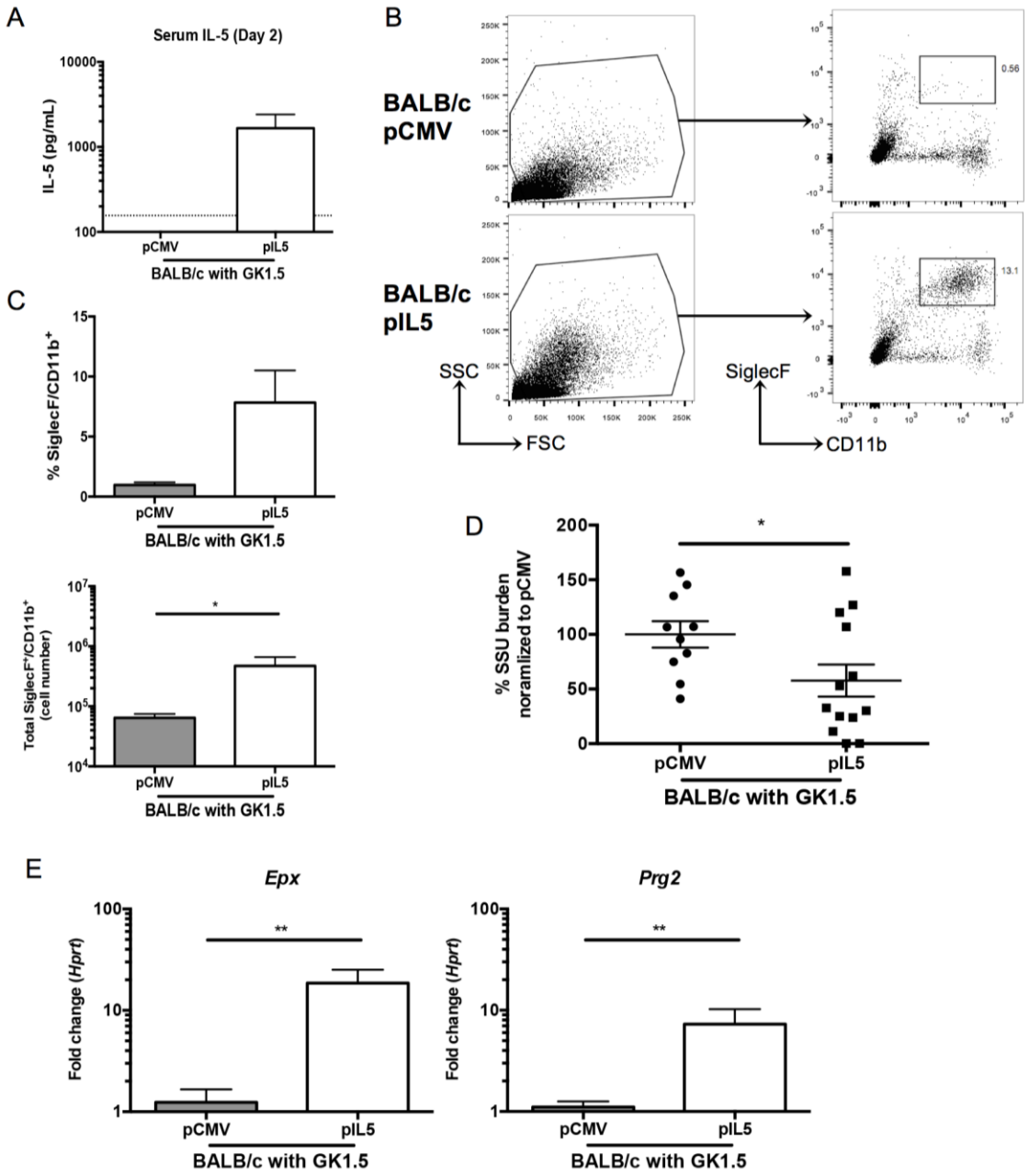


**Figure 28. pIL5 treatment can reduce *Pneumocystis* burden in CD4-depleted BALB/c mice**

A. Serum IL-5 ELISA at day 2 post infection shows over a log-fold increase in IL-5 in pIL5 treated BALB/c mice (n=10-13, dotted line represents limit of detection). B. Digested whole lung shows a high side scatter population in the pIL5 groups compared to the pCMV treated groups (left panel). The cells were gated as shown (left panel), and a SiglecF+CD11b+ population was seen in the BALB/c mice treated with pIL5 (right panel). C. pIL5 treatment resulted in an increase in percentage (top) and total number (bottom) of SiglecF+CD11b+ cells (* $p<0.05$, Mann

Whitney test). D. pIL5 treatment results in reduction in *Pneumocystis* burden as measured by qRT-PCR of small subunit ribosomal RNA at day 14 post infection (* p=0.0481 by student's t-test). E. qRT-PCR for Epx (left) and Prg2 (right) on RNA extracted from whole lung shows significant log-fold increase in expression in pIL5 treated animals compared to pCMV treated mice (** p<0.01 by Mann Whitney test). Contributors: T. Eddens and W. Elsegeiny, and B. Campfield.

In contrast, *Gata1$^{tm6Sho}$/J* mice (on a BALB/c background), mice that are deficient in eosinopoiesis, that were CD4-depleted and treated with pIL5 or pCMV as described above failed to show an effect of pIL5 on fungal burden, despite similar levels of IL-5 compared to previous mouse strains (**Figure 29A,B**). Consistent with no reduction in fungal burden, there was no observable eosinophil recruitment was detected in the lungs of *Gata1$^{tm6Sho}$/J* mice, as neither a high side-scatter population nor a SiglecF$^{+}$CD11b$^{+}$ was noted by flow cytometry (**Figure 29C,D**). Furthermore, there was no induction of *Epx* or *Prg2* in the *Gata1$^{tm6Sho}$/J* mice treated with pIL5 (**Figure 29E**).

Figure 6

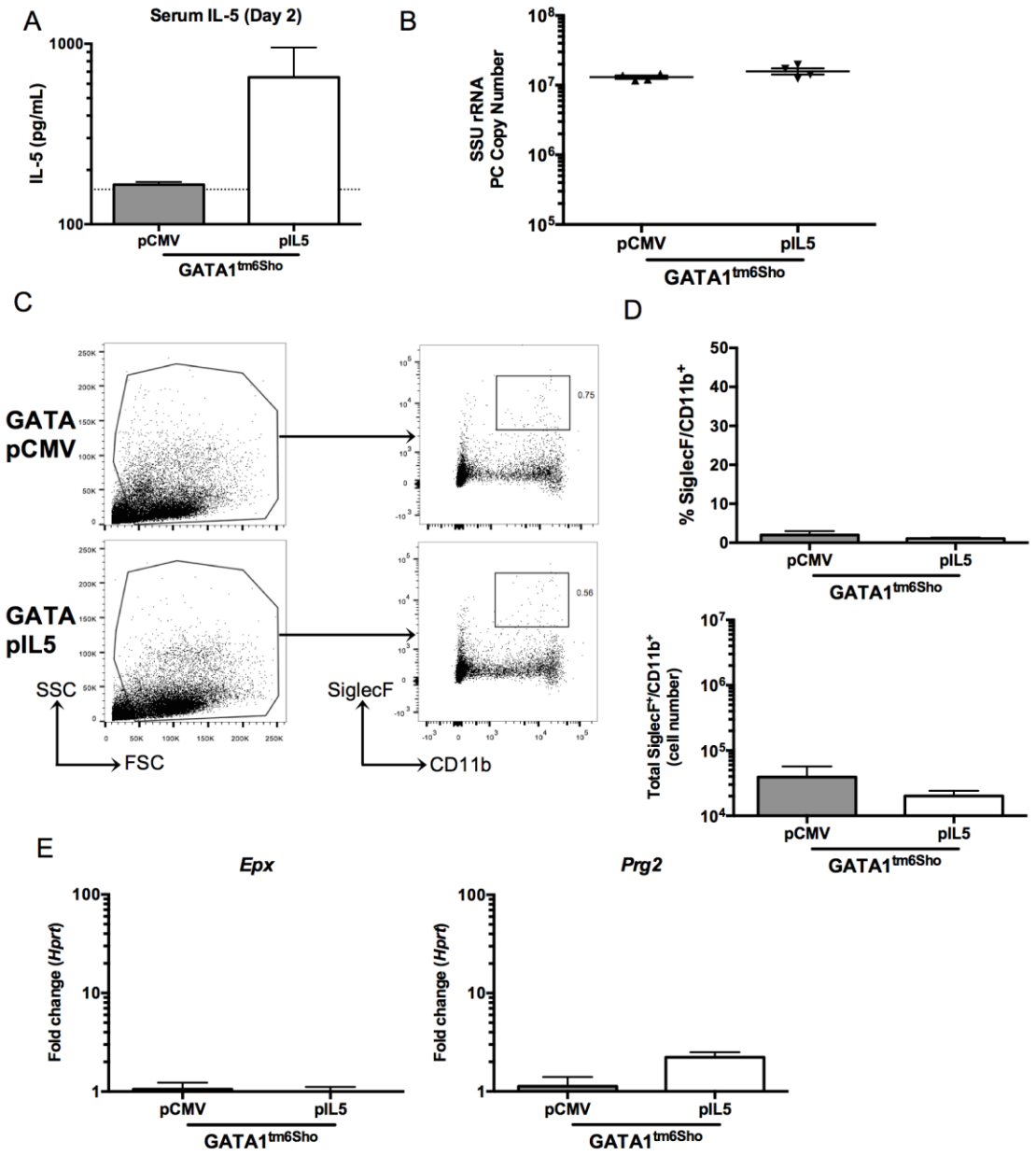


**Figure 29. pIL5 treatment cannot rescue eosinophil-deficient Gata1tm6Sho/J knockout mice**

A. Serum IL-5 ELISA at day 2 post infection shows nearly a log increase in Gata1tm6Sho/J pIL5 treated animals (n=4, dotted line represents limit of detection). B. pIL5 treatment does not reduce *Pneumocystis* burden at day 14 post infection in Gata1tm6Sho/J mice as measured by qRT-PCR of small subunit ribosomal RNA. C. Digested whole lung shows no difference in high side scatter populations (left panel) or SiglecF+CD11b+ cells (right panel) independent of pIL5 treatment status. D. pIL5 treated Gata1tm6Sho/J mice showed no difference in percentage (top)

or total number (bottom) of SiglecF+CD11b+ cells. E. qRT-PCR for Epx (left) and Prg2 (right) on RNA extracted from whole lung shows no increase in eosinophil associated genes in Gata1tm6Sho/J mice. Contributors: T. Eddens.

## A.4 DISCUSSION

The current study utilized an unbiased RNA sequencing based approach towards evaluating the role of $CD4^+$ T-cells in *Pneumocystis* infection and suggested that $CD4^+$ T-cells can recruit eosinophils to the lung by day 14 of infection by RNA sequencing. Eosinophils were also shown to have a role in immunity against *Pneumocystis* in a primary challenge model of eosinophil-deficient mice and in an eosinophil-based *Pneumocystis in vitro* killing assay. Furthermore, induction of eosinophilia via hydrodynamic injection of pIL5 was capable of reducing *Pneumocystis* burden *in vivo* in both CD4-depleted C57Bl/6 and *Rag1-/-* mice. Finally, the same technique was able to reduce *Pneumocystis* burden in CD4-depleted BALB/c mice but failed to provide any therapeutic benefit in CD4-depleted $Gata1^{tm6Sho}/J$ mice, further implicating eosinophils as a novel cell population responsible for *in vivo* antifungal activity.

$CD4^+$ T-cells have been established as crucial mediators to *Pneumocystis* due to the high incidence of *Pneumocystis* in HIV/AIDS patients with low $CD4^+$ T-cell counts [41, 164]. One clear role of $CD4^+$ T-cells in response to *Pneumocystis* is to stimulate antibody responses by providing co-stimulatory signals to B cells [173, 175]. Antibodies against *Pneumocystis* are protective; however, at day 14 of infection, prior to antibody production, *Pneumocystis* burden has already plateaued in wild type animals suggesting an antibody-independent function for CD4 cells [175]. As such, $CD4^+$ T-cells appear to recruit eosinophils early in infection while B cells are undergoing maturation into antibody-producing plasma cells and provide preliminary control

of *Pneumocystis* burden. Importantly, IL-5 transcription and eosinophil recruitment appears to be dependent on $CD4^+$ T-cells in this model, as such markers do not appear until after activation of the adaptive immune response at day 7 post-infection.

Eosinophils, classically recognized as mediators of immunity against helminths, have recently been implicated in host defense against a variety of pathogens, including bacterial and viral infections [144]. Recently, we have demonstrated that eosinophils contribute to host defense against the fungal pathogen *Aspergillus fumigates* through a secretory factor, as eosinophils could mediate fungal killing when separated using transwells [145]. The current study extends these findings by demonstrating that eosinophil-deficient mice are more susceptible to *Pneumocystis* infection and that eosinophils display antifungal activity *in vitro*. Additionally, treatment of bone marrow derived eosinophils with IL-4 and IL-13 greatly enhanced killing of *Pneumocystis*, suggesting that Th2 cytokines in the lung may augment eosinophil-dependent antifungal activity.

There are also several lines of evidence that connect *Pneumocystis* related pathology and eosinophils in both human disease and mouse models. First, eosinophilia in the bronchoalveolar lavage fluid of HIV-positive patients with *Pneumocystis* pneumonia has been well documented; however, whether a correlation exists between high eosinophil counts and lower *Pneumocystis* burden in these patients is unknown [181, 182]. Secondly, patients with a history of *Pneumocystis* or bacterial pneumonia had a significantly higher rate of physician-diagnosed asthma, a disease that has a well-established eosinophilic component in regards to pathogenesis [183]. Murine models of *Pneumocystis* have also shown Stat6, a transcription factor required for Th2 responses, is necessary for the development of airway hyperresponsiveness early in the course of infection [175]. While eosinophilia was also documented early in this murine model,

the study further links a Th2 response, and potentially eosinophilia, with pathology in the context of *Pneumocystis* infection [175]. Additionally studies have shown that $CD8^+$ T-cells may moderate the interactions between $CD4^+$ T-cells and eosinophils, although all three cell types may contribute to *Pneumocystis* driven pulmonary pathology [156].

However, the current study suggests that eosinophils are more than just the byproduct of a misguided immune response that drives airway hyperresponsiveness and pathology. The current study demonstrates that eosinophils have antifungal effects against *Pneumocystis* infection *in vitro* and *in vivo* and appear to be recruited to the lung by $CD4^+$ T-cells early in infection. Additionally, the role of eosinophils as a potential therapeutic in the setting of HIV/AIDS may warrant further exploration, as IL-5 mediated eosinophilia can provide reduced *Pneumocystis* burden even in the setting of complete loss of T cells and B cells. Furthermore, such robust eosinophilia actually appeared to mitigate airway pathology (e.g. mucus production) suggesting that *Pneumocystis* burden may play an equally important role in driving airway hyperresponsiveness. These findings provide evidence that the specific pathways responsible for protective and pathologic effects in *Pneumocystis* pneumonia may be independent and may allow for the targeted use of eosinophil-based treatments for *Pneumocystis* while avoiding concurrent pathology.

## BIBLIOGRAPHY


1. Chagas, C., *Nova tripanozomiata humana.* Mem. Inst. Oswaldo Cruz, 1909. **1**: p. 159-218.

2. F, D., *La Maladie de Chagas.* Histoire d'un Fléau Continental, 1999: p. Payot and Rivages, Paris.

3. Carinii, A., *Formas de eschizogonia do Trypanozoma lewisi.* Comm. Soc. Med. Sao Paolo, 1910. **16**: p. 204.

4. Delanoë, P.a.D., M. , *Surles rapporte des kystos de carinii le Trpanosoma lewisi.* Compt. Rend. Acad. Sci, 1912. **155**: p. 658.

5. Chabe, M., et al., *Pneumocystis: from a doubtful unique entity to a group of highly diversified fungal species.* FEMS Yeast Res, 2011. **11**(1): p. 2-17.

6. Yoneda, K.W., P. D.; Richey, C. S.; Birk, M. G., *Pneumocystis carinii: freeze-fracture study of stages of the organism.* Experimental parasitology, 1982. **53**(1): p. 68-67.

7. A, C., *Contribution to the taxonomical classification of the so-called Pneumocystis carinii.* Acta microbiologica Academiae Scientiarum Hungaricae, 1957. **4**(1): p. 1-8.

8. Jirovec, O.a.V., J., *Weitere Beitrage zur Morphologie von Pneumocystis carinii. 1st Pneumocystis carinii identisch mit Hefen oder Candiden?* Zentralblatt fur allgemeine Pathologie u. pathologische Anatomie, 1956. **94**(9-10): p. 499-517.

9. Vavra, J. and K. Kucera, *Pneumocystis carinii delanoe, its ultrastructure and ultrastructural affinities.* J Protozool, 1970. **17**(3): p. 463-83.

10. Edman, J.C., et al., *Ribosomal RNA sequence shows Pneumocystis carinii to be a member of the Fungi.* Nature, 1988. **334**(6182): p. 519-522.

11. Cushion, M.T., et al., *Transcriptome of <italic>Pneumocystis carinii</italic> during Fulminate Infection: Carbohydrate Metabolism and the Concept of a Compatible Parasite.* PLoS ONE, 2007. **2**(5): p. e423.

12. Liu, Y., et al., *Phylogenomic Analyses Support the Monophyly of Taphrinomycotina, including Schizosaccharomyces Fission Yeasts.* Molecular Biology and Evolution, 2009. **26**(1): p. 27-34.

13. Eriksson, O.E., *Pneumocystis carinii, a parasite in lungs of mammals, referred to a new family and order (Pneumocystidaceae, Pneumocystidales, Ascomycota).* System Ascomycetum, 1994. **13**: p. 165.

14. Hughes, W.T., *Pneumocystis carinii pneumonitis.* CRC Press, Inc., 1987. **1 and 2**: p. Boca Raton, Fl.

15. Gigliotti, F., et al., *Pneumocystis carinii is not universally transmissible between mammalian species.* Infect Immun, 1993. **61**(7): p. 2886-90.

16. Stringer, J.R., et al., *A New Name for Pneumocystis from Humans and New Perspectives on the Host-Pathogen Relationship.* Emerging Infectious Diseases, 2002. **8**(9): p. 891-896.

17. Sinclair, K., et al., *Pneumocystis carinii organisms derived from rat and human hosts are genetically distinct.* Mol Biochem Parasitol, 1991. **45**(1): p. 183-4.

18. Hughes, W.T., *Pneumocystis carinii versus Pneumocystis jiroveci: Another Misnomer (Response to Stringer et al.).* Emerging Infectious Diseases, 2003. **9**(2): p. 276-277.

19. Dei-Cas, E., et al., *Pneumocystis oryctolagi sp. nov., an uncultured fungus causing pneumonia in rabbits at weaning: review of current knowledge, and description of a new taxon on genotypic, phylogenetic and phenotypic bases.* FEMS Microbiol Rev, 2006. **30**(6): p. 853-71.

20. Palluault, F., et al., *Three-Dimensional Reconstruction of Rabbit-Derived Pneumocystis carinii from Serial-Thin Sections I: Trophozoite.* The Journal of Protozoology, 1991. **38**(4): p. 402-407.

21. Kwon, K.Y., S.P. Kim, and A.H. Limper, *Recognition of Pneumocystis carinii antigen on its surface by immunohistochemistry and immunoelectron microscopy.* J Korean Med Sci, 1998. **13**(2): p. 131-7.

22. Yoshikawa, H., H. Morioka, and Y. Yoshida, *Ultrastructural detection of carbohydrates in the pellicle of Pneumocystis carinii.* Parasitology Research, 1988. **74**(6): p. 537-543.

23. Palluault, F., et al., *High osmotic pressure enables fine ultrastructural and cytochemical studies onPneumocystic carinii.* Parasitology Research, 1992. **78**(5): p. 437-444.

24. De Stefano, J.A., et al., *Analysis of Pneumocystis carinii cyst wall. I. Evidence for an outer surface membrane.* J Protozool, 1990. **37**(5): p. 428-35.

25. Kovacs, J.A., et al., *Multiple genes encode the major surface glycoprotein of Pneumocystis carinii.* Journal of Biological Chemistry, 1993. **268**(8): p. 6034-40.

26. Sexton, A.C. and B.J. Howlett, *Parallels in Fungal Pathogenesis on Plant and Animal Hosts.* Eukaryotic Cell, 2006. **5**(12): p. 1941-1949.

27. Cushion, M.T., *Pneumocystis: unraveling the cloak of obscurity.* Trends in Microbiology, 2004. **12**(5): p. 243-249.

28. Vohra, P.K., et al., *Expression analysis of PCSTE3, a putative pheromone receptor from the lung pathogenic fungus Pneumocystis carinii.* Biochemical and Biophysical Research Communications, 2004. **319**(1): p. 193-199.

29. Cushion, M.T., et al., *Echinocandin Treatment of <italic>Pneumocystis</italic> Pneumonia in Rodent Models Depletes Cysts Leaving Trophic Burdens That Cannot Transmit the Infection.* PLoS ONE, 2010. **5**(1): p. e8524.

30. Morris, A., et al., *Current Epidemiology of Pneumocystis Pneumonia.* Emerging Infectious Diseases, 2004. **10**(10): p. 1713-1720.

31. Phair, J., et al., *The risk of Pneumocystis carinii pneumonia among men infected with human immunodeficiency virus type 1. Multicenter AIDS Cohort Study Group.* N Engl J Med, 1990. **322**(3): p. 161-5.

32. Hay, J.W., D.H. Osmond, and M.A. Jacobson, *Projecting the medical costs of AIDS and ARC in the United States.* J Acquir Immune Defic Syndr, 1988. **1**(5): p. 466-85.

33. Kaplan, J.E., et al., *Epidemiology of human immunodeficiency virus-associated opportunistic infections in the United States in the era of highly active antiretroviral therapy.* Clin Infect Dis, 2000. **30 Suppl 1**: p. S5-14.

34. Walzer, P.D., et al., *Early predictors of mortality from Pneumocystis jirovecii pneumonia in HIV-infected patients: 1985-2006.* Clinical infectious diseases : an official publication of the Infectious Diseases Society of America, 2008. **46**(4): p. 625-33.

35. Djawe, K., et al., *Mortality Risk After AIDS-Defining Opportunistic Illness Among HIV-Infected Persons-San Francisco, 1981-2012.* J Infect Dis, 2015.

36. Huang, L., et al., *HIV-associated Pneumocystis pneumonia.* Proc Am Thorac Soc, 2011. **8**(3): p. 294-300.

37. Malin, A.S., et al., *Pneumocystis carinii pneumonia in Zimbabwe.* Lancet, 1995. **346**(8985): p. 1258-61.

38. Ruffini, D.D. and S.A. Madhi, *The high burden of Pneumocystis carinii pneumonia in African HIV-1-infected children hospitalized for severe pneumonia.* Aids, 2002. **16**(1): p. 105-12.

39. Mikaelsson, L., G. Jacobsson, and R. Andersson, *Pneumocystis pneumonia--a retrospective study 1991-2001 in Gothenburg, Sweden.* The Journal of infection, 2006. **53**(4): p. 260-5.

40. Maini, R., et al., *Increasing Pneumocystis pneumonia, England, UK, 2000-2010.* Emerg Infect Dis, 2013. **19**(3): p. 386-92.

41. Eddens, T. and J.K. Kolls, *Pathological and protective immunity to Pneumocystis infection.* Semin Immunopathol, 2015. **37**(2): p. 153-62.

42. Monnet, X., et al., *Critical care management and outcome of severe Pneumocystis pneumonia in patients with and without HIV infection.* Crit Care, 2008. **12**(1): p. R28.

43. Mori, S. and M. Sugimoto, *Pneumocystis jirovecii infection: an emerging threat to patients with rheumatoid arthritis.* Rheumatology (Oxford), 2012. **51**(12): p. 2120-30.

44. Carmona, E.M. and A.H. Limper, *Update on the diagnosis and treatment of Pneumocystis pneumonia.* Ther Adv Respir Dis, 2011. **5**(1): p. 41-59.

45. Limper, A.H., et al., *Pneumocystis carinii pneumonia. Differences in lung parasite number and inflammation in patients with and without AIDS.* Am Rev Respir Dis, 1989. **140**(5): p. 1204-9.

46. Thomas, C.F., Jr. and A.H. Limper, *Pneumocystis pneumonia.* N Engl J Med, 2004. **350**(24): p. 2487-98.

47. Catherinot, E., et al., *Pneumocystis jirovecii Pneumonia.* Infect Dis Clin North Am, 2010. **24**(1): p. 107-38.

48. Olsson, M., et al., *Detection of Pneumocystis carinii DNA in sputum and bronchoalveolar lavage samples by polymerase chain reaction.* Journal of Clinical Microbiology, 1993. **31**(2): p. 221-226.

49. Wakefield, A.E., et al., *Detection of Pneumocystis carinii with DNA amplification.* Lancet, 1990. **336**(8713): p. 451-3.

50. Reid, A.B., S.C. Chen, and L.J. Worth, *Pneumocystis jirovecii pneumonia in non-HIV-infected patients: new risks and diagnostic tools.* Curr Opin Infect Dis, 2011. **24**(6): p. 534-44.

51. Flori, P., et al., *Comparison between real-time PCR, conventional PCR and different staining techniques for diagnosing Pneumocystis jiroveci pneumonia from bronchoalveolar lavage specimens.* J Med Microbiol, 2004. **53**(Pt 7): p. 603-7.

52. Desmet, S., et al., *Serum (1-3)-β-d-Glucan as a Tool for Diagnosis of Pneumocystis jirovecii Pneumonia in Patients with Human Immunodeficiency Virus Infection or Hematological Malignancy.* Journal of Clinical Microbiology, 2009. **47**(12): p. 3871-3874.

53. Bellamy, R.J., *HIV: treating Pneumocystis pneumonia (PCP).* BMJ Clinical Evidence, 2008. **2008**: p. 2501.

54. Helweg-Larsen, J., et al., *Clinical efficacy of first- and second-line treatments for HIV-associated Pneumocystis jirovecii pneumonia: a tri-centre cohort study.* Journal of Antimicrobial Chemotherapy, 2009. **64**(6): p. 1282-1290.

55. Kielhofner, M.A., *Trimethoprim- Sulfamethoxazole: Pharmacokinetics, Clinical Uses, and Adverse Reactions.* Texas Heart Institute Journal, 1990. **17**(2): p. 86-93.

56. Tu, G.-w., et al., *Combination of caspofungin and low-dose trimethoprim/sulfamethoxazole for the treatment of severe Pneumocystis jirovecii pneumonia in renal transplant recipients.* Nephrology, 2013. **18**(11): p. 736-742.

57. Crothers, K., et al., *Severity and outcome of HIV-associated Pneumocystis pneumonia containing Pneumocystis jirovecii dihydropteroate synthase gene mutations.* Aids, 2005. **19**(8): p. 801-5.

58. Nahimana, A., et al., *Mutations of Pneumocystis jirovecii dihydrofolate reductase associated with failure of prophylaxis.* Antimicrob Agents Chemother, 2004. **48**(11): p. 4301-5.

59. Mori, S. and P. Levin, *A brief review of potential mechanisms of immune reconstitution inflammatory syndrome in HIV following antiretroviral therapy.* Int J STD AIDS, 2009. **20**(7): p. 447-52.

60. Martin-Blondel, G., L.T. Mars, and R.S. Liblau, *Pathogenesis of the immune reconstitution inflammatory syndrome in HIV-infected patients.* Curr Opin Infect Dis, 2012. **25**(3): p. 312-20.

61. Muller, M., et al., *Immune reconstitution inflammatory syndrome in patients starting antiretroviral therapy for HIV infection: a systematic review and meta-analysis.* Lancet Infect Dis, 2010. **10**(4): p. 251-61.

62. Achenbach, C.J., et al., *Paradoxical Immune Reconstitution Inflammatory Syndrome in HIV-Infected Patients Treated With Combination Antiretroviral Therapy After AIDS-Defining Opportunistic Infection.* Clinical Infectious Diseases: An Official Publication of the Infectious Diseases Society of America, 2012. **54**(3): p. 424-433.

63. Grant, P.M., et al., *Risk factor analyses for immune reconstitution inflammatory syndrome in a randomized study of early vs. deferred ART during an opportunistic infection.* PLoS One, 2010. **5**(7): p. e11416.

64. Jagannathan, P., et al., *Life-threatening immune reconstitution inflammatory syndrome after Pneumocystis pneumonia: a cautionary case series.* Aids, 2009. **23**(13): p. 1794-6.

65. Zolopa, A., et al., *Early antiretroviral therapy reduces AIDS progression/death in individuals with acute opportunistic infections: a multicenter randomized strategy trial.* PLoS One, 2009. **4**(5): p. e5575.

66. Hirsch, H.H., et al., *Immune reconstitution in HIV-infected patients.* Clin Infect Dis, 2004. **38**(8): p. 1159-66.

67. Barry, S.M., et al., *Immune reconstitution pneumonitis following Pneumocystis carinii pneumonia in HIV-infected subjects.* HIV Medicine, 2002. **3**(3): p. 207-211.

68. Koval, C.E., et al., *Immune reconstitution syndrome after successful treatment of Pneumocystis carinii pneumonia in a man with human immunodeficiency virus type 1 infection.* Clin Infect Dis, 2002. **35**(4): p. 491-3.

69. Bozzette, S.A., et al., *The impact of concomitant viral pathogens on the course of Pneumocystis carinii pneumonia.* J Protozool, 1991. **38**(6): p. 183s-184s.

70. Hahn, P.Y., et al., *Pneumocystis carinii cell wall beta-glucan induces release of macrophage inflammatory protein-2 from alveolar epithelial cells via a lactosylceramide-mediated mechanism.* J Biol Chem, 2003. **278**(3): p. 2043-50.

71. Opelz, G., *Efficacy of rejection prophylaxis with OKT3 in renal transplantation. Collaborative Transplant Study.* Transplantation, 1995. **60**(11): p. 1220-4.

72. Revoir, W.H.B., C., *Respiratory Protection Handbook.* CRC Press, Inc., 1997.

73. Whitsett, J.A. and T. Alenghat, *Respiratory epithelial cells orchestrate pulmonary innate immunity.* Nat Immunol, 2015. **16**(1): p. 27-35.

74. Kopf, M., C. Schneider, and S.P. Nobs, *The development and function of lung-resident macrophages and dendritic cells.* Nat Immunol, 2015. **16**(1): p. 36-44.

75. Voynow, J.A. and B.K. Rubin, *MUcins, mucus, and sputum.* Chest, 2009. **135**(2): p. 505-512.

76. Thai, P., et al., *Regulation of Airway Mucin Gene Expression.* Annual Review of Physiology, 2008. **70**(1): p. 405-429.

77. Becher, B., et al., *High-dimensional analysis of the murine myeloid cell system.* Nat Immunol, 2014. **15**(12): p. 1181-1189.

78. Ornatsky, O., et al., *Multiple cellular antigen detection by ICP-MS.* Journal of Immunological Methods, 2006. **308**(1–2): p. 68-76.

79. Jahnsen, F.L., et al., *Accelerated Antigen Sampling and Transport by Airway Mucosal Dendritic Cells following Inhalation of a Bacterial Stimulus.* The Journal of Immunology, 2006. **177**(9): p. 5861-5867.

80. Neefjes, J., et al., *Towards a systems understanding of MHC class I and MHC class II antigen presentation.* Nat Rev Immunol, 2011. **11**(12): p. 823-836.

81. Vyas, J.M., A.G. Van der Veen, and H.L. Ploegh, *The known unknowns of antigen processing and presentation.* Nat Rev Immunol, 2008. **8**(8): p. 607-618.

82. Plantinga, M., et al., *Conventional and Monocyte-Derived CD11b+ Dendritic Cells Initiate and Maintain T Helper 2 Cell-Mediated Immunity to House Dust Mite Allergen.* Immunity, 2013. **38**(2): p. 322-335.

83. Schlitzer, A., et al., *IRF4 Transcription Factor-Dependent CD11b+ Dendritic Cells in Human and Mouse Control Mucosal IL-17 Cytokine Responses.* Immunity, 2013. **38**(5): p. 970-983.

84. Furuhashi, K., et al., *Mouse Lung CD103+ and CD11bhigh Dendritic Cells Preferentially Induce Distinct CD4+ T-Cell Responses.* American Journal of Respiratory Cell and Molecular Biology, 2012. **46**(2): p. 165-172.

85. Nakano, H., et al., *Pulmonary CD103+ dendritic cells prime Th2 responses to inhaled allergens.* Mucosal Immunol, 2012. **5**(1): p. 53-65.

86. Lord, J.D., J. Chen, and R.A. Kozarek, *A case of fatal idiopathic enteritis and multiple opportunistic infections associated with dendritic cell deficiencies.* J Gastrointestin Liver Dis, 2013. **22**(1): p. 87-91.

87. Carmona, E.M., et al., *Pneumocystis cell wall beta-glucans induce dendritic cell costimulatory molecule expression and inflammatory activation through a Fas-Fas ligand mechanism.* J Immunol, 2006. **177**(1): p. 459-67.

88. Lund, F.E., et al., *B Cells Are Required for Generation of Protective Effector and Memory CD4 Cells in Response to Pneumocystis Lung Infection.* The Journal of Immunology, 2006. **176**(10): p. 6147-6154.

89. Lund, F.E., et al., *Clearance of Pneumocystis carinii in Mice Is Dependent on B Cells But Not on P. carinii-Specific Antibody.* The Journal of Immunology, 2003. **171**(3): p. 1423-1430.

90. Peão, M.N.D., et al., *Morphological Evidence for Migration of Particle-Laden Macrophages through the Interalveolar Pores of Kohn in the Murine Lung.* Cells Tissues Organs, 1993. **147**(4): p. 227-232.

91. Westphalen, K., et al., *Sessile alveolar macrophages communicate with alveolar epithelium to modulate immunity.* Nature, 2014. **506**(7489): p. 503-506.

92. Bedoret, D., et al., *Lung interstitial macrophages alter dendritic cell functions to prevent airway allergy in mice.* The Journal of Clinical Investigation, 2009. **119**(12): p. 3723-3738.

93. Schneider, C., et al., *Induction of the nuclear receptor PPAR-[gamma] by the cytokine GM-CSF is critical for the differentiation of fetal monocytes into alveolar macrophages.* Nat Immunol, 2014. **15**(11): p. 1026-1037.

94. Guilliams, M., et al., *Alveolar macrophages develop from fetal monocytes that differentiate into long-lived cells in the first week of life via GM-CSF.* The Journal of Experimental Medicine, 2013. **210**(10): p. 1977-1992.

95. Gautier, E.L., et al., *Gene-expression profiles and transcriptional regulatory pathways that underlie the identity and diversity of mouse tissue macrophages.* Nat Immunol, 2012. **13**(11): p. 1118-1128.

96. Jakubzick, C., et al., *Minimal Differentiation of Classical Monocytes as They Survey Steady-State Tissues and Transport Antigen to Lymph Nodes.* Immunity, 2013. **39**(3): p. 599-610.

97. Raymond, M., et al., *Selective control of SIRP-α–positive airway dendritic cell trafficking through CD47 is critical for the development of TH2-mediated allergic inflammation.* Journal of Allergy and Clinical Immunology, 2009. **124**(6): p. 1333-1342.e1.

98. Bachem, A., et al., *Expression of XCR1 characterizes the Batf3-dependent lineage of dendritic cells capable of antigen cross-presentation.* Frontiers in Immunology, 2012. **3**.

99. Desch, A.N., et al., *CD103+ pulmonary dendritic cells preferentially acquire and present apoptotic cell–associated antigen.* The Journal of Experimental Medicine, 2011. **208**(9): p. 1789-1797.

100. Schraml, Barbara U., et al., *Genetic Tracing via DNGR-1 Expression History Defines Dendritic Cells as a Hematopoietic Lineage.* Cell, 2013. **154**(4): p. 843-858.

101. Ginhoux, F., et al., *The origin and development of nonlymphoid tissue CD103+ DCs.* The Journal of Experimental Medicine, 2009. **206**(13): p. 3115-3130.

102. Soroosh, P., et al., *Lung-resident tissue macrophages generate Foxp3+ regulatory T cells and promote airway tolerance.* The Journal of Experimental Medicine, 2013. **210**(4): p. 775-788.

103. Ricks, D., et al., *Dectin immunoadhesins and Pneumocystis pneumonia.* Infect Immun, 2013. **81**(9): p. 3451-62.

104. Downing, J.F., et al., *Gamma Interferon Stimulates Rat Alveolar Macrophages To Kill Pneumocystis carinii byl-Arginine- and Tumor Necrosis Factor-Dependent Mechanisms.* Infection and Immunity, 1999. **67**(3): p. 1347-1352.

105. Jones, T., *The effect of granulocyte-macrophage colony stimulating factor (rGM-CSF) on macrophage function in microbial disease.* Medical Oncology, 1996. **13**(3): p. 141-144.

106. Steele, C., et al., *Alveolar Macrophage–mediated Killing of Pneumocystis carinii f. sp. muris Involves Molecular Recognition by the Dectin-1 β-Glucan Receptor.* The Journal of Experimental Medicine, 2003. **198**(11): p. 1677-1688.

107. Nelson, M.P., et al., *IL-33 and M2a Alveolar Macrophages Promote Lung Defense against the Atypical Fungal Pathogen Pneumocystis murina.* The Journal of Immunology, 2011. **186**(4): p. 2372-2381.

108. Balhara, J. and A.S. Gounni, *The alveolar macrophages in asthma: a double-edged sword.* Mucosal Immunol, 2012. **5**(6): p. 605-609.

109. Le Goffic, R., et al., *Infection with influenza virus induces IL-33 in murine lungs.* American journal of respiratory cell and molecular biology, 2011. **45**(6): p. 1125-32.

110. Olmos, S., S. Stukes, and J.D. Ernst, *Ectopic activation of Mycobacterium tuberculosis-specific CD4+ T cells in lungs of CCR7-/- mice.* Journal of immunology, 2010. **184**(2): p. 895-901.

111. Dubin, P.J., et al., *Interleukin-23-mediated inflammation in Pseudomonas aeruginosa pulmonary infection.* Infection and immunity, 2012. **80**(1): p. 398-409.

112. Wong, C.K., et al., *Elevation of proinflammatory cytokine (IL-18, IL-17, IL-12) and Th2 cytokine (IL-4) concentrations in patients with systemic lupus erythematosus.* Lupus, 2000. **9**(8): p. 589-93.

113. Altare, F., et al., *Inherited interleukin 12 deficiency in a child with bacille Calmette-Guerin and Salmonella enteritidis disseminated infection.* The Journal of clinical investigation, 1998. **102**(12): p. 2035-40.

114. Elloumi-Zghal, H., et al., *Clinical and genetic heterogeneity of inherited autosomal recessive susceptibility to disseminated Mycobacterium bovis bacille calmette-guerin infection.* The Journal of infectious diseases, 2002. **185**(10): p. 1468-75.

115. de Jong, R., et al., *Severe mycobacterial and Salmonella infections in interleukin-12 receptor-deficient patients.* Science, 1998. **280**(5368): p. 1435-8.

116. Sakai, T., et al., *Missense mutation of the interleukin-12 receptor beta1 chain-encoding gene is associated with impaired immunity against Mycobacterium avium complex infection.* Blood, 2001. **97**(9): p. 2688-94.

117. Myers, A.K., et al., *Clinical and molecular findings in IPEX syndrome.* Archives of disease in childhood, 2006. **91**(1): p. 63-4.

118. Bilate, A.M. and J.J. Lafaille, *Induced CD4+Foxp3+ regulatory T cells in immune tolerance.* Annual review of immunology, 2012. **30**: p. 733-58.

119. Zhu, J., H. Yamane, and W.E. Paul, *Differentiation of Effector CD4 T Cell Populations.* Annual review of immunology, 2010. **28**: p. 445-489.

120. Shellito, J.E., et al., *Murine CD4+ T Lymphocyte Subsets and Host Defense against Pneumocystis carinii.* Journal of Infectious Diseases, 2000. **181**(6): p. 2011-2017.

121. Shipley, T.W., et al., *Persistent Pneumocystis Colonization Leads to the Development of Chronic Obstructive Pulmonary Disease in a Nonhuman Primate Model of AIDS.* Journal of Infectious Diseases, 2010. **202**(2): p. 302-312.

122. Hu, T., et al., *IFN-γ deficiency worsen Pneumocystis pneumonia with Th17 development in nude mice.* Immunology Letters, 2009. **127**(1): p. 55-59.

123. Hanano, R., K. Reifenberg, and S.H. Kaufmann, *Naturally acquired Pneumocystis carinii pneumonia in gene disruption mutant mice: roles of distinct T-cell populations in infection.* Infection and Immunity, 1996. **64**(8): p. 3201-3209.

124. Beck, J.M., et al., *Inflammatory Responses to Pneumocystis carinii in Mice Selectively Depleted of Helper T Lymphocytes.* American Journal of Respiratory Cell and Molecular Biology, 1991. **5**(2): p. 186-197.

125. Roths, J.B. and C.L. Sidman, *Both immunity and hyperresponsiveness to Pneumocystis carinii result from transfer of CD4+ but not CD8+ T cells into severe combined immunodeficiency mice.* The Journal of Clinical Investigation, 1992. **90**(2): p. 673-678.

126. Croix, D.A., et al., *Alterations in T Lymphocyte Profiles of Bronchoalveolar Lavage Fluid from SIV- and Pneumocystis carinii-Coinfected Rhesus Macaques.* AIDS Research and Human Retroviruses, 2002. **18**(5): p. 391-401.

127. Kolls, J.K., et al., *IFN-γ and CD8+ T Cells Restore Host Defenses Against Pneumocystis carinii in Mice Depleted of CD4+ T Cells.* The Journal of Immunology, 1999. **162**(5): p. 2890-2894.

128. Mc Allister, F., et al., *T Cytotoxic-1 CD8+ T Cells Are Effector Cells against Pneumocystis in Mice.* The Journal of Immunology, 2004. **172**(2): p. 1132-1138.

129. Kägi, M.K., et al., *High Proportion of Gamma-Delta T Cell Receptor Positive T Cells in Bronchoalveolar Lavage and Peripheral Blood of HIV-lnfected Patients with Pneumocystis carinii Pneumonias.* Respiration, 1993. **60**(3): p. 170-177.

130. Kuijpers, T.W., et al., *CD20 deficiency in humans results in impaired T cell-independent antibody responses.* J Clin Invest, 2010. **120**(1): p. 214-22.

131. Reff, M.E., et al., *Depletion of B cells in vivo by a chimeric mouse human monoclonal antibody to CD20.* Blood, 1994. **83**(2): p. 435-45.

132. Scott, S.D., *Rituximab: A New Therapeutic Monoclonal Antibody for Non-Hodgkin's Lymphoma.* Cancer Practice, 1998. **6**(3): p. 195-197.

133. Deborska-Materkowska, D., et al., *Fatal late-onset Pneumocystis pneumonia after rituximab: administration for posttransplantation recurrence of focal segmental glomerulosclerosis--case report.* Transplant Proc, 2014. **46**(8): p. 2908-11.

134. Martin-Garrido, I., et al., *PNeumocystis pneumonia in patients treated with rituximab.* Chest, 2013. **144**(1): p. 258-265.

135. Farkas, J.D., R.D. Clouser, and G.W. Garrison, *Pneumocystis pneumonia following rituximab.* Chest, 2014. **145**(3): p. 663-4.

136. Kurokawa, T., H. Kaya, and T. Yoshida, *Two cases of Pneumocystis jiroveci pneumonia with non-Hodgkin's lymphoma after CHOP-based chemotherapy containing rituximab.* J Clin Exp Hematop, 2010. **50**(2): p. 159-62.

137. Marcotte, H., et al., *Pneumocystis carinii infection in transgenic B cell-deficient mice.* J Infect Dis, 1996. **173**(4): p. 1034-7.

138. Canaani, J., et al., *Paradoxical Immune Reconstitution Inflammatory Syndrome Associated With Rituximab-Containing Regimen in a Patient With Lymphoma.* Journal of Clinical Oncology, 2013. **31**(11): p. e178-e180.

139. Zheng, M., et al., *CD4+ T cell-independent vaccination against Pneumocystis carinii in mice.* J Clin Invest, 2001. **108**(10): p. 1469-74.

140. Ricks, D.M., et al., *Dectin immunoadhesins and pneumocystis pneumonia.* Infect Immun, 2013. **81**(9): p. 3451-62.

141. Steele, C., et al., *Alveolar macrophage-mediated killing of Pneumocystis carinii f. sp. muris involves molecular recognition by the Dectin-1 beta-glucan receptor*. J Exp Med, 2003. **198**(11): p. 1677-88.

142. McKinley, L., et al., *Regulatory T Cells Dampen Pulmonary Inflammation and Lung Injury in an Animal Model of Pneumocystis Pneumonia.* The Journal of Immunology, 2006. **177**(9): p. 6215-6226.

143. Rostved, A.A., et al., *Outbreak of pneumocystis pneumonia in renal and liver transplant patients caused by genotypically distinct strains of Pneumocystis jirovecii.* Transplantation, 2013. **96**(9): p. 834-42.

144. Rosenberg, H.F., K.D. Dyer, and P.S. Foster, *Eosinophils: changing perspectives in health and disease.* Nat Rev Immunol, 2013. **13**(1): p. 9-22.

145. Lilly, L.M., et al., *Eosinophil deficiency compromises lung defense against Aspergillus fumigatus.* Infect Immun, 2014. **82**(3): p. 1315-25.

146. Ponce, C.A., et al., *Pneumocystis colonization is highly prevalent in the autopsied lungs of the general population.* Clin Infect Dis, 2010. **50**(3): p. 347-53.

147. Shteinberg, M., et al., *Asymptomatic Carriage of Pneumocystis jirovecii and Cytomegalovirus in Lungs of Immunocompetent Patients.* Lung, 2014.

148. Marco, H., et al., *The effect of rituximab therapy on immunoglobulin levels in patients with multisystem autoimmune disease.* BMC Musculoskeletal Disorders, 2014. **15**(1): p. 178.

149. Gigliotti, F., *Host species-specific antigenic variation of a mannosylated surface glycoprotein of Pneumocystis carinii.* J Infect Dis, 1992. **165**(2): p. 329-36.

150. Sunkin, S.M. and J.R. Stringer, *Translocation of surface antigen genes to a unique telomeric expression site in Pneumocystis carinii.* Molecular Microbiology, 1996. **19**(2): p. 283-295.

151. Sun, L., et al., *Genotyping of Pneumocystis jirovecii isolates from human immunodeficiency virus-negative patients in China.* Infect Genet Evol, 2015. **31c**: p. 209-215.

152. Shelburne, S.A., et al., *Incidence and risk factors for immune reconstitution inflammatory syndrome during highly active antiretroviral therapy.* Aids, 2005. **19**(4): p. 399-406.

153. Lai, R.P., et al., *The immunopathogenesis of the HIV tuberculosis immune reconstitution inflammatory syndrome.* Eur J Immunol, 2013. **43**(8): p. 1995-2002.

154. Longley, N., T.S. Harrison, and J.N. Jarvis, *Cryptococcal immune reconstitution inflammatory syndrome.* Curr Opin Infect Dis, 2013. **26**(1): p. 26-34.

155. Antonelli, L.R., et al., *Elevated frequencies of highly activated CD4+ T cells in HIV+ patients developing immune reconstitution inflammatory syndrome.* Blood, 2010. **116**(19): p. 3818-27.

156. Swain, S.D., N.N. Meissner, and A.G. Harmsen, *CD8 T cells modulate CD4 T-cell and eosinophil-mediated pulmonary pathology in pneumocystis pneumonia in B-cell-deficient mice.* Am J Pathol, 2006. **168**(2): p. 466-75.

157. Shipley, T.W., et al., *Persistent pneumocystis colonization leads to the development of chronic obstructive pulmonary disease in a nonhuman primate model of AIDS.* J Infect Dis, 2010. **202**(2): p. 302-12.

158. Rudner, X.L., et al., *Interleukin-23 (IL-23)-IL-17 Cytokine Axis in Murine Pneumocystis carinii Infection.* Infection and Immunity, 2007. **75**(6): p. 3055-3061.

159. Kotlarz, D., et al., *Loss-of-function mutations in the IL-21 receptor gene cause a primary immunodeficiency syndrome.* J Exp Med, 2013. **210**(3): p. 433-43.

160. Yeste, A., et al., *IL-21 induces IL-22 production in CD4+ T cells.* Nat Commun, 2014. **5**.

161. Mandujano, J.F., et al., *Granulocyte-macrophage colony stimulating factor and Pneumocystis carinii pneumonia in mice.* American Journal of Respiratory and Critical Care Medicine, 1995. **151**(4): p. 1233-1238.

162. Alvaro-Meca, A., et al., *Pneumocystis pneumonia in HIV-positive patients in Spain: epidemiology and environmental risk factors.* J Int AIDS Soc, 2015. **18**: p. 19906.

163. Antiretroviral Therapy Cohort, C., et al., *Variable impact on mortality of AIDS-defining events diagnosed during combination antiretroviral therapy: not all AIDS-defining conditions are created equal.* Clin Infect Dis, 2009. **48**(8): p. 1138-51.

164. Morris, A., et al., *Current epidemiology of Pneumocystis pneumonia.* Emerg Infect Dis, 2004. **10**(10): p. 1713-20.

165. Tansuphasawadikul, S., et al., *Clinical features, etiology and short term outcomes of interstitial pneumonitis in HIV/AIDS patients.* Southeast Asian J Trop Med Public Health, 2005. **36**(6): p. 1469-78.

166. Udwadia, Z.F., A.V. Doshi, and A.S. Bhaduri, *Pneumocystis carinii pneumonia in HIV infected patients from Mumbai.* J Assoc Physicians India, 2005. **53**: p. 437-40.

167. Martin-Garrido, I., et al., *Pneumocystis pneumonia in patients treated with rituximab.* Chest, 2013. **144**(1): p. 258-65.

168. Centers for Disease, C. and Prevention, *Pneumocystis pneumonia--Los Angeles. 1981*. MMWR Morb Mortal Wkly Rep, 1996. **45**(34): p. 729-33.

169. Colford, J.M., Jr., et al., *Temporal trends and factors associated with survival after Pneumocystis carinii pneumonia in California, 1983-1992.* Am J Epidemiol, 1997. **146**(2): p. 115-27.

170. Dworkin, M.S., D.L. Hanson, and T.R. Navin, *Survival of patients with AIDS, after diagnosis of Pneumocystis carinii pneumonia, in the United States.* J Infect Dis, 2001. **183**(9): p. 1409-12.

171. Lundgren, I.S., et al., *Outcomes and duration of Pneumocystis jiroveci pneumonia therapy in infants with severe combined immunodeficiency.* Pediatr Infect Dis J, 2012. **31**(1): p. 95-7.

172. Casper, J.T., et al., *Successful treatment with an unrelated-donor bone marrow transplant in an HLA-deficient patient with severe combined immune deficiency ("bare lymphocyte syndrome").* J Pediatr, 1990. **116**(2): p. 262-5.

173. Lund, F.E., et al., *B cells are required for generation of protective effector and memory CD4 cells in response to Pneumocystis lung infection.* J Immunol, 2006. **176**(10): p. 6147-54.

174. Shellito, J., et al., *A new model of Pneumocystis carinii infection in mice selectively depleted of helper T lymphocytes.* J Clin Invest, 1990. **85**(5): p. 1686-93.

175. Swain, S.D., et al., *Pneumocystis elicits a STAT6-dependent, strain-specific innate immune response and airway hyperresponsiveness.* Am J Respir Cell Mol Biol, 2012. **46**(3): p. 290-8.

176. Yu, C., et al., *Targeted deletion of a high-affinity GATA-binding site in the GATA-1 promoter leads to selective loss of the eosinophil lineage in vivo.* J Exp Med, 2002. **195**(11): p. 1387-95.

177. Zheng, M., et al., *CD4+ T cell-independent DNA vaccination against opportunistic infections.* The Journal of clinical investigation, 2005. **115**(12): p. 3536-44.

178. Beck, J.M., et al., *Inflammatory responses to Pneumocystis carinii in mice selectively depleted of helper T lymphocytes.* Am J Respir Cell Mol Biol, 1991. **5**(2): p. 186-97.

179. Dyer, K.D., et al., *Functionally competent eosinophils differentiated ex vivo in high purity from normal mouse bone marrow.* J Immunol, 2008. **181**(6): p. 4004-9.

180. Nakagome, K., et al., *IL-5-induced hypereosinophilia suppresses the antigen-induced immune response via a TGF-beta-dependent mechanism.* J Immunol, 2007. **179**(1): p. 284-94.

181. Fleury-Feith, J., et al., *Bronchoalveolar lavage eosinophilia associated with Pneumocystis carinii pneumonitis in AIDS patients. Comparative study with non-AIDS patients.* Chest, 1989. **95**(6): p. 1198-201.

182. Sadaghdar, H., Z.B. Huang, and E. Eden, *Correlation of bronchoalveolar lavage findings to severity of Pneumocystis carinii pneumonia in AIDS. Evidence for the development of high-permeability pulmonary edema.* Chest, 1992. **102**(1): p. 63-9.

183. Gingo, M.R., et al., *Asthma diagnosis and airway bronchodilator response in HIV-infected patients.* J Allergy Clin Immunol, 2012. **129**(3): p. 708-714 e8.